4502

STUDIES OF HUMAN SERUM ALBUMIN-LIGAND INTERACTIONS USING SITE-DIRECTED MUTANTS AND RECOMBINANT FRAGMENTS OF THE PROTEIN

A DISSERTATION SUBMITTED TO THE GRADUATE DIVISION OF THE UNIVERSITY OF HAWAI'I IN PARTIAL FULFILLMENT OF THE REQUIREMENTS FOR THE DEGREE OF

DOCTOR OF PHILOSOPHY

IN

BIOMEDICAL SCIENCES
(BIOCHEMISTRY)

AUGUST 2004

By
Jinsheng Yang

Dissertation Committee:

Nadhipuram V. Bhagavan, Chairperson

Richard J. Guillory
Howard F. Mower
Marguerite Volini
Philip C. Loh

© Copyright (2004)

by

Jinsheng Yang

ACKNOWLEDGEMENSTS

I would like to express my deep gratitude to Dr. Nadhipuram V. Bhagavan, my research advisor, for his support and guidance throughout my studies. I would also like to thank Dr. Marguerite Volini, Dr. Philip C. Loh, Dr. Howard F. Mower and Dr. Richard J. Guillory for their valuable help. Also, I would to thank Dr. Charles E. Petersen, Dr. Chung-Eun Ha and Ji-Sook Ha, for being nice and helpful colleagues over the years. Last, I would like to thank my dear wife, Dr. Zerong You, who has shared with me the stresses and the excitements in my pursuit of a Ph. D. degree.

ABSTRACT

Human serum albumin (HSA) is the most abundant protein in the blood circulation. Binding reversibly many endogenous and exogenous compounds with moderate to high affinity, HSA principally functions as a transport and depot protein. HSA-ligand interactions affect pharmacokinetics of drugs. Due to its high concentration, HSA can assume additional functions. Structurally, it is a single chain protein with three homologous domains, each domain having distinct features.

The use of recombinant fragments and mutants of HSA is emerging as an important way to explore HSA-ligand interactions and structural transitions of HSA at the molecular level. In this work, domains I, II, III and domain III with Y411W mutation were expressed in *Pichia pastoris* as stand-alone proteins and were characterized by fluorescence techniques. The results indicated that the isolated domain fragments retain many of the binding properties that have been mapped to them in the intact HSA. A domain II construct with desirable cleavage at the secretion signal sequence was obtained and a preliminary rule for designing an efficient cleavage site has been proposed.

HSA undergoes structural changes around neutral pH, known as the N-B transition, which was suggested to have physiological significance. Previous work has suggested a dominant role for five histidine residues at positions 9, 39, 67, 105, 128 or 146 of domain I in this transition. In the present work, by using site-directed mutants, the five positions have been resolved to be 9, 67, 105, 128 and 146 and the role of the histidine residues has been confirmed.

The metabolism of many arachidonic acid metabolites is altered when bound to HSA. The mechanism by which prostaglandins bound to subdomain IIA of HSA are metabolized by catalytic processes was studied in this work. The breakdown of the prostaglandin 15-keto-PGE_2 to 15-keto-PGA_2 and 15-keto-PGB_2 in the presence of wild type HSA and a number of subdomain IIA mutants was examined using a previously validated spectroscopic method. The results support the involvement of certain basic amino residues in the catabolism of HSA-bound 15-keto-PGE_2, and suggest that metabolism of HSA-bound prostaglandins may be a more complex and specific process than previously thought.

TABLE OF CONTENTS

Acknowledgments.....iv

Abstract.....v

List of Tables.....x

List of Figures.....xi

Chapter 1. Introduction.....1

Human serum albumin.....1

Research Overview.....9

Fragment studies.....9

Role of histidine residues of domain I in the N-B transition of HSA.....12

Structural basis for HSA-mediated catalysis of prostaglandin metabolism.....18

Chapter 2. Expression and characterization of recombinant domain fragments.....22

Materials and methods.....22

Synthesis and purification of recombinant fragments of HSA.....22

Binding of fluorescent probes to the fragments.....24

Displacement of fluorescent probes from the fragments by drugs.....26

Quenching of tryptophan fluorescence.....26

General experimental parameters.....27

Analysis of data.....28

Results.....29

Expression of domain fragments and tuning of the N-terminal.....29

Binding of fluorescent probes to the fragments.....37

Displacement of fluorescent probes from the fragments by drugs.....43

Quenching of tryptophan fluorescence.....53

Discussion.....54

Chapter 3. Study of the role of histidine residues of domain I in the N-B transition 60

Materials and methods.....61

Synthesis and purification of recombinant mutants of HSA.....61

Introduction of mutations into the HSA coding region.....61

Expression of recombinant mutants.....61

Verification of the DNA sequence of HSA mutants 61

Purification of recombinant mutants.....62

Measurement of fluorescence of mutant-warfarin complexes.....62

Background.....62

General experimental parameters.....64

Analysis of data 65

Measurement of the fluorescent enhancement of mutant-bound Warfarin at pH 6.0, 7.4 and 9.0.....65

Measurement of dissociation constants of mutant-warfarin complexes at pH 6.0, 7.4 and 9.0.....66

Measurement of fluorescence of mutant-bound warfarin as a function of pH.....66

Results.....66

Measurement of fluorescence enhancement of mutant-bound warfarin at pH 6.0, 7.4 and 9.0.....66

Measurement of dissociation constants of mutant-warfarin complexes at pH 6.0, 7.4 and 9.0.....67

Measurement of fluorescence of mutant-bound warfarin as a function of pH.....68

Discussion.....98

Chapter 4. Study of the structural basis for HSA-mediated catalysis of prostaglandin metabolism.....109

Synthesis and purification of recombinant HSA.....110

Introduction of mutations into the HSA coding region.....110

Verification of the DNA sequence of HSA clones.....110

Purification of recombinant HSA.....111

Synthesis and purification of recombinant HSA fragments.....111

Cloning of coding regions for domains I, II and III.....112

Verification of DNA sequence of clones and protein expression and purification.....113

Spectroscopic assay of 15-keto-prostaglandin E_2 (15 keto-PGE_2) breakdown...113

Background.....113

General experimental parameters.....115

Analysis of data.....116

Results.....117

Discussion.....125

Chapter 5. Conclusions.....134

References.....137

LIST OF TABLES

Table		Page
1.	Dissociation constants of warfarin binding for the mutants as well as for rHSA at pH 6.0, 7.4 and 9.0.	74
2.	pH_{50} and Hill constant values for the mutants in the presence and in the absence of $CaCl_2$	95
3.	Relative rate constants for step 1 and for step 2	124

LIST OF FIGURES

Figure		Page
1.	X-ray crystallographic structure of natural HSA	7
2.	Structures of the three individual domains of HSA	8
3.	Influence of down-stream sequence context around the supposed cleavage site of Lex2 on the cleavage as determined by N-terminal sequencing	32
4.	Initially used primer pairs for domains I, II and III, and the modified 5' primers	33
5.	Re-designed 5' primers for domains II	34
6.	SDS-PAGE of expression products of domain II showing the effect of down-stream sequence context on the cleavage	35
7.	SDS-PAGE of expression products of domains I, II and III	36
8.	Structural representation of warfarin and dansylsarcosine	39
9.	Structural representation of iophenoxic acid, phenylbutazone, bilirubin and ibuprofen	40
10.	Fluorescence emission spectra of warfarin bound to recombinant HSA (rHSA) and domain fragments	41
11.	Fluorescence emission spectra of dansylsarcosine bound to rHSA and domain fragments	42
12.	Saturation of rHSA and domain II with warfarin	46
13.	Saturation of rHSA and domain III with dansylsarcosine	47
14.	Drug-induced changes in the fluorescence of warfarin bound to rHSA	48
15.	Drug-induced changes in the fluorescence of warfarin bound to domain II	49
16.	Drug-induced changes in the fluorescence of dansylsarcosine bound to rHSA	50

17. Drug-induced changes in the fluorescence of dansylsarcosine bound to domain III.....51

18. Drug-induced changes in the fluorescence of dansylsarcosine bound to domain III-Y411W.....52

19. Quenching of the tryptophanyl fluorescence of rHSA, Domain II and Domain III-Y411W by iophenoxate.....57

20. Fluorescence spectra of rHSA, domain II and domain III-Y411W with excitation at 295 nm.....58

21. Stern-Volmer plot of acrylamide quenching of rHSA, domain II and domain III-Y411W with excitation at 295 nm.....59

22. Warfarin fluorescence enhancement for the mutants at pH 6.0, 7.4 and 9.0.....72

23. Fractional changes in fluorescence enhancement for the mutants at pH 7.4.....73

24. Association constants (Ka) for the mutants as well as rHSA at pH 6.0, 7.4 and 9.0.....75

25. Effect of pH on the fluorescence of warfarin bound to rHSA in the absence and presence of 2.5 mM $CaCl_2$.....76

26. Effect of pH on the fluorescence of warfarin bound to H9F in the absence and presence of 2.5 mM $CaCl_2$.....77

27. Effect of pH on the fluorescence of warfarin bound to H9S in the absence and presence of 2.5 mM $CaCl_2$.....78

28. Effect of pH on the fluorescence of warfarin bound to H39F in the absence and presence of 2.5 mM $CaCl_2$.....79

29. Effect of pH on the fluorescence of warfarin bound to H39S in the absence and presence of 2.5 mM $CaCl_2$.....80

30. Effect of pH on the fluorescence of warfarin bound to H67F in the absence and presence of 2.5 mM $CaCl_2$.....81

31. Effect of pH on the fluorescence of warfarin bound to H67S in the absence and presence of 2.5 mM $CaCl_2$.....82

32. Effect of pH on the fluorescence of warfarin bound to H105F in the absence and presence of 2.5 mM $CaCl_2$.....83

33. Effect of pH on the fluorescence of warfarin bound to H105S in the absence and presence of 2.5 mM $CaCl_2$.....84

34. Effect of pH on the fluorescence of warfarin bound to H128F in the absence and presence of 2.5 mM $CaCl_2$.....85

35. Effect of pH on the fluorescence of warfarin bound to H128S in the absence and presence of 2.5 mM $CaCl_2$.....86

36. Effect of pH on the fluorescence of warfarin bound to H146F in the absence and presence of 2.5 mM $CaCl_2$.....87

37. Effect of pH on the fluorescence of warfarin bound to H146S in the absence and presence of 2.5 mM $CaCl_2$.....88

38. Fractional changes in the fluorescence of warfarin bound to H9F or H9S in the absence or presence of 2.5 mM $CaCl_2$ as a function of pH.....89

39. Fractional changes in the fluorescence of warfarin bound to H39F or H39S in the absence or presence of 2.5 mM $CaCl_2$ as a function of pH.....90

40. Fractional changes in the fluorescence of warfarin bound to H67F or H67S in the absence or presence of 2.5 mM $CaCl_2$ as a function of pH.....91

41. Fractional changes in the fluorescence of warfarin bound to H105F or H105S in the absence or presence of 2.5 mM $CaCl_2$ as a function of pH.....92

42. Fractional changes in the fluorescence of warfarin bound to H128F or H128S in the absence or presence of 2.5 mM $CaCl_2$ as a function of pH.....93

43. Fractional changes in the fluorescence of warfarin bound to H146F or H146S in the absence or presence of 2.5 mM $CaCl_2$ as a function of pH.....94

44. Effect of pH on the fluorescence of warfarin bound to rHSA in the absence and presence of 2.5 mM $CaCl_2$ and 5 mM $CaCl_2$.....96

45. Effect of ionic strength on the pH titration of warfarin-rHSA complex.....97

46. Contact surface and neighbor residues of His9.....103

47. Contact surface and neighbor residues of His39.....104

48. Contact surface and neighbor residues of His67.....105

49. Contact surface and neighbor residues of His105.....106

50. Contact surface and neighbor residues of His128.....107

51. Contact surface and neighbor residues of His146.....108

52. Proposed mechanism by which 15-keto-PGE_2 is converted to 15-keto-PGB_2...114

53. Time course for a two-step consecutive reaction 120

54. Effects of albumin species (group A) on 15-keto-PGE_2 catalysis.....121

55. Effects of albumin species (group B) on 15-keto-PGE_2 catalysis.....122

56. Effects of albumin species (group C) on 15-keto-PGE_2 catalysis.....123

57. Sequence alignment of serum albumins from human, pig, horse, dog, cow and rabbit, focusing on domain IIA.....131

CHAPTER 1
INTRODUCTION

HUMAN SERUM ALBUMIN

Owing to its availability, ease of purification, low cost and important physiological functions, human serum albumin (HSA) is probably the most studied protein. In the past 30 years, more than 15,000 articles have been published with albumin as the study subject; there have been many well-written reviews about albumin (e.g. Spector, 1986; Carter and Ho, 1994; Curry *et al.*, 1999; Kragh-Hansen *et al.*, 2002); Peters (1996) has authored an excellent monograph about albumin, a classic in albumin research literature.

As is often quoted, albumin investigation dates back to more than 160 years ago, when serum albumin (in fact the total protein of the fluids) was recognized as a principal component of blood by H. Ancell (1839). In the early days, researchers developed dialysis, salt fractionation and crystallization to purify albumin. Using then the new technique of ultracentrifugation, T. Svedberg identified albumin as a 4S band with a molecular mass of about 70,000 Da in 1930s; A. Tiselius, in the Svedberg laboratory, separated albumin as well as globulin into bands by electrophoresis in 1937. During the 1940s, E.J. Cohn developed cold alcohol fractionation procedures to prepare albumin in pure form and in large quantity, which also encouraged the adoption of albumin as a model protein by biochemists. Many well-know scientists have contributed to the understanding of albumin.

Human serum albumin is the most abundant protein in the blood circulation with a normal concentration of about 42 mg/ml (about 0.6 mM). It is also distributed to the

interstitial fluid of the tissues, with concentration ranging from 15 to 30 mg/ml. An adult has total body HSA of about 360 grams. HSA is known to have many important physiological functions. Among these are: providing 80% of the colloid osmotic blood pressure in the circulatory system, playing a major role in maintaining blood pH (Figge *et al.*, 1991), binding ions such as calcium (Pedersen, 1971; Kragh-Hansen and Vorum, 1993), and binding small organic molecules that have a low water solubility. As stated in an editorial, the concentration of albumin in serum has long been recognized as an indicator of the state of general health and nutrition of an individual (Williams, 1992). Albumin synthesis is closely regulated by blood osmotic pressure (Brown and Shockley, 1982). An increase in osmotic pressure leads to a decrease in albumin synthesis while a decrease in osmotic pressure leads to an increase in albumin synthesis. Binding of ions reduces the concentration of the unbound ions and provides a reservoir of bound ions that are available for rapid dissociation when unbound ions are needed. The most outstanding function is the binding of small organic ligands that have a low water solubility. Albumin binds a great variety of ligands reversibly with moderate to high affinity. It is known as the transport function of albumin since it facilitates the movement of the organic ligands. Among organic ligands of endogenous origin are fatty acids, bilirubin, amino acids such as tryptophan and hormones such as thyroxine while many commonly prescribed drugs such as warfarin, digoxin, furosemide, and ibuprofen are examples of ligands of exogenous origin. Fatty acid transport is believed to be the primary role of albumin. Under normal physiological condition albumin binds 0.5 to 2 fatty acid molecules per albumin molecule. Due to its affinity for so many ligands and high concentration, additional functions of albumin can also be of physiological importance. HSA affects

pharmacokinetics of many drugs; its interactions with drugs are a key factor in drug design. Binding of bilirubin also protects the body against the toxic effect of this heme derivative. Recently, albumin has been identified as an important reservoir of nitric oxide, a key signal molecule in the body system (Stamler *et al.*, 1992). HSA also has several enzymatic or enzyme-like activities. For instance, it promotes the conversion of prostaglandin E_2 to prostaglandin A_2 and prostaglandin A_2 to prostaglandin B_2. Recently, the Co(II)-albumin test was evaluated for the assessment of myocardial ischemia and myocardial infarction (Bhagavan *et al.*, 2003). The understanding of albumin is far from complete; there will be more surprises for the albumin researchers.

Puzzled by the unique binding capacity of albumin, early researchers suggested that albumin bind ligands in a "sponge-like" manner. This picture of albumin-ligand interaction gave way to the more interesting view of specific binding when Sudlow *et al.* (1975), by using fluorescence probes, demonstrated that many of the ligands studied fell into two groups and within each group, the ligands competed for one binding site. The two specific binding sites in the two groups were named "site I" and "site II" respectively; for site I, dimethylaminonapthalene-1-sulfonamide (DNSA) and warfarin were the classical probes, and for site II, dansylsarcosine was the preferred probe. The displacement of either DNSA/warfarin or dansylsarcosine was used as a measure of the specificity and relative strength of binding of drugs to the two sites.

In 1975, the complete sequence of HSA was determined by two groups of researchers (Meloun *et al.*, 1975; Behrens *et al.*, 1975), which for the first time provided a structural framework for albumin studies. HSA is a single chain protein made of 585 amino acid residues with a MW of 66.5 kD. It has 35 cysteines forming 17 S-S pairs,

which accounts for its high stability. Cys34 is the only free cysteine residue, which may be involved in nitric oxide binding (Keaney *et al.*, 1993). Primary sequence, disulfide loop pattern, and intron-exon pattern for the gene suggest a three domain structural arrangement of HSA. Supported also by primary sequences of albumins from other vertebrate species, HSA is presumed to have evolved from gene triplication of a 190-amino acid "protoalbumin". The three homologous repeats was predicted to fold into three domains (I, II and III).

Thanks to the multiple disulfide loops, HSA is a very stable protein; for example, it can survive 10-hour heating at 60°C. Nevertheless, HSA is also a very flexible molecule because the disulfide loops are formed locally within each individual domain and there is no inter-domain disulfide bond. The spatial arrangement between domains can alter readily under various conditions. It has long been known that HSA undergoes reversible conformational isomerization at pH values above 8-9 and below 4 (Foster, 1977). Observing electrophoretic heterogeneity, Foster classified as "F", the fast migrating form produced at pH value less than 4; "N", the normal form, which is predominant at neutral pH; and "B", the basic form occurring at pH above 8.

A sustained interest has been maintained in determining the shape of HSA in solution. The data accumulated over years seems intriguing. The favored view, which was largely based on hydrodynamic and low-angle X-ray scattering measurements, was that in solution HSA has the cigar-shaped form of a prolate ellipsoid with a 3:1 axial ratio. However, there also have been data suggesting a spherical shape for albumin. For instance, in agreement with a more folded structure like a U shape, fluorescent quenching data suggested nearly equal distances between Cys34, Trp214 and Tyr411, each of which

is located in a different domain (Hagag *et al.*, 1983). Based on the results from acid-base titration experiments with HSA, a large peptic fragment and a large tryptic fragment, Bos *et al.* (1989b) also reasoned that domain I has direct interactions with domain III thus favoring the folded U structure of albumin.

Using greatly improved techniques, He and Carter (1992) obtained the X-ray crystallographic structure of HSA at a resolution of 3.2 Å, which marked a monumental achievement in obtaining usable crystals of albumin. Curry *et al.* (1998) resolved the crystal structure of HSA complexed with myristate. Sugio *et al.* (1999) published the crystal structure of unliganded HSA at 2.5 Å. Sugio and colleagues determined the three-dimensional structures of HSA derived from pool plasma and from a *Pichia pastoris* expression system; both structures are virtually identical, with an r.m.s. deviation of 0.24 Å. Since then more crystal structures of HSA have been reported, such as the crystal structure of HSA-warfarin-myristate complex (Petitpas *et al.*, 2001), rHSA-thyroxine, R218H-thyroxine, R218P-thyroxine, rHSA-thyroxine-myristate and R218H-thyroxine-myristate complexes (Petitpas *et al.*, 2003).

The crystal structure of albumin reveals a molecule of roughly the shape of an equilateral triangle with sides of about 80 Å and a depth of about 30 Å (Figure 1). This is known as the heart-shaped HSA in contrast to the cigar-shaped HSA suggested by many earlier studies. Under neutral pH conditions, the structure of HSA has an axial ratio of about 2.66, which He and Carter interpreted as being in good agreement with the value of 3.0 predicted by earlier data from physical experiments. HSA is predominantly α-helical, with a content value of 67%. The tertiary structure is composed of three homologous domains as suggested by earlier work and each domain can be divided further into

subdomains A and B, which are composed of six and four α-helices (Figures 1 and 2). Domains I (residues 1-195), II (196-383) and III (384-585) are not only topologically identical but also very similar in tertiary structure. On the other hand, the global assembly of the three domains is highly asymmetric. Subdomain IIB has hydrophobic and hydrogen bond interactions with the interface region between subdomain IA and subdomain IB while domain III only interacts only with subdomain IIB. There is a large channel formed by subdomains IB, IIIA and IIIB, which limits the contacts between domain I and domain III. X-ray studies have placed site I in domain IIA and site II in domain IIIA (Figures 1 and 2). Deep hydrophobic pockets with positively charged residues at the entrances are located at similar positions in subdomain IIA and subdomain IIIA whereas subdomain IA does not have a similar pocket. Domain IIA has the lone tryptophan residue of HSA (W214). Binding of fatty acids causes dramatic conformational changes (Curry *et al.*, 1998): globally, fatty acid binding induces relative rotations of the three domains with very modest distortion of the individual domains; locally, there is no significant main chain movement upon fatty acid binding and rotations of side chains are the principal local adjustments to accommodate the bound ligand. Curry suggested that physiologically, global conformation changes may allow the 'HSA receptor' to discriminate between loaded and empty HSA, which may help deliver fatty acids efficiently.

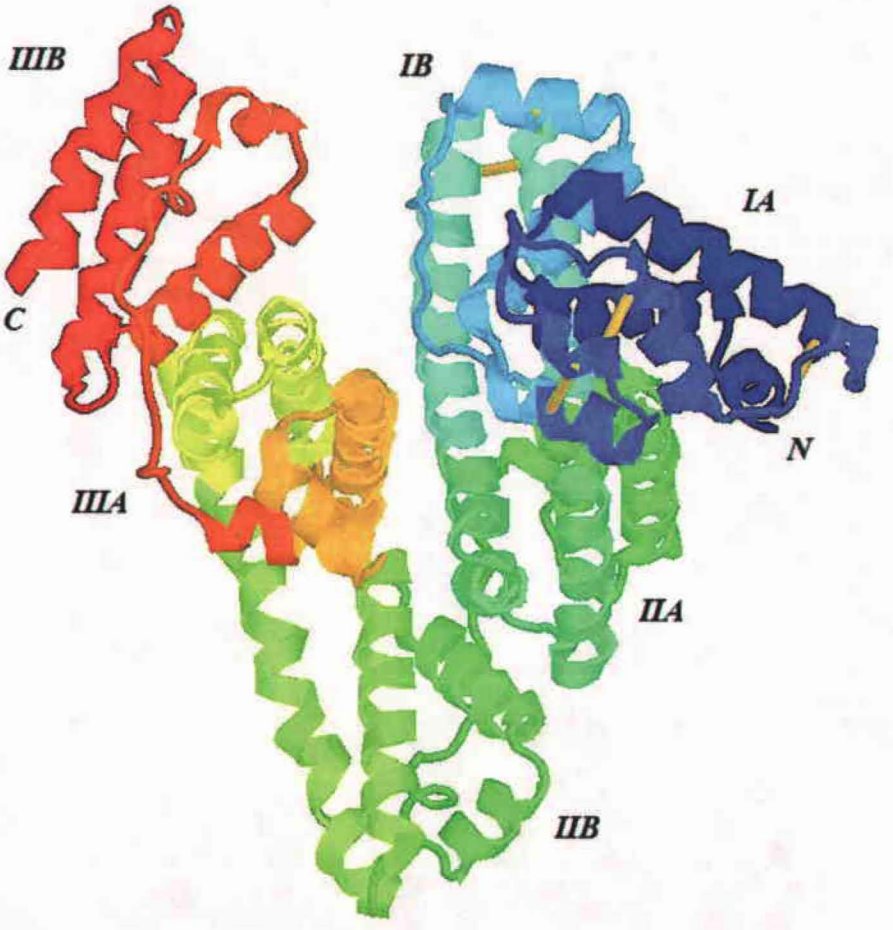

Figure 1. X-ray crystallographic structure of natural HSA. The figure was produced using Protein Explorer (Martz, 2000) and the PDB ID of the structure is 1BM0 (Sugio S *et al.*, 1999).

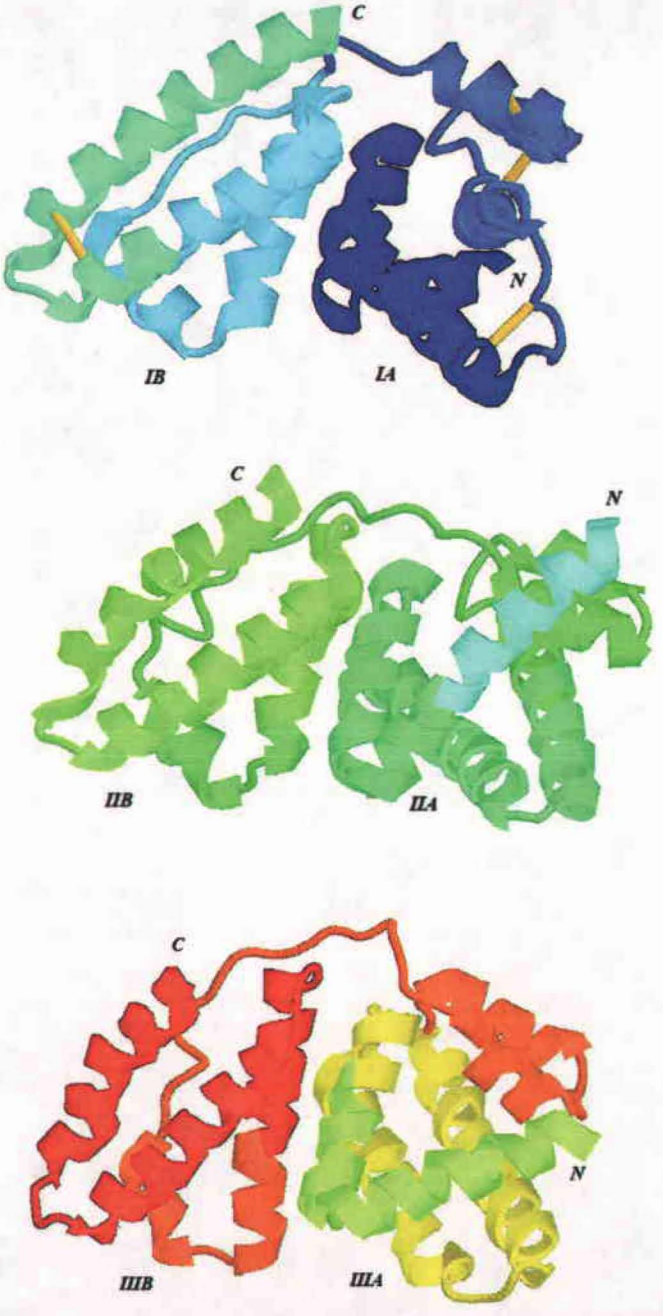

Figure 2. Structures of the three individual domains of HSA. Each domain consists of two subdomains (A and B), which have a pseudo C_2 symmetry. The figure was produced using Protein Explorer (Martz, 2000) and the PDB ID of the structure is 1BM0 (Sugio S *et al.*, 1999).

Currently, the crystal structures offer the most detailed pictures of albumin and have proved to be most valuable in reconciling the accumulated data and providing guidance for future research. However, due to its 'snapshot' nature, the information provided by the X-ray crystal structure has many missing links. Therefore, the complementary information obtained by other techniques is indispensable.

RESEARCH OVERVIEW

Fragment studies

Fragments produced either by chemical cleavage or proteolytic digestion have been useful in structural and functional studies of albumin. They have been used for determining amino acid sequence, disulfide bonding pattern, loci of antigenic and ligand-binding, interactions between different regions, and structural origin of conformational transitions. Since proteolytic cleavage can be achieved under mild conditions with a reduced chance of modification to the sensitive residues, proteinases have been the preferred cleavage reagent. Pepsin or trypsin digestion of albumin has proved to be the most useful; under appropriate conditions, they exhibit enhanced selectivity. Two proteolytic fragments have been widely used in ligand-binding and conformation transition studies. One is a large peptic fragment bracketing residues 1-387 (domains I and II) and the other is a tryptic fragment bracketing residues 198-585 (domains II and III). The peptic fragment binds bilirubin displaying similar induced circular dichroism (CD) signal as that for the bilirubin-HSA complex (Geisow and Beaven, 1977). Using the two large fragments in CD and equilibrium dialysis experiments, Bos *et al.* (1988a) suggested that the tryptic fragment contains the primary diazepam-binding site and the

peptic fragment one or more secondary binding sites for diazepam. In a comparative study of warfarin-binding properties of the two fragments using the CD method, Bos *et al.* (1988b) found that the induced ellipticity of the warfarin-peptic fragment complex was pH dependent and the dependence was in the pH range of the so-called N-B transition while the CD signal for the warfarin-tryptic fragment complex was pH independent. The peptic fragment and albumin showed similar warfarin-binding properties, and equilibrium dialysis results revealed that the affinity of warfarin to the peptic fragment and to HSA was practically the same while the tryptic fragment showed a value 2-8 fold lower. Thus it was concluded that the primary binding site for warfarin is located in domain II of HSA and that domain I plays an important role in the N-B transition. Bos *et al.* (1989b) carried out acid/base titration studies and ^{1}H-NMR spectroscopic studies on the large tryptic fragment and the large peptic fragment of HSA. The titration results indicated that Ca^{+2} ions induce a downward pK shift of several histidine residues of the peptic fragment and of HSA while Ca^{+2} ions have little influence on the pK of histidine residues of the tryptic fragment. A correspondence existed between the number of histidines detected by acid-base titration and the NMR experiments. It was concluded that in domain I at least five histidine residues play a dominant role in the N-B transition. The binding of the steroid hormones testosterone and pregenolone to HSA and the two fragments was examined by Fisher *et al.*(1993). The binding sites for both steroids were located in domain II. Both steroids showed pH-dependent binding profiles in the case of HSA and peptic fragment.

However, the use of proteolytic fragments suffers some disadvantages. The location of the cleavage sites on the primary sequence of HSA allows for a very limited

choice of sizes and boundaries of proteolytic fragments, which has precluded the use of fragments in many situations. In addition, unwanted cleavages or nicks within the fragment can be found occasionally.

Currently, recombinant technique and protein expression systems combined with site-directed mutagenesis are among the most powerful tools in structure-function studies of proteins. Recombinant fragments can be well designed with natural border based on the primary and tertiary structures of HSA. Compared with the whole-length protein molecule, the smaller sized fragments will be more amenable to NMR studies. In view of the drawbacks of proteolytic fragments, Kjeldsen *et al.* (1998) succeeded in expressing domain I and III fragments in *Saccharomyces cerevisiae*. Our laboratory has expressed half HSA comprising IA, IB and IIA subdomains in *Pichia pastoris* (Park *et al.*, 1999). Dockal *et al.* (1999) expressed all three domains in *Pichia pastoris* system and examined some properties of the fragments. These advances in preparing recombinant fragments have inspired more experiments with HSA fragments (e.g., Subramaniam *et al.*, 2000; Liu *et al.*, 2004).

In practice, the recombinant fragments have all been expressed in a secreted form to enhance their yields and simplify their purification. However, standard cloning strategy requires that extra residues be introduced into the N-terminal of the fragments when a non-native secretion signal sequence is used, which often results in heterogeneous removal of the signal sequence from the N-terminal. In the case of fragments with N-terminal different from the natural one, it seems unavoidable to have some extra residues attached to the new N-terminals during the cloning procedures. The introduction of extra residues can also pose problems in some situations. In this study, the cause of

heterogeneous processing of the secretion signal sequence and its remedy was investigated. Further characterization of the domain fragments was attempted using fluorescence probes and site-specific drugs. To facilitate fluorescent spectroscopic study, a tryptophan was introduced into a domain III fragment. The feasibility of using individual domains as stand-alone model proteins for the study of HSA was tested further in this study.

Role of histidine residues of domain I in the N-B transition of HSA

HSA undergoes isomerization with varying pH:

	E ⟷ F ⟷ N ⟷ B ⟷ A				
pH of transition:		2.7	4.3	8	10
name of isomer:	expanded	fast	neutral	basic	aged

Originally, Leonard *et al.* (1963) observed a drop in specific rotation at 313.2 nm around pH 8 in an optical rotatory dispersion (ORD) study of HSA and attributed it to changes in tertiary structure of HSA. They proposed that the drop is due to decreased inter-residue contacts in the isomeric form, i.e., the form at slightly alkalilne pH, and the rearrangement is small since hydrodynamic parameters appeared constant. The transition from the neutral form, or the N form to the basic form or the B form has been termed 'neutral transition' or N-B transition. By using differential hydrogen ion titration as well as ORD measurements, Harmsen *et al.* (1971) studied the N-B transition of bovine serum albumin (BSA), a close homologue of HSA, in the presence of KCl or $CaCl_2$. Their results strongly suggested that the N-B transition causes pK shift of imidazole groups and that in the low pH conformation, several histidine residues are involved in salt bridges. An important observation was made that in the presence of calcium ions, the N-B

transition steepens and shifts to lower pH values, which are in the physiological range, suggesting physilogical relevance of this phenominon.

The N-B transition involves largely the interactions between domain I and domain II. Wanwimolruk and Birkett (1982) investigated the effects of the N-B transition of HSA on the specific drug-binding sites. They found that the B conformation has increased affinity for drugs and fluorescent probes at site I whereas no effect was observed on drug binding at site II. Fatty acid binding induces similar changes in drug binding as the N-B transition does; however, the effects of pH and fatty acids are additive, suggesting independent conformational changes. As in binding site studies, HSA Fragments have also found their use in this endeavor. In a comparative study of warfarin-binding properties of a tryptic fragment bracketing residues 198-585 (domains II and III) and a peptic fragment bracketing residues 1-387 (domains I and II) using CD method, Bos *et al.* (1988b) found that the induced ellipticity of the warfarin-peptic the fragment complex was pH dependent and the dependence was in the pH range of the N-B transition while the CD signal for the warfarin-tryptic fragment complex was pH independent. Thus it was concluded that domain I plays an important role in the N-B transition. By applying fluorescence and near-UV circular dichroism techniques to stand-alone domain fragments, Dockal *et al.* (2000) found that in the pH range of the N-B transition, HSA domain I and domain II experienced a tertiary structural isomerization, whereas with domain III no changes in tertiary structure was observed. Drug binding studies also lend supporting evidence. The binding of the steroids testosterone and pregenolone to HSA and the two fragments was examined by Fisher *et al.* (1993). The binding sites for both steroids were located in domain II. Both steroids showed pH-

dependent binding profiles in the case of HSA and peptic fragment. Loop diuretics bind to site I of HSA and the binding was found to be sensitive to the N-B transition (Takamura *et al.*, 1996). Using typical site-specific drugs, i.e., warfarin, phenylbutazone, ibuprofen and diazepam, Kosa *et al.* (1998) examined the species differences of serum albumins during the N-B transitions. They found that the N-B transition occurred in albumins from all species examined and suggested that the amino acid residues responsible for the transition were some of the histidine residues in domain I.

Domain III appears to play little role in the transition and site II is not affected by the transition. For instance, based on fluorescence displacement data, the primary binding site of carprofen to HSA was predicted to be in the N-terminal part of domain III and this binding site was independent of the N-B transition (Rahman *et al.* 1993). By using dialysis and displacement of fluorescent probes binding to known sites of HSA, Maruyama *et al.* (1993) discovered that suprofen binds to site II of HSA, which is located in domain III, and the binding is independent of N-B transition. The primary binding site of benzothiadiazides was located in site II and the binding is insensitive to the N-B transition (Takamura *et al.*, 1994).

Since the early work by Harmsen *et al.* (1971), the importance of histidine residues in the N-B transition has been proposed by many researchers. By measuring the induced CD of oxyphenylbutazone-albumin complex, Droge *et al.* (1983) interpreted the effect of calcium ion on the N-B transition in terms of the two-state model and suggested that a decrease in the apparent pK values of the histidines was involved in N-B transition. The changes in apparent pK of the histidines were more dramatic with increasing calcium ion concentration. Acid-base titration indicated that in the presence of calcium ions,

fewer histidines were titratable than in the absence of calcium ions. They predicted that at least four to five histidines are involved in the N-B transition. Labro and Janssen (1986) studied the proton titration behavior of the histidine residues of HSA by means of 500 MHz ^{1}H-NMR spectroscopy. They found that some of the NMR signals had pH dependent resonance intensities and were observed in part of the pH range only. It was reasoned that the N-B transition was responsible for this behavior and the spectral changes upon addition of Ca^{2+} was caused by a downward pK shift for several histidine residues and a concomitant downward shift in the midpoint of the N-B transition. Bos *et al.* (1989b) carried out acid/base titration studies and ^{1}H-NMR spectroscopic studies on the large tryptic fragment and the large peptic fragment of HSA. The titration results indicated the calcium ions induce a downward pK shift of several histidine residues of the peptic fragment and of HSA while calcium ions have little influence on the pK of histidine residues of the tryptic fragment. The pH-dependent His C-2 proton resonances were assigned number 1-17 in albumin and the corresponding resonances could be identified on the fragments. A correspondence existed between the number of histidines detected by acid-base titration and the NMR experiments. Bos *et al.* concluded that in domain I at least the histidine residues corresponding to the His C-2 resonances 1-5 play a dominant role in the N-B transition; His3, which is involved in Cu^{2+} binding, does not take a part in the N-B transition. Thus among a total of seven histidine residues of domain I, the role of remaining six residues at positions 9, 39, 67, 105, 128 and 146 of domain I each has to be determined.

Warfarin, an anticoagulant with pK 5.0 and a fluorescent molecule, also found its wide use in the studies of the N-B transition. Wilting *et al.* (1979) used warfarin as a

sensitive circular dichroism (CD) marker to monitor the N-B transition and found the induced CD signal had the same pH dependence as the albumin alone suggesting that the warfarin-binding site on albumin is affected by the transition. The parallel between the N-B transition and the binding properties of warfarin to HSA was confirmed in more details by further studies (Wilting *et al.*, 1980). It was shown that over the pH range 6 to 9, the pH dependence of the fluorescent intensity of the warfarin-HSA complex at low drug to protein ratios parallels the N-B transition monitored by CD methods and over this pH range HSA has only one strong binding site for warfarin. Using the two large proteolytic fragments of HSA, Bos *et al.* (1988b) studied the induced ellipticity of the warfarin-fragment complexes and concluded that the primary binding site for warfarin is located in domain II of HSA and that domain one plays an important role in the N-B transition. Peterson *et al.* (2002) in our laboratory investigated the structure of the warfarin-binding site on HSA using site-directed mutagenesis and found some novel behavior for the mutants by measuring the fluorescence change as a function of pH. The mutants examined, which had specific substitution in subdomain IIA, showed 2-10 fold changes in their affinity for warfarin binding.

The physiological signifcance of this transition has been discussed by many researchers. Zurawski and Foster (1974) suggested possible physiological roles of the transition: enhanced hydrogen-ion buffering and buffering for calcium ions. Bos *et al.* (1989a, 1989b) discussed the role of the N-B transition in the transport and cellular uptake mechanisms of endogenous and exogenous compounds. Since domain I is not primarily involved in ligand binding, domain I may be the site that make contact with several membranes, e.g., the hepatocyte membrane. The ligands are released and

transported across the membrane through the N-B transition. The lower pH at membrane surfaces of several tissues may facilitate the transition. The conformational change may facilitate the recognition of the loaded HSA. The influence of pH on the microenvironment around Cys 34 of HSA was studied by using acrylodan, a Cys-specific fluorescence probe by Narazaki *et al.* (1997). The results revealed that the exposure around Cys34 in the B form was less than that in the N form and the effects of pH and oleate on the microenvironment are independent and additive. They concluded that physiologically changes in the reactivity of Cys34 with pH might be related to changes in mercaptide ion content.

Recombinant mutants of HSA have provided new insights into ligand-HSA interactions. In the present work, the six histidine residues at positions 9, 39, 67, 105, 128 and 146 of domain I were each mutated to serine and phenylalanine and their role in the N-B transition examined. Due to the sensitivity of fluorescence methods, the changes in the fluorescence of warfarin-mutant complexes were measured to monitor the conformational changes during the transition.

The result was discussed in terms of a two-state model (Monod *et al.*, 1965). This model has been commonly adopted in previous studies of the N-B transition. For example, when the proton is considered as the ligand, having the highest affinity for the N conformation, the allosteric two-state model can be used to describe the behavior of the N-B transition (Janssen *et al.*, 1981). The model was used to analyze results such as: the cooperativity in proton binding, enhanced by calcium ion; the difficulty in measuring this cooperativity experimentally; the fraction of albumin present in one of the two

conformations; and the effects of calcium ions and warfarin on the L, the allosteric constant, of the two-state model.

Structural basis for HSA-mediated catalysis of prostaglandin metabolism

The structures of two prostaglandins, prostaglandins E_1 and $F_{1\alpha}$ (PGE_1 and $PGF_{1\alpha}$) were elucidated in 1962. As more prostaglandins were discovered it soon became clear that they all shared a similar chemical structure, namely they were 20-carbon unsaturated carboxylic acids with a cyclopentane ring, all of which were derived from the precursor arachidonic acid. It was soon found that arachidonic acid was a precursor for other chemically related biologically active molecules such as prostacyclin (PGI_2), thromboxanes and leukotrienes. For a more complete background and synthesis pathways showing the interrelationships between the above compounds, the reader is referred to the pharmacology text by Campbell and Halushka (1996).

The general instability of prostaglandins and related compounds in aqueous media has complicated attempts to unravel the many biological roles played by these highly active signaling molecules. It became apparent early on in prostaglandin research that proteins in the blood might play an important role in modulating the biological activities of these compounds by binding to and stabilizing or destabilizing certain prostaglandins. A series of binding studies using radio-labeled PGE_1, PGE_2 PGA_2, and PGF_2 found that the only plasma protein that significantly bound to the above prostaglandins was human serum albumin (HSA) (Raz 1972). Although the affinity of HSA for a variety of biologically active arachidonic acid metabolites is relatively low (Kd = 10^{-5} M) (Unger 1972; Gueriguian 1976), the high serum HSA concentration (40 g/L) makes these

interactions physiologically significant. For example one study showed that HSA catalyzes the conversion of prostaglandin H_2 (PGH_2) a precursor of thromboxane A_2 (TXA_2), a stimulator of platelet aggregation to prostaglandin D_2 (PGD_2), an inhibitor of platelet aggregation (Watanabe *et al.* 1982). HSA has also been shown to stabilize PGI_2 (Wynalda and Fitzpatrick 1980) another unstable but potent inhibitor of platelet aggregation derived from PGH_2. However, HSA stabilizes the potent stimulant of irreversible platelet aggregation TXA_2 (Folco *et al.* 1977) enhancing its activity. In addition HSA binds to leukotriene A_4 (LTA_4) (Fitzpatrick *et al.* 1981) the unstable precursor of most leukotrienes preventing its rapid non-enzymatic degradation to biologically inactive metabolites in aqueous media.

A number of competitive binding studies with warfarin and other site I ligands have shown that the above interactions of HSA with arachidonic acid metabolites (Folco *et al.* 1977; Fitzpatrick and Wynalda, 1981; Fitzpatrick *et al.* 1984) occurs at ligand binding site I on HSA, that is, the effect of HSA on metabolism of the above arachidonic acid metabolites can be eliminated by adding high concentrations of ligands that compete for binding to site I, but not by ligands that bind to other sites on HSA. X-ray crystallographic studies (He and Carter, 1992; Carter and Ho, 1994; Curry *et al.* 1998; Petitpas *et al.* 2001) and experiments with recombinantly produced HSA fragments (Dockal *et al.* 1999, 2000) have shown that ligand-binding site I on HSA is located in subdomain IIA. Although HSA enhances the activity of both inhibitors and stimulators of platelet aggregation it should be noted that a number of studies have shown that the overall effect of HSA on platelet aggregation is strongly inhibitory (Silver *et al.* 1973; Remuzzi *et al.* 1979.). In light of the many epidemiological studies that have found a

strong inverse correlation between serum HSA concentration and risk of death from cardiovascular disease, one might propose that prostaglandin/HSA interactions could play an important role in the development of coronary heart disease.

The present study was based on a previous investigation which found that the half-life of PGD_2, PGE_1, PGE_2, 6-keto-PGE_1 and 15-keto-PGE_2 were reduced in the presence of HSA, relative to their half-lives in aqueous buffer at pH 7.4 (Fitzpatrick and Wynalda, 1981). By comparing the breakdown products obtained for the above prostaglandins in the presence of HSA to those obtained at various pH values the authors concluded that all of the prostaglandins above bind to the same site on HSA, which has an alkaline microenvironment with a local pH greater than or equal to 10.0. These authors proposed that this alkaline microenvironment in the HSA/prostaglandin binding site is responsible for the accelerated breakdown of these prostaglandins in the presence of HSA.

The above hypothesis is consistent with the large number of basic and hydrophobic amino acid residues protruding into the subdomain IIA-binding pocket. By comparing the half-life for PGE_2 and PGD_2 in the presence of albumin from various mammalian species an important observation was made (Fitzpatrick and Wynalda, 1981). The relative effects of each albumin species on the half-lives of PGE_2 and PGD_2 were similar, that is, those albumin species which caused the greatest reduction in the half-life of PGE_2 also caused the greatest reduction in the half-life of PGD_2. Similarly, those albumin species that caused the smallest reduction in the half-life of PGE_2 also showed the smallest reduction in the half-life of PGD_2. In total, the above results suggested a similar mechanism for the breakdown of PGD_2 and PGE_2, strengthening the idea that a

similar mechanism may be involved in the breakdown of all the prostaglandins listed above.

In the above study, the breakdown of prostaglandins bound to HSA was monitored using high performance liquid chromatography (HPLC) with ultraviolet spectrophotometric detection. A further study that measured the breakdown products obtained from 15-keto-PGE_2 incubated with HSA by similar methodology and by a visible spectrophotometric method (Fitzpatrick *et al.* 1984) found that both methods gave the same reaction rates. Namely, the breakdown of 15-keto-PGE_2 leads to the formation of a keto-enol tautomer intermediate with a peak absorbance at 505 nm (Figure 52). Thus, one can monitor the rate at which HSA catalyzes the breakdown of 15-keto-PGE_2 to the keto-enol tautomeric hybrid, which is formed instantaneously from 15-keto-PGA_2, by monitoring absorbance at 505 nm. This study found that albumin from different species had dramatically different effects on the breakdown of 15-keto PGE_2 (Fitzpatrick *et al.* 1984), suggesting that subtle changes in the subdomain 2A binding site, that is, amino acid substitutions, could alter the catalytic rate for 15-keto PGE_2 breakdown to the keto-enol tautomers and ultimately to 15-keto-PGB_2 (Figure 52). Unfortunately, the many amino acid differences between species make it difficult to draw specific structural conclusions about reaction mechanism from the above data.

Our present study was undertaken to obtain insights into the above HSA/prostaglandin interaction by comparing the rate at which specific site-directed mutants of HSA with substitutions in subdomain 2A catalyze the breakdown of 15-keto-PGE_2 to the keto-enol tautomer intermediate and to the final reaction product PGB_2.

CHAPTER 2
EXPRESSION AND CHARACTERIZATION OF RECOMBINANT DOMAIN FRAGMENTS OF HSA

HSA fragments have been of important use in studying the binding sites of ligands on the protein. However, their application was restricted by the cleavage site for the techniques used, e.g. cleavage by chemical agents or by proteases, until the advent of recombinant technique. Currently, recombinant technique and protein expression systems combined with site-directed mutagenesis are among the most powerful tools in structure-function study of proteins. Recombinant fragments can be well designed with natural border based on the primary and tertiary structures of HSA. Compared with the full-length protein molecule, the smaller sized fragments will be more amenable to NMR studies. To facilitate fluorescent spectroscopic study, a tryptophan will be introduced into domain III fragment. The feasibility of using individual domains as stand-alone model proteins for the study of HSA will be tested in this study.

MATERIALS AND METHODS

Synthesis and purification of recombinant fragments of HSA

We used a protocol that was a modification of a previously published technique to express and purify domains I, II and III of HSA (Dockal *et al.* 1999). Each pPIC9-domain I/II/III expression cassette coding for a particular domain fragment plus the alpha mating factor secretion signal sequence was introduced into the yeast species *Pichia Pastoris* by electroporation. A yeast clone which contains the expression cassette stably integrated into the chromosomal DNA was isolated in each case.

To produce domain III/Y411W fragment, tyrosine 411 in domain III was replaced by tryptophan using standard techniques as previously described (Petersen *et al.* 1996, 1997, 2000). Y411 is known to line the binding pocket of site II; substitution of tryptophan for Y411 in HSA showed minimal effect on digoxin binding (Ha CE *et al.*, 1999).

The total genomic DNA from each *Pichia Pastoris* clone used to produce a particular HSA fragment was isolated using standard techniques. The genomic DNA isolated from each clone was used as template to amplify the entire coding region of the fragment by Polymerase Chain Reaction (PCR). For each clone, the entire coding region was sequenced using the dideoxy nucleic acid chain termination technique, and the translation product corresponding to this sequence was found to match a previously published HSA sequence at amino acid positions involved except for the mutation introduced into a particular mutant.

A secreted HSA domain fragment was isolated from growth media as follows. The medium was brought to 50% saturation with ammonium sulfate at room temperature. The temperature was then lowered to 4°C, and the pH was lowered to 4.4, the isoelectric point of HSA (assuming that the each domain has a similar value). The precipitated protein was collected by centrifugation and resuspended in distilled water. Dialysis was carried-out for 72 hours against 100 volumes of phosphate buffered saline (PBS) (137 mM NaCl, 2.7 mM KCl, 4.3 mM Na_2HPO_4, 1.4 mM KH_2PO_4, pH 7.4) with one change of buffer. The solution was loaded onto a column of Cibacron Blue immobilized on Sepharose 6B (Sigma, St. Louis, MO). After the column was washed with 10 bed volumes of PBS, the protein was eluted with 3 M NaCl. The eluent was dialyzed against

PBS and passed over a column of Lipidex-1000 (Packard Instruments) to remove hydrophobic ligands possibly bound to the protein (Glatz and Veerkamp 1983). The resulting protein exhibited only one band on SDS-PAGE. Protein concentrations were determined by the BCA method, a modification of the Lowry procedure in which bicinchoninic acid is substituted for tartrate (Smith *et al.*, 1985).

To examine the cleavage at secretion signal sequence attached to the N-terminal of a fragment, the sample was subjected to N-terminal protein sequencing on an Applied Biosystems, Inc. Model 476A protein sequencer. The first 11 amino acids were determined.

Binding of fluorescent probes to the fragments

When excited at 320 nm, warfarin emits fluorescence with peak intensity at around 380 nm. This fluorescent intensity, or quantum yield, is remarkably enhanced when warfarin is restricted in its internal rotation of the acetobenzyl group. The HSA-bound warfarin shows a 10 to 20 fold enhancement of fluorescence over that of unbound warfarin. This property of warfarin-HSA complex has long been exploited to determine the concentration of HSA-bound warfarin in solution, which is the basis for HSA/warfarin dissociation constant determination by fluorescent techniques.

The method to determine the dissociation constant Kd for warfarin binding to the primary binding site on HSA involves two experiments. The first experiment is devised to measure the fluorescence enhancement of HSA-bound warfarin for the primary binding site. In order to obtain stoichiometric binding of warfarin to HSA, a high-concentration solution of HSA, usually 10 μM, is titrated with warfarin up to a

warfarin/HSA molar ratio about 1/10 with the fluorescence recorded for each addition of warfarin. Under the above-mentioned condition, a linear relationship between fluorescent intensity and total warfarin concentration should be observed indicating stoichiometric binding. The same titration is also done with the HSA solution replaced by a blank, i.e., the same buffer used for the HSA solution. Under condition of stoichiometric binding, linear regression analysis of the data can be performed to calculate the slopes of fluorescence intensity versus warfarin concentration in the presence or absence of HSA. The ratio of two slopes is defined as the fluorescence enhancement. The second experiment involves titration of a low-concentration solution of HSA, usually 1 μM, with warfarin to cover an appropriate range of warfarin bound per HSA molecule, usually up to a total warfarin/HSA mole ratio of 10. As can be shown with ease, the fraction of warfarin bound to HSA over the warfarin added (bound and unbound warfarin), assuming a single binding site on HSA, is determined by the equation:

$$\text{Fraction of warfarin bound} = (F - F_0)/(F_0 (E - 1)) \qquad (1)$$

where F is the fluorescence intensity measured; F_0 is the fluorescence intensity measured for the same total amount of warfarin in the absence of HSA; E is the fluorescence enhancement determined by the first experiment. This equation can be used for each point in the titration if binding occurs only at the primary binding site, which is largely satisfied if the molar ratio of bound warfarin/HSA is less than one.

Dansylsarcosine displays similar fluorescent enhancement upon binding to HSA when excited at 370 nm and monitored at 475 nm. Therefore, similar procedures can be used for dansylsarcosine binding study. The principle is the same for fragment experiments using fluorescent markers.

Displacement of fluorescent probes from the fragments by drugs

To ensure that a fluorescent probe, i.e., warfarin or dansylsarcosine, binds mostly to the primary binding sites in HSA or a fragment, sample solutions containing 1 μM probe and 10 μM HSA or the fragment were used. Solutions containing only the proteins being studied were used as blank. The initial fluorescence of a sample solution was measured before the addition of drugs. A drug was then added to concentrations of 10 μM, 20 μM, 30 μM or 40 μM stepwise, with the fluorescence measured upon each addition of the drug.

Quenching of tryptophan fluorescence

HSA has a single tryptophan residue in domain II, which is located near the entrance of the hydrophobic pocket of site I. In domain III-Y411W, a tryptophan residue was substituted for the original tyrosine residue (Y411) found at a position homologous to that for W214 in domain II. The single tryptophan of HSA has been exploited in many studies on HSA-ligand interactions. The wavelength of maximum fluorescence intensity of tryptophan (340 nm) overlaps with the absorption band of many drugs, so, quenching by Forster energy transfer mechanism is observed in many ligand-HSA complexes. Measurement of the quenching of the single tryptophan residue of HSA has been used to calculate the affinity of ligands for HSA (e.g., Steiner *et al.*, 1966; Sudlow *et al.*, 1973; Levine, 1977).

Collisional fluorescence quenching has also been employed to examine the accessibility of the single tryptophan residue to solute quencher; the acrylamide quenching reaction was shown to be very discriminating in sensing the exposure of

fluorescing tryptophanyl residues in globular proteins (Eftink and Ghiron, 1976). In the present work, acrylamide quenching of the single tryptophan residue of HSA, domain II, and domain III-Y411W was studied in order to compare the difference in the matrix enveloping the tryptophan residue of the respective proteins. To selectively excite the tryptophan residue, a wavelength of 295 nm was used for the excitation and the fluorescence was monitored at 340 nm.

General experimental parameters

Fluorescence intensity measurements were performed with a QM-1 spectrafluorometer (Photon Technologies International). The half-band was set to 2 nm for both excitation and emission. A 10 mm x 4 mm quartz cuvette was used to hold 1 ml of a sample and the temperature was maintained at 25 °C by using a constant temperature circulator. For warfarin fluorescence experiments, samples were excited at 320 nm and emission was monitored at 380 nm; for measurement of dansylsarcosine fluorescence, samples were excited at 370 nm and emission was monitored at 475 nm; for tryptophan fluorescence quenching studies, samples were excited at 295 nm and emission was monitored at 340. In all experiments, inner-filter effect was kept low by careful selection of the upper limits of concentration for both proteins and ligands. The sodium salt of warfarin was directly dissolved in H_2O to make a 10 mM stock solution, which was diluted further to prepare working solutions for titration studies; dansylsarcosine was dissolved in small volume of 0.1N NaOH before it was diluted to prepare a 10 mM stock solution. For measurement of the fluorescence enhancement of HSA-bound warfarin at the primary binding site, a solution of 10 μM HSA, was titrated with warfarin up to a

warfarin/HSA mole ratio about 1/10 with the fluorescence recorded for each addition of warfarin. The titration was repeated with the HSA solution replaced by a blank, i.e., the same buffer used for the HSA solution. For the second experiment, a 1-μM HSA solution, was titrated with warfarin up to a total warfarin/HSA mole ratio of 10. For experiments with dansylsarcosine, the same procedure was used. For the fragments were treated in a similar way as HSA.

Analysis of data

By using equation (1), a set of concentrations of free ligand (i.e., unbound warfarin) and mole ratio of ligand bound/HSA data pair was calculated. The data were fit to single binding site (hyperbola) curve using the following equation:

Mole ratio of ligand bound = Bmax * X / (Kd + X)

where Bmax is the maximum of mole ratio of ligand bound, X is the concentration of the free ligand and Kd is the dissociation constant. Nonlinear regression method of the Prism computer program (GraphPad) was employed. In this study Bmax should be one; however, due to variances in HSA/fragments quantification, Bmax can deviate from unity to some degree. As can be shown, if free ligand concentration and ratio of ligand bound/HSA can be determined correctly, variance in Bmax will not affect Kd value determined.

For acrylamide quenching experiments, the data were analyzed by the Stern-Volmer equation (Lakowicz, 1986):

$$F_0 / F = 1 + K_{sv} [Q]$$

where F_0 is the initial fluorescent intensity, F the fluorescent intensity after the addition of the quencher, in this case, acrylamide, K_{sv}, the Stern-Volmer constant for collisional quenching process, and [Q] the concentration of the quencher. Linear regression method of the Prism computer program (GraphPad) was employed.

RESULTS

Expression of domain fragments and tuning of the N-terminal

When constructing a yeast expression system for a cloned sequence of a protein, in particular, for a system that will secrete the product into the media, a signal peptide sequence is usually added upstream of the target sequence. An expression system that has the expressed protein secreted directly into the culture media facilitates purification of the product greatly. The commonly used signal sequence is that of the alpha mating factor of yeast *Saccharomyces cerevisiae*. The secretion signal sequence of the alpha mating factor is shown along with the native secretion signal sequence of HSA in Figure 3. To facilitate the construction of the expression construct, the introduction of specific endonuclease recognition sequences, i.e. enzyme cutting sites into the construct is a common practice and in some cases is inevitable. This gives rise to extra or changed amino acid residues. Generally, the added residues have minimal effects on the global structure of the protein of interest. Dockal et *al.* (1999) studied the UV-CD and drug-induced CD using fragments of the three individual domain of HSA with extra Glu-Phe residues at the N-terminal and found that the fragments were similar to the whole HSA in many characteristics and much of the binding capability was retained in these fragments.

Initially, the natural boundaries between the domains as defined by Dockal *et al.* (1999), were adopted with domain I encompassing 1-197, domain II 189-385 and domain III 381-585. Sequencing results of eleven amino acid residues at the N-terminal of each domain initially constructed in the present work showed variable cleavage at the juncture of signal peptide and target sequence. By examining several constructs containing the secretion signal sequence, we observed that splicing the signal peptide with arbitrary fragments of protein often does not provide the cleavage site required for the correct processing of the signal peptide. The correct cleavage seems to demand some constraints on the sequence linked to the signal peptide sequence. For example, when using the initially designed primers IF/IR, IIF/IIR and IIIF/IIIR (Figure 4), whereas domain I construct yielded the expected product, the product of domain III construct lost one more residue (valine in this case) than expected. The product of domain II construct lost six residues, which could partly account for the observed reduction in the binding constants for some ligands in our preliminary studies (Figure 3). To minimize the perturbation of the domain structure caused by truncation and loss of important amino acid residues or introduction of extra amino acid residues, the constructs were re-designed. Briefly, three new 5' primers, F1N, F2N and F3N, were designed, in which the region encoding the four downstream residues, i.e., Glu Ala Glu Ala, at the cleavage site were removed from the 5' primers (Figure 4). The three modified construct were introduced into yeast hosts; however, the expression products failed to be secreted into the media (data not shown). In a renewed effort, the following strategy was adopted in designing the primers for domains I and II. The new domain I construct used the native signal peptide of HSA, which was confirmed to result in correct cleavage by this laboratory. Since domain III

products only lacked one valine residue at the N-terminal compared to the one initially expected, no new construct for domain III was attempted. Four new 5' primers were designed with possibly favorable patterns of sequence around the cleavage site (Figure 5). The products of these redesigned constructs were subject to N-terminal sequencing to find the optimal constructs. One primer, IIF187, resulted in an efficient cleavage of the signal peptide and the N-terminal exposed at position 187 of HSA, two residues ahead of position 189, which was taken as the N-terminal for domain II fragment by Dockal *et al.* (1999). In their work, two extra foreign or non-native residues, Glu-Phe, were attached to the natural sequence starting at position 189 in the final product, which might increase the ellipticity for CD below 265 nm making the interpretation of CD data more difficult. The other three primers all resulted in heterogeneous cleavage shown in SDS-PAGE as doublet band (Figure 6).

The determination of the optimal construct design at the N-terminal will also make the construction of Domain I-II and Domain II-III straightforward, which will allow more studies to be attempted.

The purified products of domains I (using the natural signal sequence of HSA), II (using primer IIF187) and III by Cibacron Blue column were analyzed by SDS-PAGE (Figure 7). The apparent sizes were, within the accuracy of SDS-PAGE, in agreement with the calculated molecular weight of about 23 kD.

Human serum albumin
(Prepro)
Met Lys Trp Val Thr Phe Ile Ser Leu Leu Phe Leu Phe Ser Ser
(mature)
Ala Tyr Ser Arg Gly Val Phe Arg Arg ^* Asp Ala His Lys ...

α-Factor in pPIC9 vector (for domain I, II and III)

Met Arg Phe Pro Ser Ile Phe Thr Ala Val Leu Phe Ala Ala Ser

Ser Ala Leu Ala Ala Pro Val Asn Thr Thr Thr Glu Asp Glu Thr

Ala Gln Ile Pro Ala Glu Ala Val Ile Gly Tyr Ser Asp Leu Glu

Gly Asp Phe Asp Val Ala Val Leu Pro Phe Ser Asn Ser Thr Asn

Asn Gly Leu Leu Phe Ile Asn Thr Thr Ile Ala Ser Ile Ala Ala

Lys Glu Glu Gly Val Ser Leu Glu Lys Arg ^ Glu Ala Glu Ala ...

Domain I
... **Leu Glu Lys Arg ^* Glu Ala Glu Ala** Asp Ala His Lys Ser ...

Domain II
... **Leu Glu Lys Arg ^ Glu Ala Glu Ala** Gly Lys Ala Ser Ser Ala Lys * Gln Arg Leu Lys Cys ...

Domain III
... **Leu Glu Lys Arg ^ Glu Ala Glu Ala** Val * Glu Glu Pro Gln Asn Leu Ile Lys ...

Figure 3. Influence of down-stream sequence context around the supposed cleavage site of Lex2 on the cleavage as determined by N-terminal sequencing. ^, supposed cutting site; *, cutting revealed by N-terminal sequencing of the expressed proteins. The underlined residues are, according to the manual for pPIC9 vector (Invitrogen), required for correct processing of the leader sequence.

IF, 49mer
GTA TCT CTC GAG AAA AGA GAG GCT GAA GCT GAT GCA CAC AAG AGT GAG G

IR, 38mer
GCG GTG AGC GAA TTC TTA TCT CTG TTT GGC AGA CGA AG

IIF, 54mer
GTA TCT CTC GAG AAA AGA GAG GCT GAA GCT GGG AAG GCT TCG TCT GCC AAA CAG

IIR, 39mer
GCG GTG AGC GAA TTC TTA CTG AGG CTC TTC CAC AAG AGG

IIIF, 54mer
GTA TCT CTC GAG AAA AGA GAG GCT GAA GCT GTG GAA GAG CCT CAG AAT TTA ATC

IIIR, 38mer
GCG GTG AGC GAA TTC TTA TAA GCC TAA GGC AGC TTG AC

F1N, 37mer
GTA TCT CTC GAG AAA AGA GAT GCA CAC AAG AGT GAG G

F2N, 42mer
GTA TCT CTC GAG AAA AGA GGG AAG GCT TCG TCT GCC AAA CAG

F3N, 42mer
GTA TCT CTC GAG AAA AGA GTG GAA GAG CCT CAG AAT TTA ATC

Figure 4. Initially used primer pairs for domains I, II and III, and the modified 5' primers. IF/IR, IIF/IIR and IIIF/IIIR, the initial primer pairs for domains I, II and III, respectively, with which the Leu Glu Lys Arg ^ Glu Ala Glu Ala site was restored during cloning. F1N, F2N and F3N, the modified 5' primers for domains I, II and III, respectively, in which the region encoding the four downstream residues, i.e., Glu Ala Glu Ala , at the cleavage site were removed from the 5' primers.

IIF183, 50mer

```
GTA TCT CTC GAG AAA AGA GAG GCT GAA GCT GAT GAA CTT CGG
      … Leu Glu Lys Arg Glu Ala Glu Ala Asp Glu Leu Arg


GAT GAA GG
Asp Glu Gly …
```

IIF184, 51mer

```
GTA TCT CTC GAG AAA AGA GAG GCT GAA GCT GAA CTT CGG GAT
      … Leu Glu Lys Arg Glu Ala Glu Ala Glu Leu Arg Asp

GAA GGG AAG
Glu Gly Lys …
```

IIF187, 52mer

```
GTA TCT CTC GAG AAA AGA GAG GCT GAA GCT GAT GAA GGG AAG
      … Leu Glu Lys Arg Glu Ala Glu Ala*Asp Glu Gly Lys

GCT TCG TCT G
Ala Ser Ser …
```

IIF188, 49mer

```
GTA TCT CTC GAG AAA AGA GAG GCT GAA GCT GAA GGG AAG GCT
      … Leu Glu Lys Arg Glu Ala Glu Ala Glu Gly Lys Ala

TCG TCT G
Ser Ser Ala …
```

Figure 5. Re-designed 5' primer for domains II. The underlined residues are, according to the manual for pPic9 vector (Invitrogen), required for correct processing of the leader sequence. Product of the construct using IIF187 as 5' primer resulted in a single cleavage at the C-end of the signal sequence, which is indicated by symbol * .

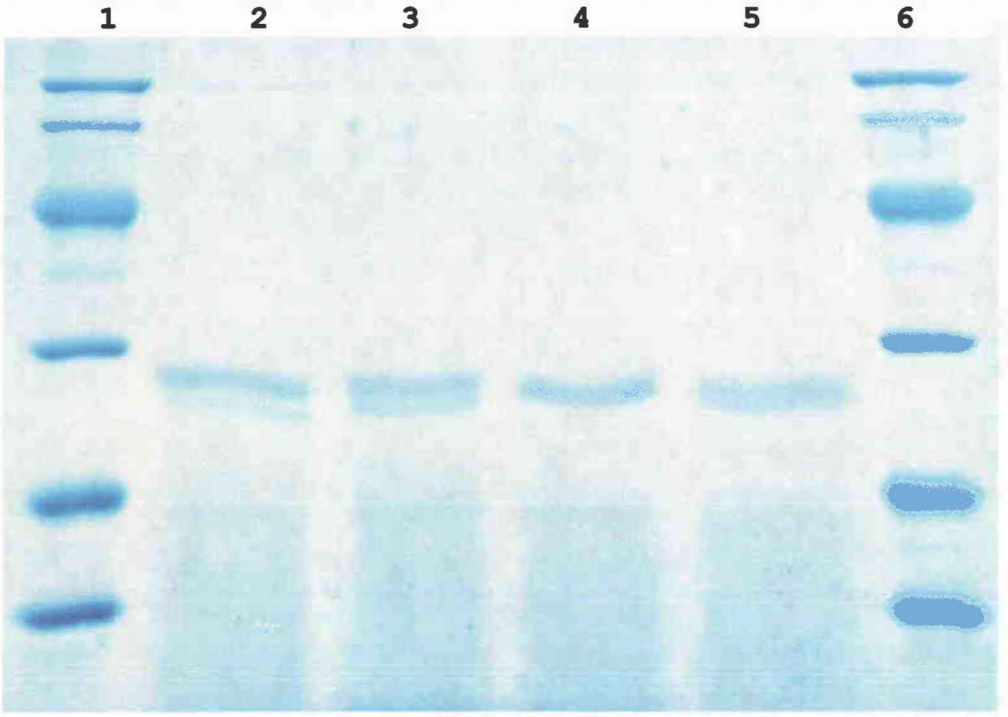

Figure 6. SDS-PAGE of expression products of domain II showing the effect of down-stream sequence context around the supposed cleavage site of Lex2 on the cleavage. Lane 1 and Lane 6, BioRad Low-range molecular weight protein marker; lane 2, 3, 4 and 5 expression products corresponding to primer IIF183, primer IIF184, primer IIF187 and primer IIF188, respectively.

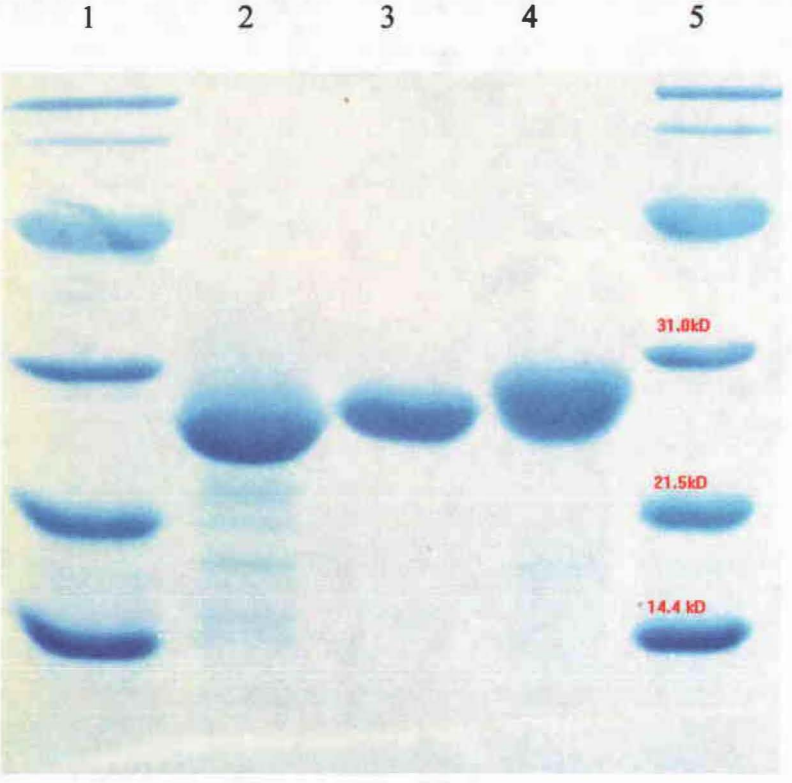

Figure 7. SDS-PAGE of the expression products of domains I, II and III. Lane 1 and Lane 5, BioRad Low-range molecular weight protein marker; lane 2, 3, and 4, domain fragments I, II and III.

Binding of fluorescent probes to the fragments

Due to their well-known specific binding for HSA and high quantum yield of fluorescence when bound to HSA, warfarin and dansylsarcosine (Figure 8) were used to probe the properties of the fragment and HSA in a comparative way. Also, the structures of some commonly used drugs in HSA studies as well as that of a heme metabolite, bilirubin, are shown in Figure 9. The fluorescence emission spectra of warfarin and dansylsarcosine (1 μM) bound to HSA and the domain fragments (10 μM) are shown in Figures 10 and 11, respectively. When bound to HSA and domain II, warfarin exhibited strong fluorescence. Under the conditions used, warfarin bound to HSA approximately in a stoichiometric way. The reduction in the fluorescence for domain II was likely caused by both decrease in the fluorescent enhancement and reduction in the fraction of warfarin bound. As can be seen later from the results of other experiments, the amount of domain II fragment appeared consistently overestimated by BCA protein assay. Because BCA protein assay uses BSA as a reference, it is expected that the whole HSA, due to its high homology to BSA, can be quantified accurately whereas other proteins may be underestimated or overestimated (Smith *et al.*, 1985). So, the true difference between HSA and domain II with respect to warfarin binding may be smaller than what Figure 10 suggested. Domain III displayed a fluorescent signal not much higher than free warfarin, which is known be about one tenth of the intensity of warfarin-HSA complex. Domain III-Y411W showed some weak binding of warfarin. Compared with HSA, the fragments red-shifted a little the fluorescent emission suggestive of less hydrophobic interaction with warfarin. For dansylsarcosine, similar to the results for warfarin, the fragments red-shifted the fluorescence when compared with rHSA. Domain III-Y411W exhibited the

same amount of fluorescence intensity as HSA while domain III had only about half of the intensity of HSA. Domain II had appreciable binding for dansylsarcosine in view of the much lower fluorescence emission of dansylsarcosine in the unbound state than warfarin.

The dissociation constants of rHSA and domain II for warfarin binding were determined using fluorescent techniques. Fractional saturation curves of wild type recombinant HSA (rHSA) and domain II (Dom II) with warfarin are shown in Figure 12. The curves were fitted to the data using nonlinear regression method of the Prism computer program (GraphPad). The samples were in PBS buffer with pH 7.4. Domain II had a slightly reduced affinity for warfarin than rHSA (4 μM versus 2.3 μM). The dissociation constants of HSA and domain III for dansylsarcosine were determined in a similar way (Figure 13). Domain III had 3-4 fold reduced affinity for dansylsarcosine than HSA (7 μM versus 2.2 μM). The dissociation constants determined for rHSA here compared favorably with the published values for HSA.

The results were consistent with the current knowledge about sites I and II of HSA, suggesting that the fragments retain much of their properties with respect to the binding of the two classical fluorescent markers. The recombinant HSA appeared identical to the natural HSA from human in drug binding behaviors.

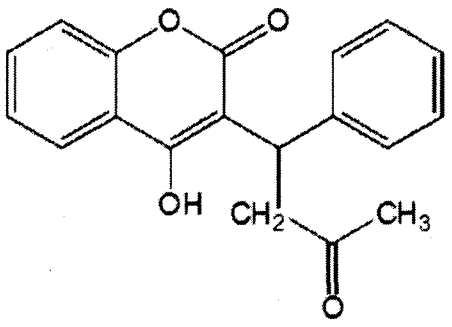

Warfarin

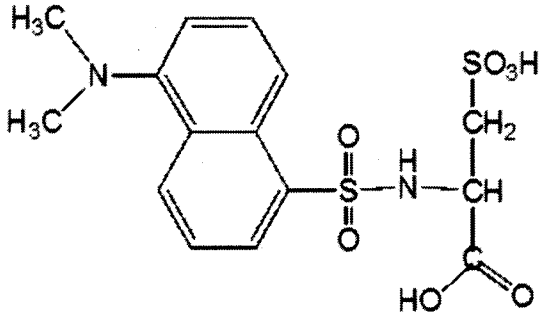

Dansylsarcosine

Figure 8. Structural representation of warfarin and dansylsarcosine.

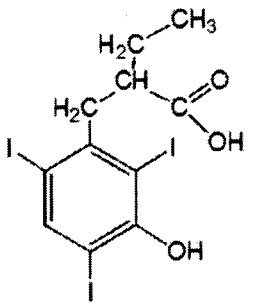

Iophenoxic acid

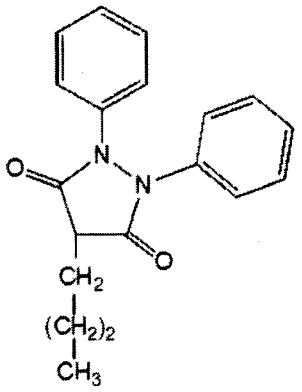

Phenylbutazone

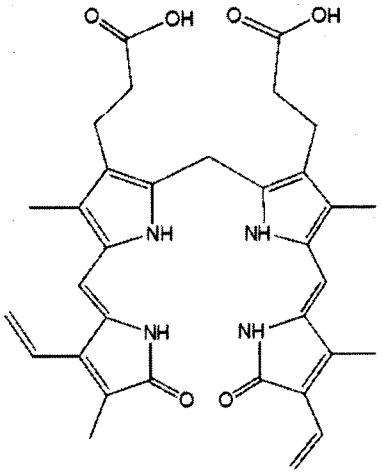

Bilirubin

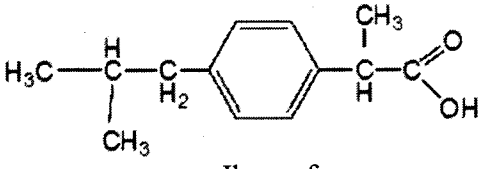

Ibuprofen

Figure 9. Structural representation of iophenoxic acid, phenylbutazone, bilirubin and ibuprofen.

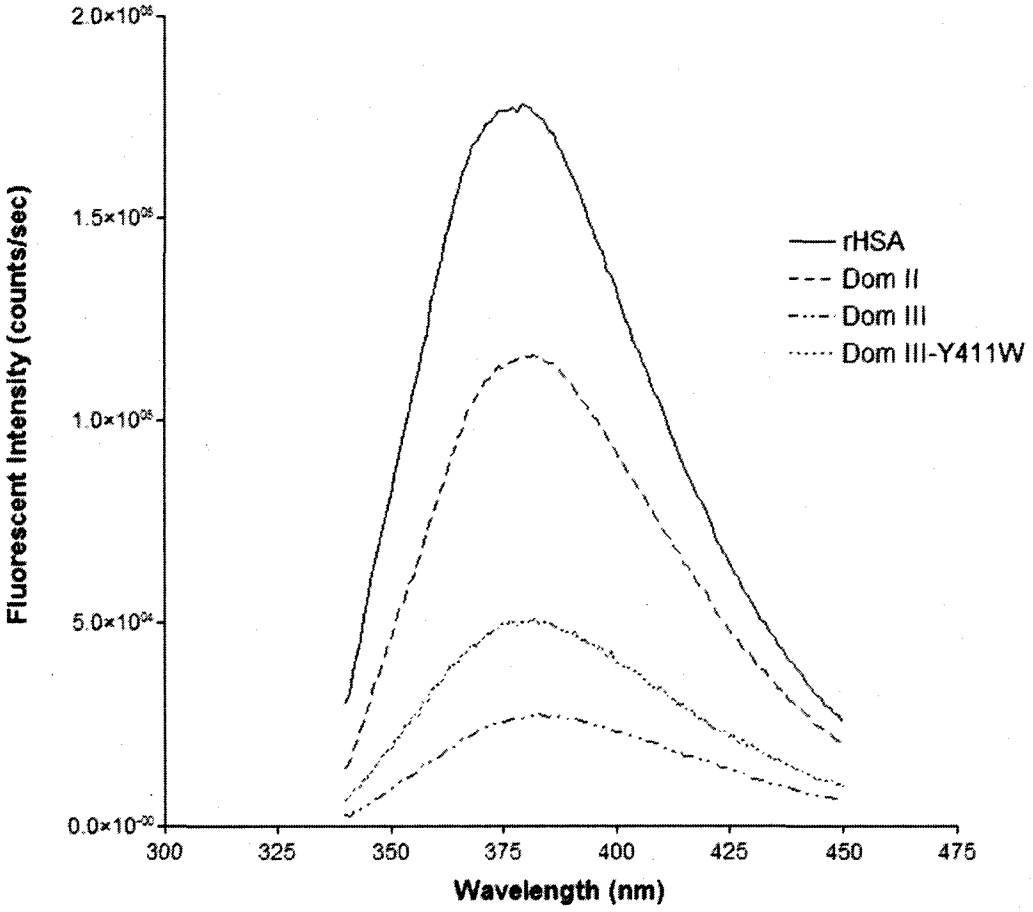

Figure 10. Fluorescence emission spectra of warfarin (1 μM) bound to wild type recombinant HSA (rHSA) and the domain fragments (10 μM). The excitation wavelength was 320 nm.

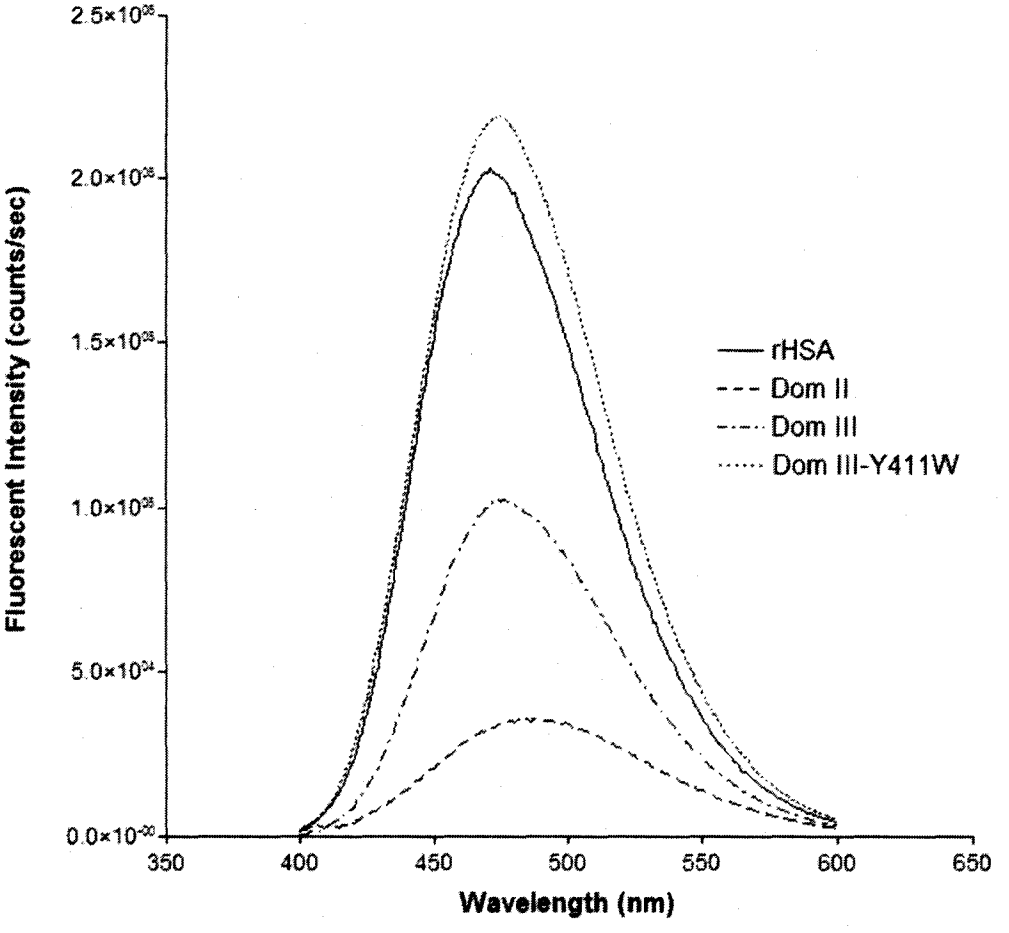

Figure 11. Fluorescence emission spectra of dansylsarcosine bound to rHSA and the domain fragments. The excitation wavelength was 370 nm.

Displacement of fluorescent probes from the fragments by drugs

Sudlow *et al.* (1975, 1976) validated the use of fluorescent probes in the drug displacement studies. By comparing the results obtained by monitoring fluorescence changes with the results obtained by equilibrium dialysis, it was concluded the changes in fluorescence is largely caused by the displacement of the fluorescence probes and that the changes in fluorescence quantum yield do not contribute significantly to changes in fluorescence intensity.

Drug-induced changes in fluorescence of warfarin bound to rHSA are shown in Figure 14. Site I specific drugs, phenylbutazone and iophenoxic acid, and site II specific drug ibuprofen were used in the displacement experiments. Though not a drug, bilirubin, the most studied ligand for HSA, was also included in the experiments. It is documented that phenylbutazone and iophenoxic bind to site I of HSA with dissociation constants of 1.4 μM and 0.012 μM, respectively; ibuprofen binds to site II of HSA with a dissociation constant of 0.37 μM (Peters, 1996). Due to the technical difficulties in quantifying the high affinity of bilirubin for site I, the published values for its dissociation constant vary considerably, often more than 10 fold; the "most probable value" is about 0.01 μM.

Essentially, iophenoxate was the most effective in reducing the fluorescence of warfarin-rHSA. At ligand to rHSA molar ratio of 4:1, bilirubin was the most effective; which, however, was probably caused by the inner-filter effect of the high concentration bilirubin. Also, at ligand to rHSA molar ratio of 1:1, bilirubin appeared to be not as effective as its dissociation constant suggests, which was presumably attributed to the decrease in true concentration due to the high instability of bilirubin under the experimental conditions. Phenylbutazone decreased the fluorescence in agreement with

its known Kd. In good agreement with Sudlow *et al.* (1976), ibuprofen first enhanced the fluorescence to about 10 % at 1:1 molar ratio and then reduced the fluorescence slightly in an approximately linear way. Ibuprofen binds specifically to site II of HSA with high affinity and the binding induces a conformational change that enhances the quantum yield of fluorescent probes (Sudlow *et al.*, 1976). Upon saturation of the primary binding site at site II, further addition of ibuprofen might cause weak competition with warfarin at site I.

Similar observation of changes in the fluorescence of domain II-warfarin complex was made. However, there were subtleties worthy of examination. Phenylbutazone seemed to be more effective in reducing fluorescence of domain II-warfarin suggesting that the relative affinity of phenylbutazone over warfarin for domain II was enhanced. An alternative explanation could be that rHSA has more secondary binding sites than the domain II fragment to buffer the competition. Ibuprofen decreased the fluorescence slightly in a linear way without any lag like that for rHSA. Because of the absence of site II or domain III, the above-mentioned quantum yield enhancing conformational change was missing. The fluorescence lowering by ibuprofen was more apparent than for rHSA suggesting that ibuprofen has slightly enhanced affinity for domain II or the absence of secondary binding sites in domain II fragment to buffer the competition. The displacement profiles for rHSA and domain II by bilirubin were very similar suggesting similar binding affinity for bilirubin in both cases. Kd determination for bilirubin, though liable to system errors, appeared supportive of this suggestion (data not shown).

Drug displacement results for dansylsarcosine-rHSA, dansylsarcosine-domain III and dansylsarcosine-domain III-Y411W are shown in Figures 16, 17 and 18, respectively. As expected, ibuprofen reduced the fluorescence substantially and to similar extent for all

three proteins. It is not clear whether changes in affinity or removal of secondary binding sites has a role in the cases of domain III and domain III-Y411W. For dansylsarcosine-rHSA, the displacement by phenylbutazone displayed a lag at 1:1 molar ratio, suggesting the saturation of phenylbutazone at site I of rHSA. The displacement by iophenoxic acid showed a lag at 3:1 molar ratio, suggesting saturation of three sites in rHSA before an increased displacement occurred. For dansylsarcosine-domain III, displacement by phenylbutazone did not show a lag at 1:1 molar ratio, and the reduction in fluorescence was more apparent than for rHSA, suggesting either adjustments of domain III structure to allow for better binding of this drug or effects of losing of secondary binding sites. The increase in displacement was most dramatic for iophenoxic so that it almost superimposed the profile for ibuprofen. This could be partly accounted for by the extremely high affinity of iophenoxate for HSA and by the existence of three iophenoxate binding site in HSA (Fehske and Muller, 1978). Since the effect of iophenoxate on dansylsarcosine-domain III-Y411W complex was not as dramatic, the structural perturbation in domain III favoring iophenoxate binding might be the major cause of the effect of iophenoxate on dansylsarcosine-domain III.

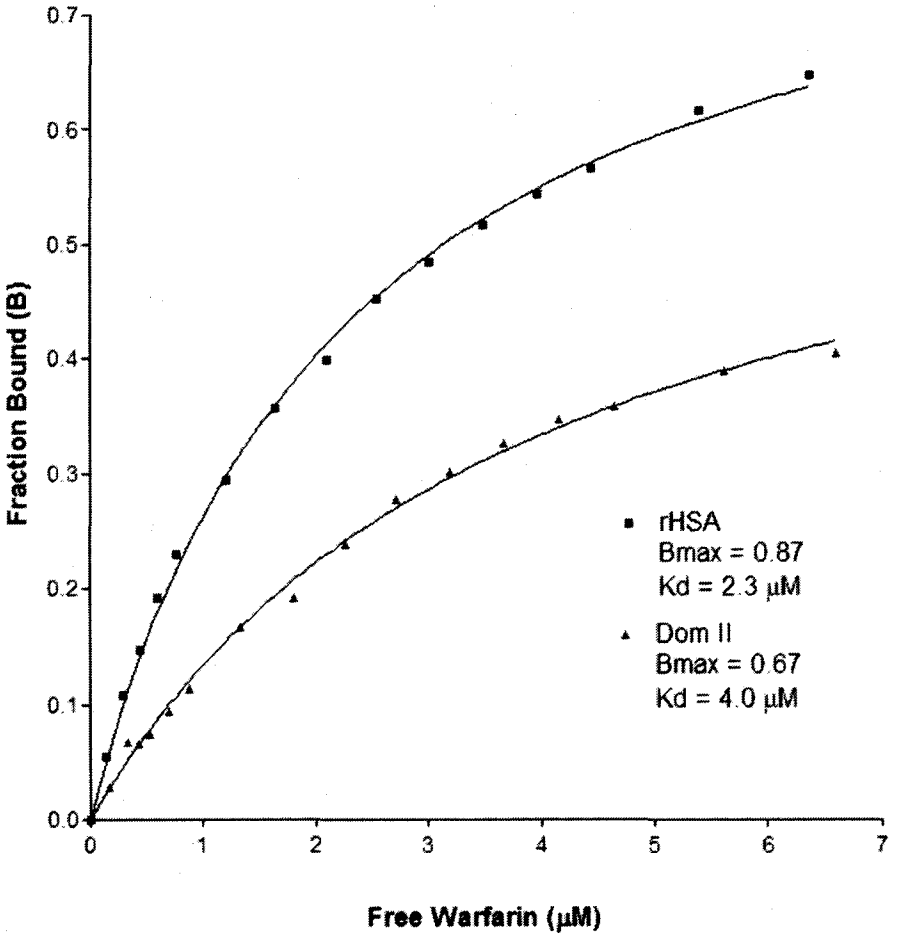

Figure 12. Saturation of rHSA and domain II (Dom II) with warfarin. The curves were fitted to the data using nonlinear regression method of the Prism computer program (GraphPad). The samples were in PBS buffer, pH 7.4.

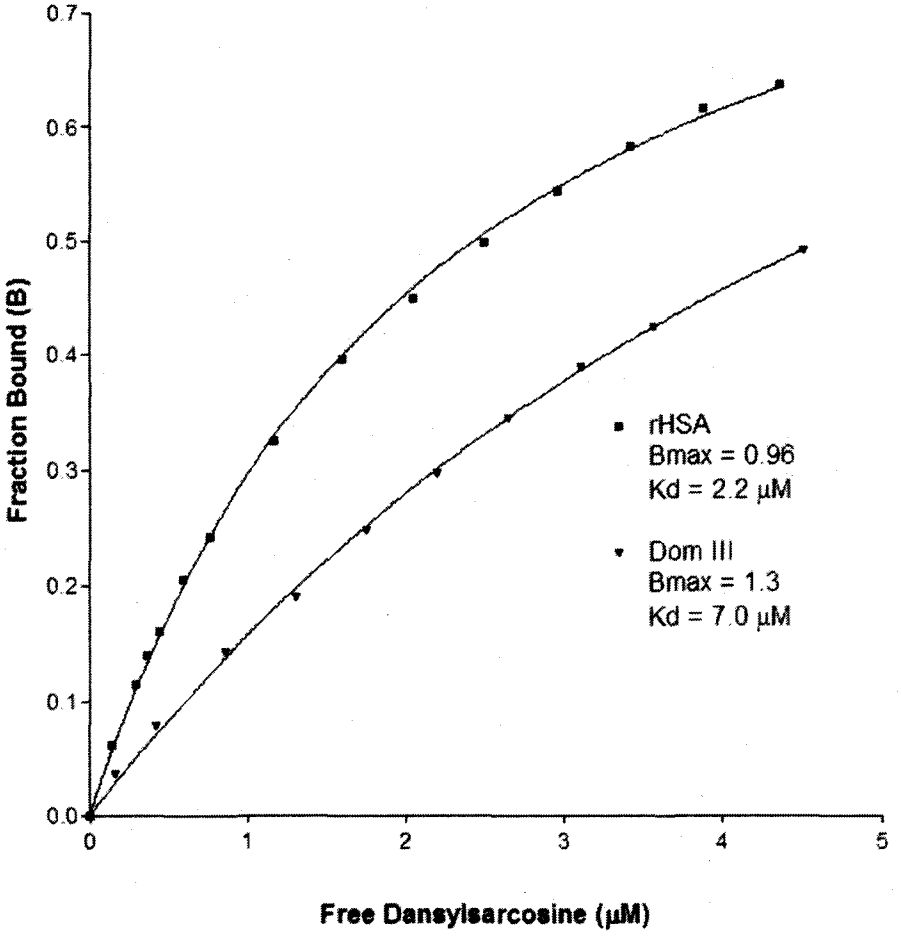

Figure 13. Saturation of rHSA and domain III (Dom III) with dansylsarcosine. The curves were fit to the data using nonlinear regression method of the Prism computer program (GraphPad). The samples were contained in PBS buffer, pH 7.4.

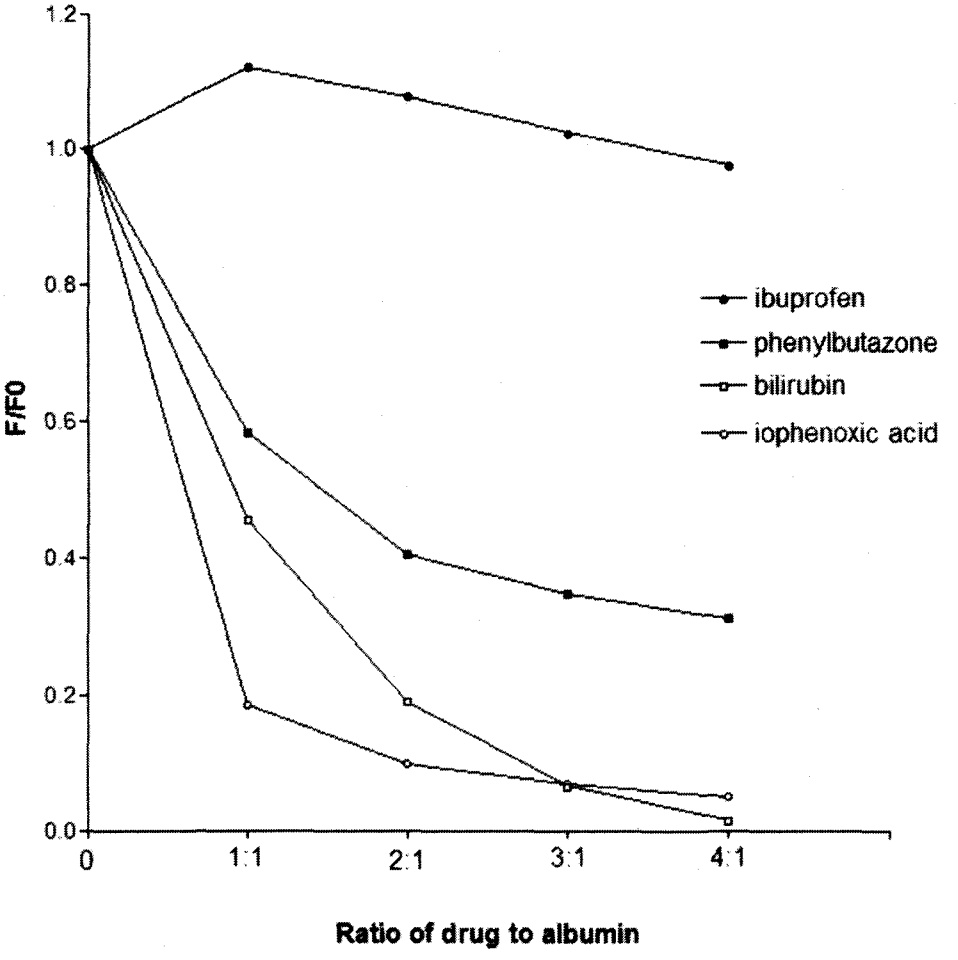

Figure 14. Drug-induced changes in the fluorescence of warfarin bound to rHSA. The samples were in PBS buffer, pH 7.4. To ensure the fluorescent probe, i.e., warfarin, binds mostly to the primary binding site in rHSA, sample solutions containing 1 μM probe and 10 μM rHSA were used. Solutions containing only rHSA was used as blank. The initial fluorescence of a sample solution (F_0) was measured before the addition of drugs. A drug was then added to concentrations of 10 μM, 20 μM, 30 μM or 40 μM stepwise, with the fluorescence measured (F) upon each addition of the drug. Fluorescence was measured at 380 nm with excitation at 320 nm. Though not a drug, Bilirubin, the most studied ligand for HSA, was also included in the experiments.

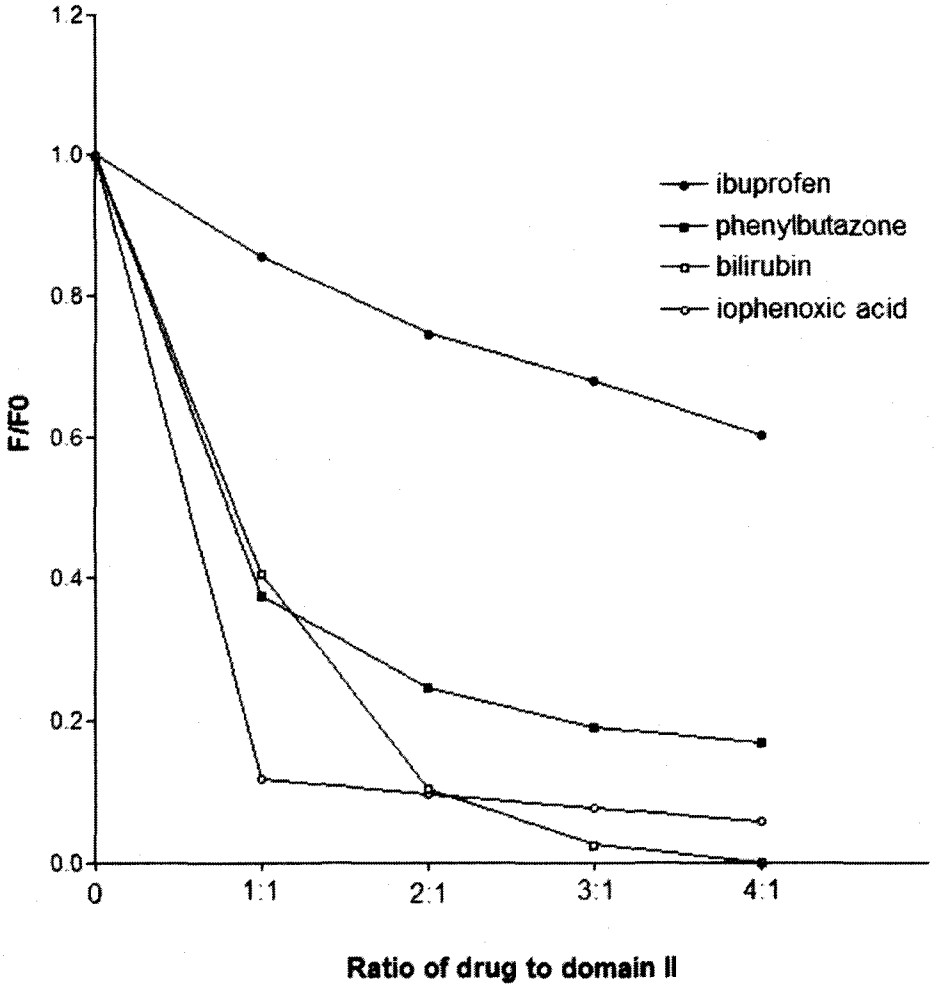

Figure 15. Drug-induced changes in the fluorescence of warfarin bound to domain II. The samples were in PBS buffer, pH 7.4. To ensure the fluorescent probe, i.e., warfarin, binds mostly to the primary binding site in domain II, sample solutions containing 1 μM probe and 10 μM domain II were used. Solutions containing only domain II was used as blank. The initial fluorescence of a sample solution (F_0) was measured before the addition of drugs. A drug was then added to concentrations of 10 μM, 20 μM, 30 μM or 40 μM stepwise, with the fluorescence measured (F) upon each addition of the drug. Fluorescence was measured at 380 nm with excitation at 320 nm.
Though not a drug, Bilirubin, the most studied ligand for HSA, was also included in the experiments.

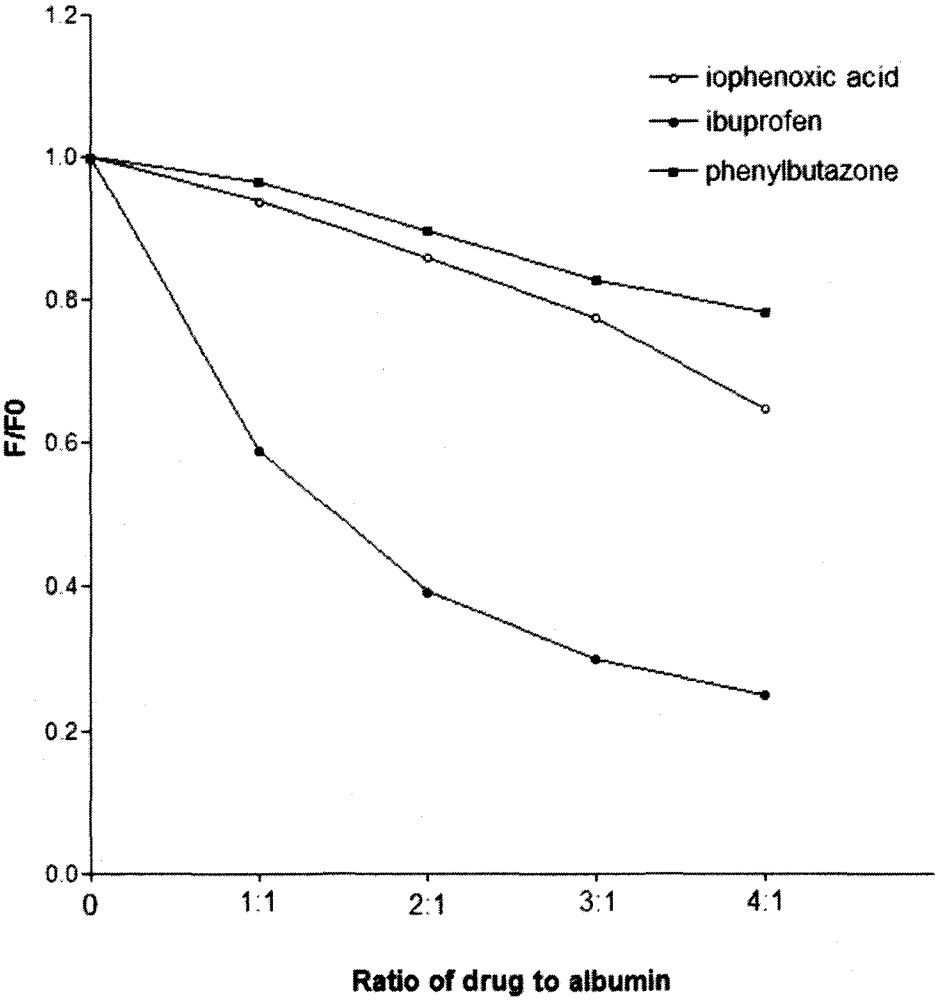

Figure 16. Drug-induced changes in the fluorescence of dansylsarcosine bound to rHSA. The samples were in PBS buffer with pH 7.4. To ensure the fluorescent probe, i.e., dansylsarcosine, binds mostly to the primary binding site in rHSA, sample solutions containing 1 μM probe and 10 μM rHSA were used. Solution containing only HSA was used as blank. The initial fluorescence of a sample solution (F_0) was measured before the addition of drugs. A drug was then added to concentrations of 10 μM, 20 μM, 30 μM or 40 μM stepwise, with the fluorescence measured (F) upon each addition of the drug. Fluorescence was measured at 475 nm with excitation at 370 nm.

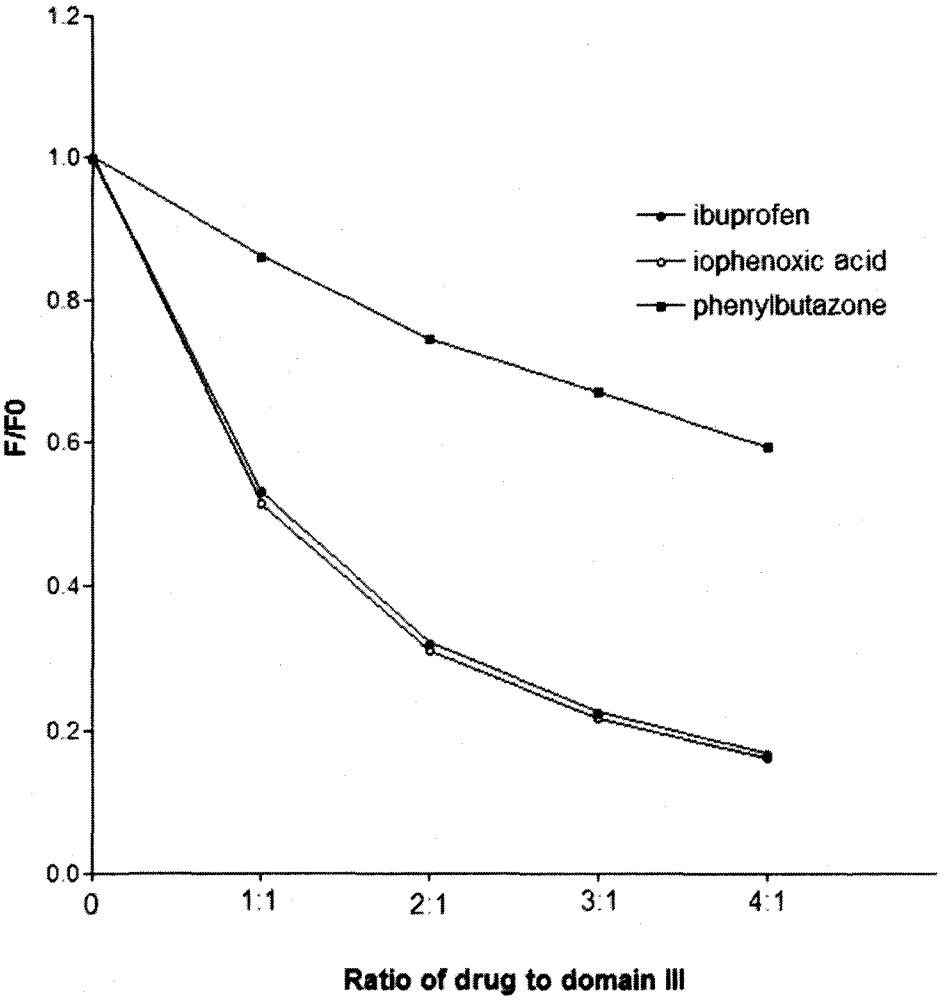

Figure 17. Drug-induced changes in the fluorescence of dansylsarcosine bound to domain III. The samples were in PBS buffer with pH 7.4. To ensure the fluorescent probe, i.e., dansylsarcosine, binds mostly to the primary binding site in domain III, sample solutions containing 1 μM probe and 10 μM domain III were used. Solution containing only domain III was used as blank. The initial fluorescence of a sample solution (F_0) was measured before the addition of drugs. A drug was then added to concentrations of 10 μM, 20 μM, 30 μM or 40 μM stepwise, with the fluorescence measured (F) upon each addition of the drug. Fluorescence was measured at 475 nm with excitation at 370 nm.

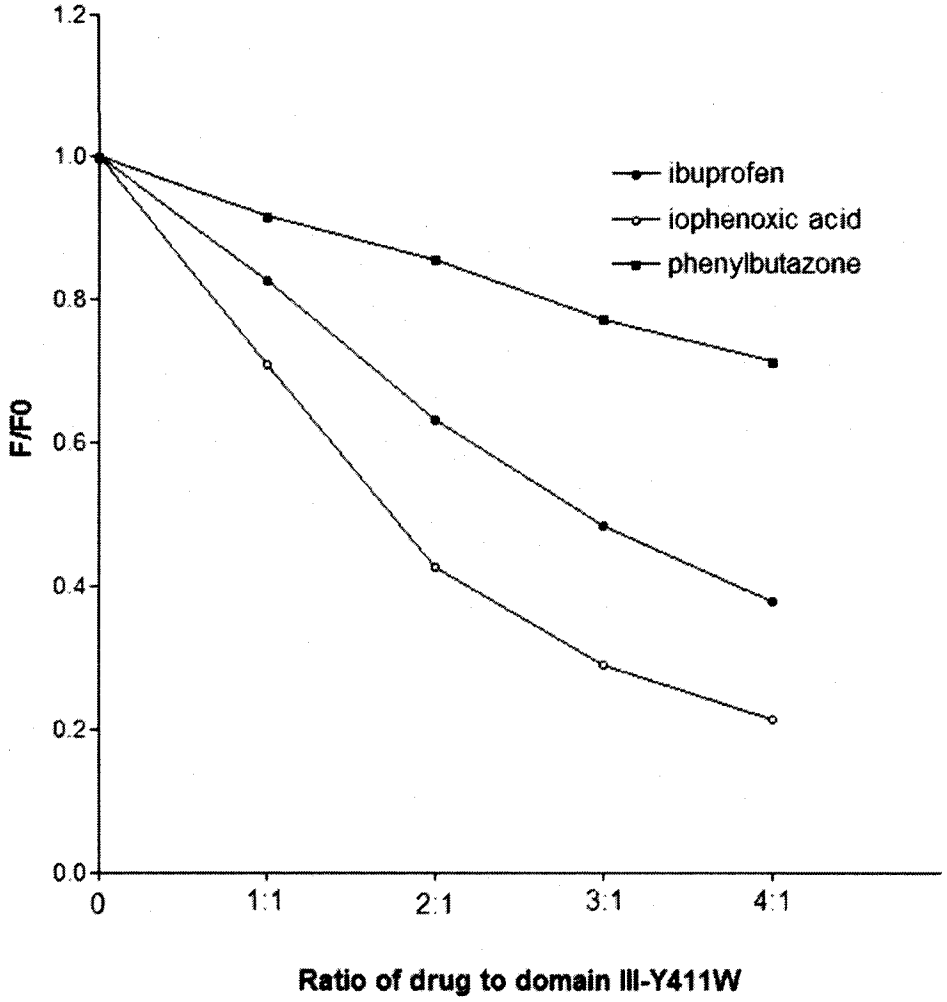

Figure 18. Drug-induced changes in the fluorescence of dansylsarcosine bound to domain III-Y411W. The samples were in PBS buffer with pH 7.4. To ensure the fluorescent probe, i.e., dansylsarcosine, binds mostly to the primary binding site in domain III-Y411W, sample solutions containing 1 μM probe and 10 μM domain III-Y411W were used. Solutions containing only domain III-Y411W was used as blank. The initial fluorescence of a sample solution (F_0) was measured before the addition of drugs. A drug was then added to concentrations of 10 μM, 20 μM, 30 μM or 40 μM stepwise, with the fluorescence measured (F) upon each addition of the drug. Fluorescence was measured at 475 nm with excitation at 370 nm.

Quenching of tryptophan fluorescence

Quenching of tryptophanyl fluorescence of rHSA, domain II and domain III-Y411W by iophenoxate is shown in Figure 19. Samples (1 μM) were titrated with iophenoxic acid. Fluorescence was measured at 340 nm with excitation at 295 nm.

In agreement with the results of fluorescent probe displacement by iophenoxic acids as well as the published dissociation constant for HSA, the tryptophanyl fluorescence of rHSA was almost linearly quenched by iophenoxate up to a molar ratio of 1:1 suggesting approximate stoichiometric binding of iophenoxate to rHSA. Domain II behaved similarly. The curve observed for Domain III-Y411W suggested that iophenoxate was bound more weakly by Domain III-Y411W.

Fluorescence spectra of rHSA, domain II and domain III-Y411W with excitation at 295 nm are shown in Figure 20. Compared with rHSA, domain II and domain III-Y411W exhibited reduced fluorescence. Since the amount of domain II was suspected to be overestimated by BCA assay, the fluorescence might be higher than Figure 20 indicated. Domain II showed a small blue-shift while domain III-Y411W blue-shifted the emission maximum to 330 nm. This suggests that among the three proteins, the environment around the single tryptophan residue is the most hydrophobic in domain III-Y411W and the least in rHSA.

Consistent with the observed blue-shift in emission maximum, the acrylamide collisional quenching studies gave the K_{sv}, the Stern-Volmer constant as follows: 9.6, 6.2 and 2.6 M^{-1}, respectively for rHSA, domain II and domain III-Y411W.

The results suggests that the tryptophan residue is most accessible to solute quenching in rHSA, less accessible in domain II and least accessible in domain III-

Y411W. So, there are some changes in the local structure enveloping the single tryptophan residue. The difference in the tryptophanyl accessibility may also reflect the inherent difference in the environments around W214 of rHSA and W411 of domain III-Y411W.

DISCUSSION

Fragments have been of important use in dissecting the array of ligand binding site on HSA. In this work, domain fragments with well-defined boundaries were expressed in *Pichia pastoris* expression system. CD data indicated that the domain fragments retained a similar α-helical content as HSA (data not shown). They retained many of the structural characteristics found in the domains inside the context of the whole HSA molecule. The single tryptophan residue substituted for tyrosine at position 411 of domain III exhibited fluorescence quenching when a quenching ligand was bound to domain III-Y411W, which may facilitate the use of this fragment as a surrogate protein in many studies. In general, the displacement of fluorescent markers bound to a specific site on the fragments by drugs showed similar behavior as expected for the corresponding domain in the intact HSA. For example, site I specific ligands such as bilirubin, iophenoxate, phenylbutazone and warfarin, bind to domain II fragment with affinity comparable with that for intact HSA. Domain III and Domain III-Y411W fragments bind site II specific ligands, such as ibuprofen and dansylsarcosine, as expected. Due to the lack of inter-domain interactions, small to moderate structural changes were observed in some case when monitored by a certain method, which is in agreement with previous studies (Dockal *et al.*, 1999; Liu *et al.*, 2004). By means of acrylamide quenching, it was

found that the tryptophan residue is most accessible to solute quenching in rHSA, less accessible in domain II and least accessible in domain III-Y411W. The results were consistent with the current consensus on the properties of site I and site II (Kragh-Hansen *et al.*, 2002). Site I appears large, enough to habor a ligand as big as bilirubin, flexible and to have many individual ligand-binding subsites that are independent of each other in some cases and interact with each other in other cases. Site II seems smaller and less flexible (data not shown).

One important observation in this work is the effect of the sequence flanking the C-terminal of the α-factor secretion signal sequence (i.e., signal peptide) on the cleavage of the signal peptide. Though the study of sequence patterns as well as functions of the signal peptide is an active field, much attention has been directed to the signal sequence *per se* and the influence of downstream flanking sequence on the cleavage is rarely documented. However, the designing of an efficient cleavage site for a protein that does not have a natural signal sequence, such as domains II and III, is of practical significance, because a secreted protein is usually folded properly and produced in high yield facilitating its purification. It was found in this work that in most cases, an arbitrary N-terminal sequence spliced with a recommended signal sequence will lead to cleavage at a site shifted into the N-terminal region, multiple cleavage resulting in a heterogeneous population, or a complete failure to secret into the media, which was probably the cause of the failure to express domain II by Kjeldsen *et al.* (1998). By comparing the flanking sequences and the cleavage patterns of several expression constructs in the present work, a preliminary rule for designing an efficient cleavage site for *Pichia pastoris* expression system can be proposed as follows. When using the recommended α-factor signal

sequence ...Leu Glu Lys Arg Glu Ala Glu Ala, to effect an efficient cleavage, two requirements should be met: (1) the N-terminal, i.e., position 1 of the final product to be exposed by cleavage should start with Asp, Glu or Gln; (2) the residue three or seven residue downstream, i.e., position 4 or 8 of the final product should be Lys. An important role Leu Glu Lys Arg Glu Ala Glu Ala seems to provide positive charges since the signal sequence for HSA is ... Arg Arg Asp Ala His Lys, which is efficiently processed by the *Pichia pastoris* expression system. The results of four constructs as well as the processing of the natural HSA fit this rule perfectly (Figures 3, 5 and 6). It appears an α-helix secondary structure may be involved in the signal peptide processing as the requirement for Lys at position 4 or 8 suggests. This periodicity agrees with α-helix secondary structure. Most efficient cleavage occurs when Lys is at position 4.

The determination of the optimal construct design at the N-terminal also make the construction of Domain I-II and Domain II-III straightforward, which will allow for the study of the properties of the interfaces and interactions between domains II and III or domains I and II.

The proposed rule can be a useful guide when quasi-arbitrary boundaries for fragments are needed. By selecting a suitable region of the parent sequence or by attaching an extra sequence clip to the target sequence in accordance with the rule proposed here, efficient expression constructs could be made.

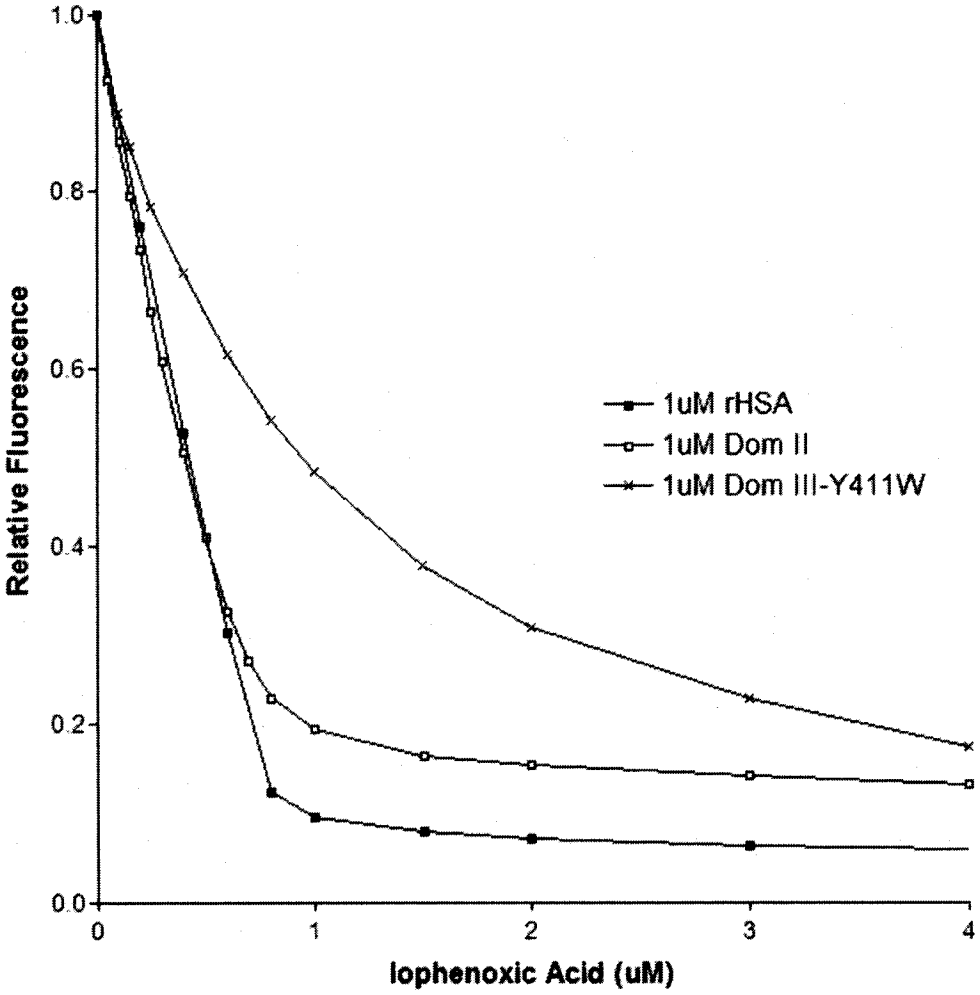

Figure 19. Quenching of tryptophanyl fluorescence of rHSA, Domain II and Domain III-Y411W by iophenoxate. Samples (1 μM) were titrated with iophenoxic acid. Fluorescence was measured at 340 nm with excitation at 295 nm.

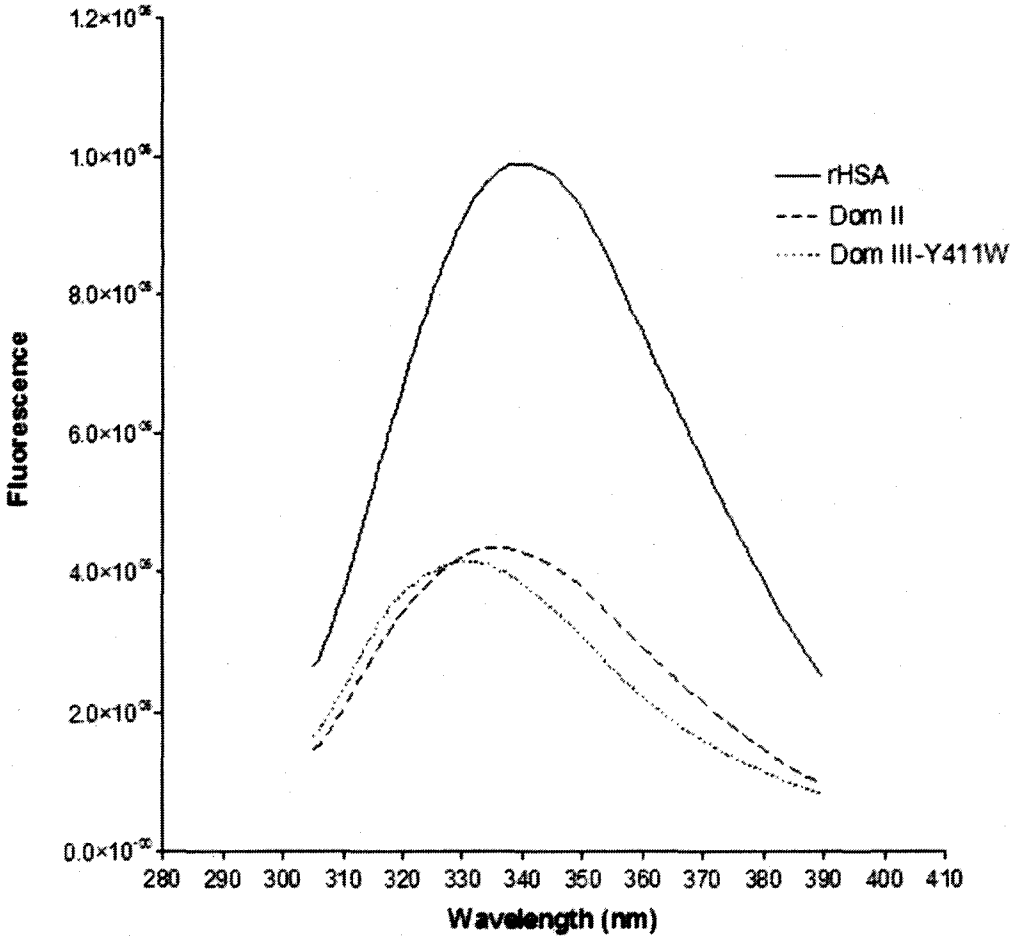

Figure 20. Fluorescence spectra of rHSA, domain II and domain III-Y411W with excitation at 295 nm. The samples were in equal molar concentration (10 μM).

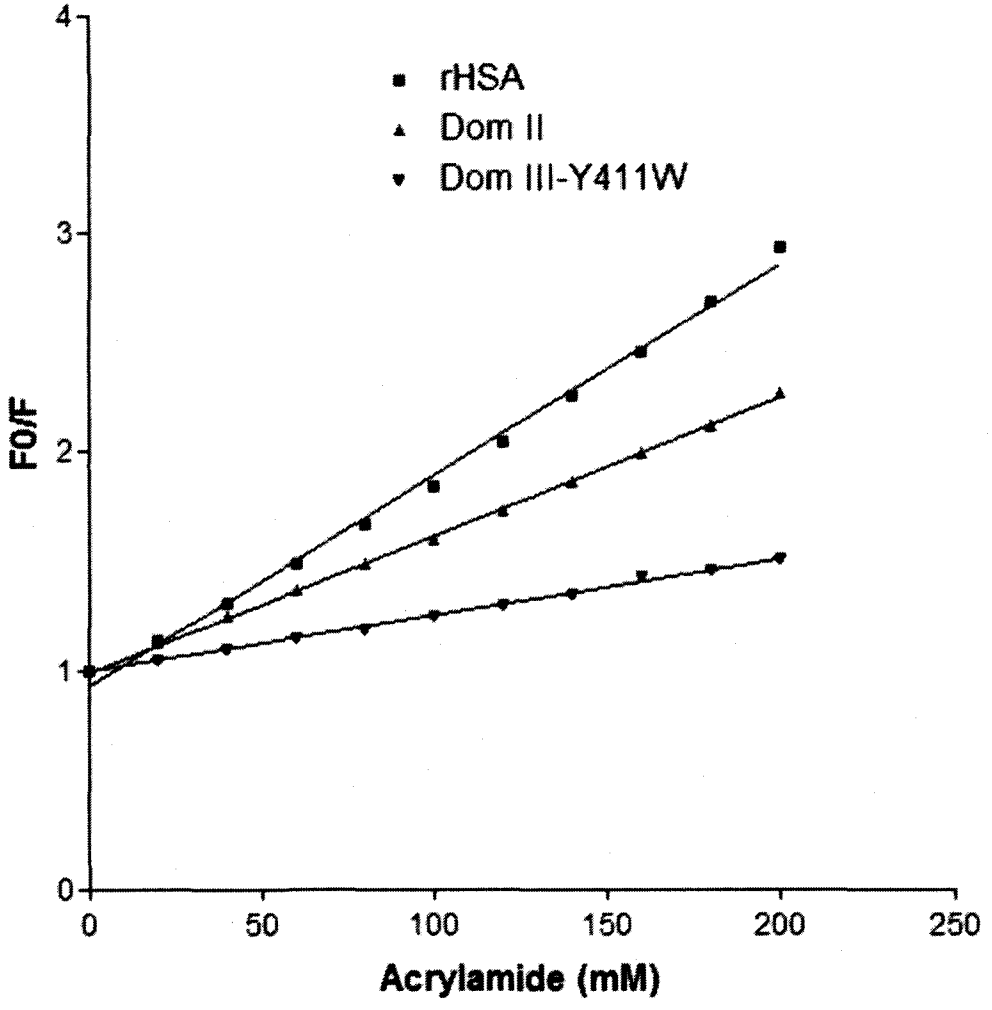

Figure 21. Stern-Volmer plot of acrylamide quenching of rHSA, domain II and domain III-Y411W with excitation at 295 nm. Each sample was 10 μM in PBS. F_0 is the initial fluorescent intensity, F the fluorescent intensity after the addition of the quencher, acrylamide.

CHAPTER 3
STUDY OF THE ROLE OF HISTIDINE RESIDUES OF DOMAIN I IN THE N-B TRANSITION

Originally, Leonard (1963) observed a drop in specific rotation around pH 8 in an ORD study of HSA and attributed it to a comformational change. The N-B transition has its basis in the unusual pK of imidazoles and has physiological significance. The presence of Ca^{2+} reduces the mid-point pH for the transition. Many physicochemical changes of HSA as a function of pH parallel the N-B transition. Many site I ligands show increased affinity for the B form of albumin. The B conformer shows increased volume and surface area. ^{1}H NMR studies have suggested that in domain I at least the histidine residues corresponding to the His C-2 resonances 1-5 play a dominant role in the N-B transition; His3, which is involved in Cu^{2+} binding, does not take a part in the N-B transition. Among a total of seven histidine residues of domain I, six residues at positions 9, 39, 67, 105, 128 and 146 of domain I were each mutated to serine and phenylalanine, respectively, and their role in the N-B transition examined. Due to the sensitivity of fluorescence methods, the changes in the fluorescence of warfarin-mutant complexes were used to monitor the conformational changes during the transition.

MATERIALS AND METHODS

Synthesis and purification of recombinant mutants of HSA

Introduction of mutations into the HSA coding region

Specific mutations were introduced into the HSA coding region in a plasmid vector containing the entire HSA coding region (pHiL-D2 HSA) using standard techniques as previously described (Petersen, Ha, Jameson and Bhagavan, 1996; Petersen, Ha, Harohalli, Park and Bhagavan, 1997; Petersen, Ha, Harohalli, Park and Bhagavan, 2000).

Expression of recombinant mutants

Each pHiL-D2 HSA expression cassette coding for a particular HSA mutant was introduced into the yeast species *Pichia Pastoris* by electroporation. A yeast clone that contained the expression cassette stably integrated into the chromosomal DNA was isolated in each case.

Verification of the DNA sequence of mutants

The total genomic DNA from each *Pichia Pastoris* clone used to produce a particular HSA species was isolated using standard techniques. The genomic DNA isolated from each clone was used as template to amplify the entire HSA coding region by PCR. For each clone, the entire HSA coding region was sequenced using the dideoxy nucleic acid chain termination technique, and the translation product corresponding to this sequence was found to match a previously published HSA sequence at all amino acid positions except for the mutation introduced into a particular HSA mutant.

Purification of recombinant mutants

The secreted HSA was isolated from growth media as follows. The medium was brought to 50% saturation with ammonium sulfate at room temperature. The temperature was then lowered to 4°C, and the pH was lowered to 4.4, the isoelectric point of HSA. The precipitated protein was collected by centrifugation and resuspended in distilled water. Dialysis was carried-out for 72 hours against 100 volumes of phosphate buffered saline, 137 mM NaCl, 2.7 mM KCl, 4.3 mM Na_2HPO_4, 1.4 mM KH_2PO_4, pH 7.4 (PBS) with one change of buffer. The solution was loaded onto a column of Cibacron Blue immobilized on Sepharose 6B (Sigma). After the column was washed with ten bed volumes of PBS, HSA was eluted with 3 M NaCl. The eluent was dialyzed against PBS and passed over a column of Lipidex-1000 (Packard Instruments) to remove hydrophobic ligands possibly bound to HSA (Glatz and Veerkamp, 1983). The resulting protein exhibited only one band on SDS-PAGE. Protein concentrations were determined by the BCA method, a modification of the Lowry procedure in which bicinchoninic acid is substituted for tartrate (Smith *et al.*, 1985).

Measurement of the fluorescence of mutant-warfarin complexes

Background

When excited at 320 nm, warfarin emits fluorescence with peak intensity at around 380 nm. This fluorescence, or quantum yield, is remarkably enhanced when warfarin is restricted in its internal rotation of the acetobenzyl group, such as when in a viscous solution or bound to HSA. The HSA-bound warfarin shows a 10 to 20 fold enhancement of fluorescence over that of unbound warfarin. This property of the

warfarin-HSA complex has long been exploited to determine the concentration of HSA-bound warfarin in solution, which is the basis for HSA/warfarin dissociation constant determination by fluorescent techniques.

The method to determine the dissociation constant Kd for warfarin binding to the primary binding site on HSA involves two experiments. The first experiment is devised to measure the fluorescence enhancement of HSA-bound warfarin at the primary binding site. In order to obtain stoichiometric binding of warfarin to HSA, a high-concentration solution of HSA, usually 10 μM, is titrated with warfarin up to a warfarin/HSA mole ratio about 1/10 with the fluorescence recorded for each addition of warfarin. Under the above-mentioned condition, a linear relationship between fluorescent intensity and total warfarin concentration should be observed indicating stoichiometric binding. The same titration is also done with the HSA solution replaced by a blank, i.e., the same buffer used for the HSA solution. Under condition of stoichiometric binding, linear regression analysis of the data can be performed to calculate the slopes of fluorescence intensity versus warfarin concentration in the presence or absence of HSA. The ratio of two slopes is defined as the fluorescence enhancement. The second experiment involves titration of a low-concentration solution of HSA, usually 1 μM, with warfarin to cover an appropriate range of warfarin bound per HSA molecule, usually up to a total warfarin/HSA mole ratio of 10. As can be shown with ease, the fraction of warfarin bound to HSA over the warfarin added (bound and unbound warfarin), assuming a single binding site on HSA, is determined by the equation:

$$\text{Fraction of warfarin bound} = (F - F_0)/(F_0*(E - 1)) \quad (1)$$

where F is the fluorescence intensity measured; F_0 is the fluorescence intensity measured for the same total amount of warfarin in the absence of HSA; E is the fluorescence enhance determined by the first experiment. This equation can be used for each point in the titration if binding occurs only at the primary binding site, which is largely satisfied if the molar ratio of bound warfarin/HSA is less than one.

General experimental parameters

Fluorescence intensity measurements were performed with a QM-1 spectrafluorometer (Photon Technologies International). Samples were excited at 320 nm and emission was monitored at 380 nm. The slit-width was set to 2 nm for both excitation and emission. A 10 mm x 3 mm quarts cuvette was used to hold 1 ml of a sample and the temperature was maintained at 25 °C by using a constant temperature circulator. The sodium salt of warfarin was directly dissolved in H_2O to make a 10 mM stock solution, which was diluted further to prepare working solutions for titration studies. For measurement of the fluorescence enhancement of HSA-bound warfarin at the primary binding site, a 10 μM HSA solution, was titrated with warfarin up to a warfarin/HSA molar ratio about 1/10 with the fluorescence recorded upon each addition of warfarin. The titration was repeated with the HSA solution replaced by a blank, i.e., the same buffer used for the HSA solution. For the second experiment, a 1 μM HSA solution was titrated with warfarin up to a total warfarin/HSA mole ratio of 10.

These experimental parameters were applied to the mutants as well.

Analysis of data

By using equation (1), a set of concentration of free ligand (i.e., unbound warfarin) and mole ratio of ligand bound/HSA data pair was calculated. The data were fit to single binding site (hyperbola) curve using the following equation:

Mole ratio of ligand bound = Bmax * X / (Kd + X)

where Bmax is the maximum of mole ratio of ligand bound, X is the concentration of the free ligand and Kd is the dissociation constant. Nonlinear regression method of the Prism computer program (GraphPad) was employed. In this study Bmax should be one; however, due to variance in HSA quantification, Bmax can deviate from unity to some degree. If free ligand concentration and ratio of ligand bound/HSA can be determined correctly, variance in Bmax will not affect Kd value.

Measurement of the fluorescent enhancement of mutant-bound Warfarin at pH 6.0, 7.4 and 9.0

10 μM HSA samples were titrated with warfarin up to a final warfarin concentration of 1 μM. For measurement of fluorescence enhancement at pH6.0, HSA samples were diluted in PBS (adjusted to pH 6.0 with 0.1 N HCl). For measurement of fluorescence enhancement at pH7.4, HSA samples were diluted in PBS. For measurement of fluorescence enhancement at pH 9.0, HSA samples were diluted in PBSG (PBS plus 5 mM glycine adjusted to pH 9.0 with 0.1 N HCl). Linear regression analysis of the data was performed to calculate the slopes of fluorescence intensity versus warfarin concentration in the presence or absence of HSA. The ratio of two slopes was calculated as the fluorescence enhancement for each sample at each pH value.

Measurement of dissociation constants of mutant-Warfarin complex at pH 6.0, 7.4 and 9.0

A 1-μM mutant solution, was titrated with warfarin up to a total warfarin / mutant mole ratio of 10.

Measurement of the fluorescence of mutants-bound warfarin as a function of pH

Warfarin was added to a 10-μM HSA solution to get a final concentration of 0.5 μM. At the start of each titration, the pH value was adjusted to 5-6 with 0.1 N HCl. Then the warfarin/HSA solution was titrated to a final pH value above 9 with 0.1 N NaOH; the titration was controlled in such a way that each addition of NaOH increased the pH value of the solution by 0.2-0.3 unit. The fluorescence intensity of the solution was recorded for each pH value measure. The fluorescence was measured at 380 nm with excitation at 320 nm.

RESULTS

Measurement of fluorescence enhancement of mutant-bound warfarin at pH 6.0, 7.4 and 9.0

Comparison of fluorescence enhancement for all the thirteen HSA species is shown in Figure 22. The variance in fluorescence enhancement for all the thirteen HSA species at pH 6.0 or pH 9.0 was small while the values for the sample at pH 7.4 displayed significant variance. The increases in enhancement values when pH was changed from 6.0 to 9.0 were about two fold, in good agreement with data reported by other researchers (e.g., Petersen *et al.*, 2002). In general, the values for a pair of mutations (F/S) for the same histidine residue showed the same trend. For example, H39F/H39S behaved the in

parallel at all three pH values and resembled the wild type HSA. All the other HSA species exhibited increased fluorescence enhancement values at pH 7.4 compared with that of wild type. The values for H146F/H146S pair at pH 7.4 displayed remarkable difference; still, both values were significantly larger than that for wild type HSA, which can be better visualized when the fractional difference is shown (Figure 23).

Measurement of dissociation constant of mutant-warfarin complex at pH 6.0, 7.4 and 9.0

The dissociation constants (Kd) for the mutants as well as for rHSA at pH 6.0, 7.4 and 9.0 are shown in Table 1 (page 74). For easy comparison of data, association constants converted from the dissociation constants are shown in Figure 24. The data showed a similar profile to that of the fluorescence enhancement data. The variances were larger between mutants at the same pH values than those of the fluorescence enhancement data. The increased variances can be accounted for by the differences in the procedures used to obtain the two sets of data. Enhancement measurement is straightforward and involves one experiment whereas dissociation constant (Kd) determination is indirect and involves two experiments. Therefore error propagation is entailed in the Kd determination. However, the principal cause for the increased variances lies in the low concentration of protein required for Kd titration. Over the useful range of saturation of the protein by warfarin, the fluorescence signal is several fold weaker than that for the enhancement measurement. Due to this deteriorated signal/noise ratio, the relative standard deviation for Kd was about 20 % in contrast to that of about 5 % for fluorescence enhancement, which was in agreement with a previous

study (Petersen *et al.*, 2002). The majority of the mutants exhibited increased affinity for warfarin when compared with wild type HSA. At pH 6.0 and 9.0, the fractional change in the affinity for warfarin binding for each mutant relative to that for rHSA was less than 50 %, which indicated that the mutation-caused perturbation in the structure of warfarin-binding site was small. There were no significant difference between serine substitution and phenylalanine substitution.

Measurement of fluorescence of mutant-bound warfarin as a function of pH

The effects of pH on the fluorescence intensities of warfarin (0.5 μM) bound to rHSA and the mutants (10 μM) in the absence and in the presence of 2.5 mM $CaCl_2$ are shown in Figures 25 to 37. Because warfarin has a pK 5.0, the fluorescent quantum yield of unbound warfarin is almost constant over the pH range of 6 to 9. Thus at the molar ratio of 0.5:10, the changes in the fluorescent intensity of a protein-warfarin complex reflect the changes in the fluorescence enhancement of the protein-warfarin complex. In the absence of calcium ions, the titration curves were of a typical sigmoid shape while in the presence of calcium ions, the titration curves were of complex shapes. In the presence of calcium ions, most of the titration curves had an inflection between pH 7.5 and 8.0. The inflection was easily observed in the cases of rHSA, H9S, H39F, H67F, H105F, H105S, H128F, H128S and H146F. In the cases of H9F, H39S, H67S and H146S, the inflection was barely noticeable. Apparent variances in fluorescent intensity existed among the protein-warfarin complexes at an identical pH value; the variances were less than 50 % in all cases, which was in agreement with the Kd data. As in the case of dissociation constants, the variances were larger than those for the fluorescence

enhancement measurements, which was probably due to the spread of the titration experiments over several days.

By visual inspection, the midpoint pH (pH_{50}) values of the titration curves for many mutants shifted to lower pH values relative to that for rHSA. To facilitate the comparison of midpoint pH values shift, the following analysis of the data was performed: the titration data for a mutant were fitted to the equation

Y=Bottom + (Top-Bottom)/(1+10^((LogEC50-X)*HillSlope))

where X is the logarithm of concentration, or the pH value in this case; Y is the response , or the fluorescent intensity in this case; Y starts at Bottom and goes to Top with a sigmoid shape; LogEC50 is pH_{50} in this case. The fitting was done by using nonlinear regression function of Prism computer program (GraphPad). It should be noted that protons bind to the N form of a HSA species and the relative fluorescent intensity of a mutant-warfarin complex reflects the relative amount of the B form. However, when pH is used instead of $\log[H^+]$, the fluorescent intensity can be directly used.

By using the above-mentioned analysis, the pH_{50}, the HillSlope (Hill constant), Top and Bottom can be obtained. The Top and Bottom represent the B conformer and the N conformer respectively. A fractional change or relative change in fluorescent intensity is defined as

(F - Bottom) / (Top – Bottom)

where F is the fluorescent intensity of the warfarin-mutant complex at the concomitant pH during titration. A plot of fractional changes versus pH can be drawn. This transformation does not affect the pH_{50}, and the HillSlope (Hill constant).

The fractional changes in fluorescent intensity of the mutants in the absence and in the presence of calcium ions are shown in Figures 38 to 43. For ease of comparison, the fractional changes in fluorescent intensity of rHSA in the absence and in the presence of calcium ions are also shown in each plot. Table 2 shows the computer-derived values of pH_{50} and Hill constant for the HSA species in the presence and in the absence of $CaCl_2$.

The changes in the pH_{50} values of the mutants in the absence of calcium ions were most unambiguously observed. The most dramatic shifts of pH_{50} towards lower pH were found for H9F/S (about 0.7 unit) and H67F/S (about 0.5 unit). H105F/S and H146 had moderate reduction in pH_{50}, with a value around 0.35 unit. The mutant pair at position 128, i.e., H128F/S showed a small change in pH_{50}, which was about 0.15 on the average for the two mutants. The two mutants at position 39, H39F/S, exhibited virtually the same pH_{50} as rHSA. In fact, H39S had a shift of pH_{50} towards high pH (less than 0.1 units), which was considered to be within the error range of the experiment. The pH titration of the mutant-warfarin complexes was performed under low ionic strength condition, in which the principal contribution of ionic strength was from the NaOH used in titration. Though the fluorescence enhancement measurement was done in PBS, the results by the two methods were in good agreement lending strong evidence to the following conclusion: histidine residues at positions 9, 67, 105 and 146 play dominant role in the N-B transition; His 128 also contributes to the transition; H39 is not involved in the N-B transition.

This conclusion was also supported by the results from the titration in the presence of calcium ions, though less convincing than by the results from the calcium-

free experiments. The ambiguity in some results for pH titration in the presence of calcium ions probably had its origin in the deviation of the titration behavior from a typical sigmoid curve. The data were more difficult to fit to the theoretical equation than the data of titration in the absence of calcium ions. When the above-mentioned inflection was apparent, only data points at pH less than 7.5 were used whereas when the inflection was not observable, data points over a larger pH range were included. The inclusion of data points above pH 7.5 in the latter case was required since otherwise the Top derived would be subject to large variance leading to error in pH_{50} estimation. However, the inclusion of data points above pH 7.5 would surely result in inconsistence in the treatment of data. Due to this dilemma, the data from experiments in the absence of calcium ions are considered superior in quality.

The effect of pH on the fluorescence of warfarin (0.5 μM) bound to rHSA (10 μM) in the presence of 2.5 mM and 5 mM $CaCl_2$ is shown in Figure 44. The data points at pH lower than 7, of the two titrations could be fitted to sigmoid curves and the higher calcium concentration resulted in a higher Hill constant, which was in agreement with previous observations.

Most published studies on the N-B transition were carried out in moderate ionic strength, which is higher than that used in the current work. The effect of ionic strength on the pH titrations of warfarin-rHSA complex is shown in Figure 45. Higher ionic strength resulted in the lowering of pH_{50} in the absence of calcium ions, which explains why the pH_{50} values in this work were higher than those reported by others. It is interesting to note that higher ionic strength reduced the effect of calcium ions.

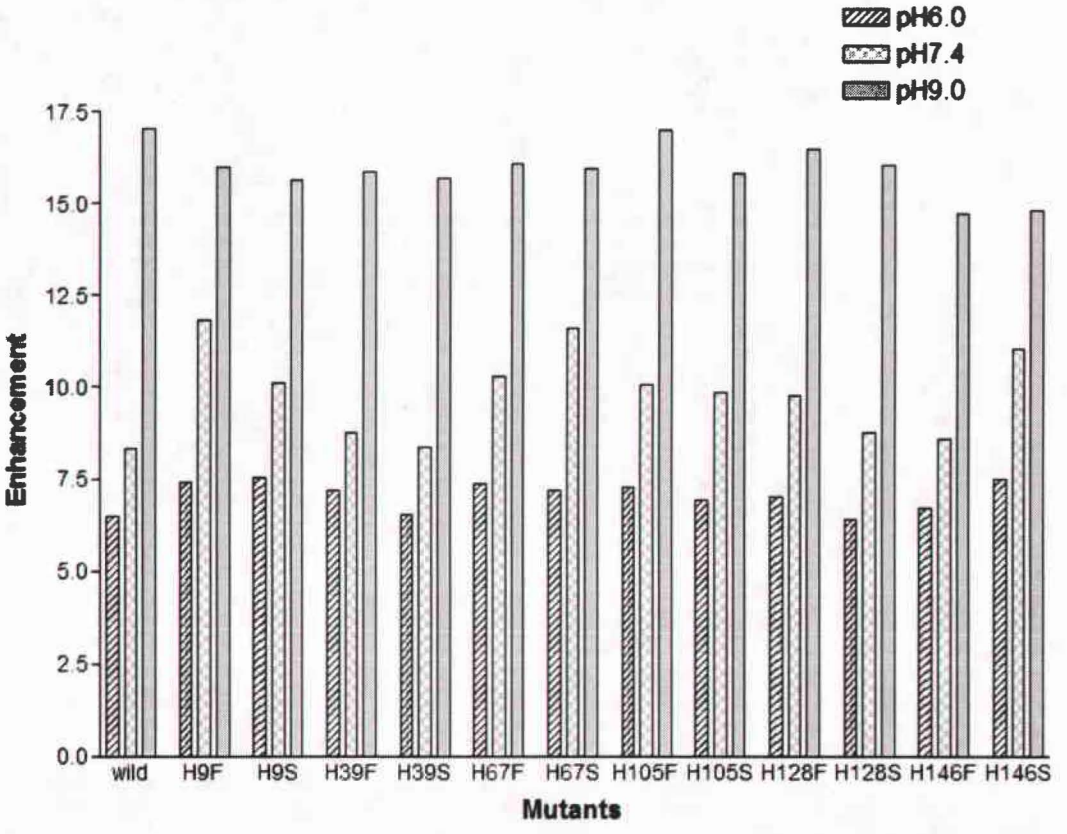

Figure 22. Warfarin fluorescence enhancement for the mutants at pH 6.0, 7.4 and 9.0. The enhancement is defined as the ratio of the fluorescence of warfarin bound to a mutant complex to the fluorescence of the same amount of warfarin free in the buffer. The fluorescence was excited at 320 nm and monitored at 380 nm.

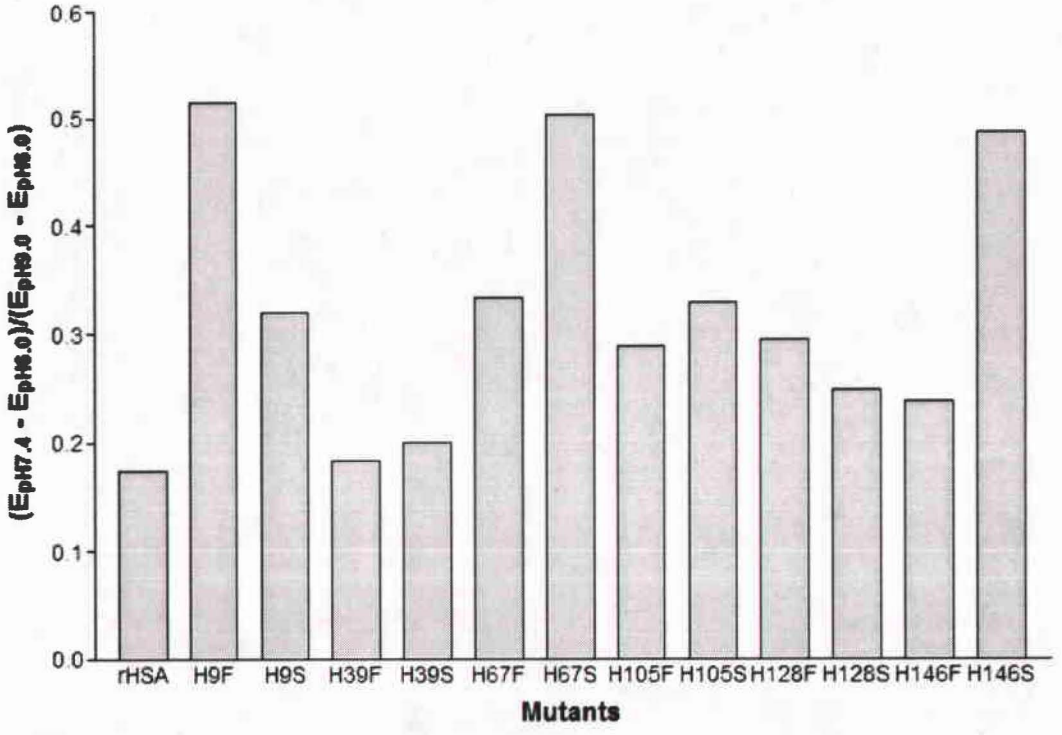

Figure 23. Fractional changes in fluorescence enhancement for the mutants at pH 7.4. A fractional change for a mutant is defined as

$$(E_{pH7.4} - E_{pH6.0}) / (E_{pH9.0} - E_{pH6.0})$$

where $E_{pH7.4}$ is the enhancement at pH 7.4, $E_{pH6.0}$ the enhancement at pH6.0, and $E_{pH9.0}$ the enhancement at pH9.0.

Table 1. Dissociation constants (Kd) for the mutants as well as rHSA at pH 6.0, 7.4 and 9.0. The buffers were PBS with pH adjusted to 6.0 with HCl, PBS with pH 7.4, and PBSG (PBS plus 5 mM glycine) adjusted to pH 9.0, respectively.

Mutants	Kd (μM) at pH 6.0	Kd (μM) at pH 7.4	Kd (μM) at pH 9.0
rHSA	2.4	2.1	1.1
H9F	1.8	1.2	0.9
H9S	2.1	1.7	1.0
H39F	2.2	1.8	0.8
H39S	1.8	1.6	1.0
H67F	2.4	2.1	1.2
H67S	1.9	1.8	1.2
H105F	2.1	1.8	0.9
H105S	2.4	1.6	0.9
H128F	1.7	1.4	1.0
H128S	2.4	1.9	0.9
H146F	2.4	1.8	0.9
H146S	1.7	1.3	0.8

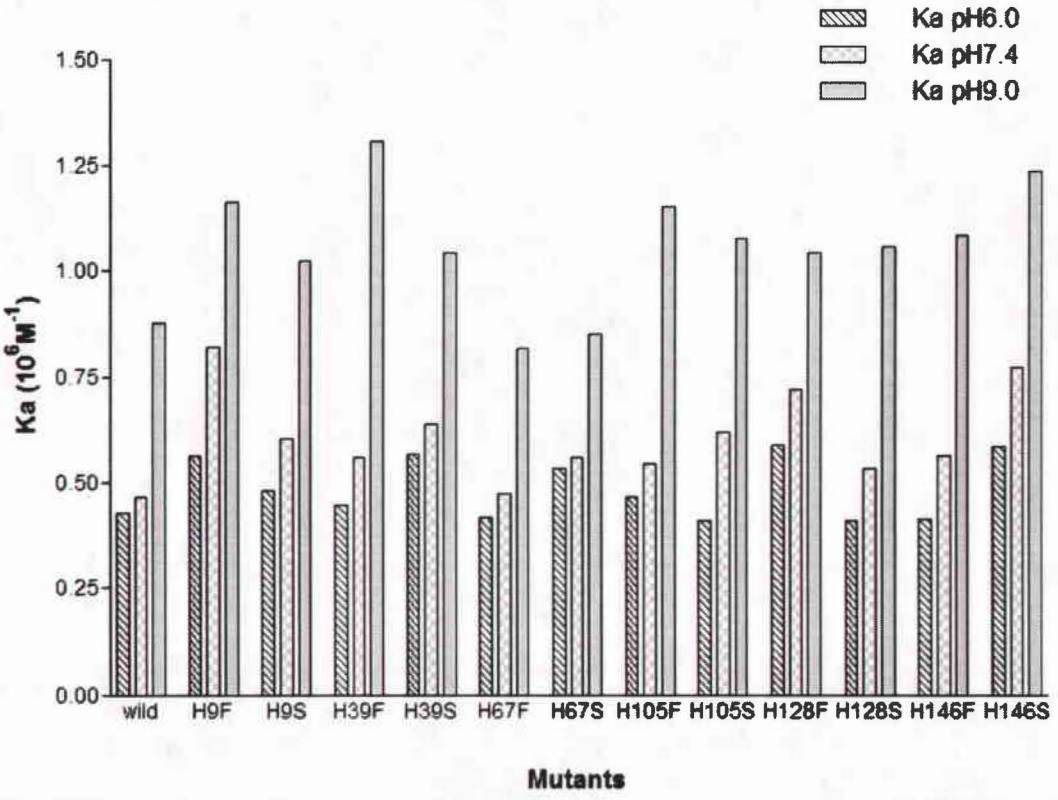

Figure 24. Association constants (Ka) for the mutants as well as rHSA at pH 6.0, 7.4 and 9.0. The buffers were PBS with pH adjusted to 6.0 with HCl, PBS with pH 7.4, and PBSG (PBS plus 5 mM glycine) adjusted to pH 9.0, respectively. The fluorescence was excited at 320 nm and monitored at 380 nm.

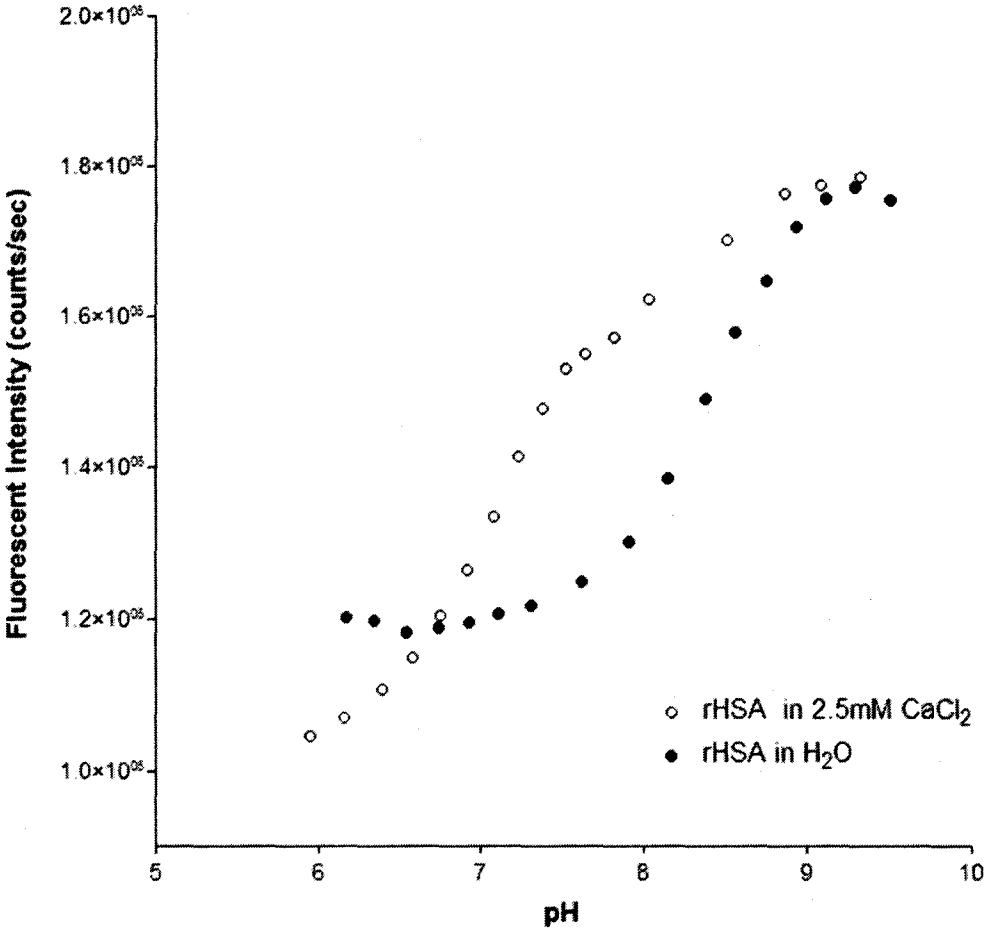

Figure 25. Effect of pH on the fluorescence of warfarin (0.5 μM) bound to rHSA (10 μM) in the absence and presence of 2.5 mM $CaCl_2$. The pH was adjusted with addition of aliquots of 0.1 N NaOH and if necessary, the pH was brought down to 5-6 with 0.1 N HCl at the start of titration. The fluorescence was measured at 380 nm with excitation at 320 nm.

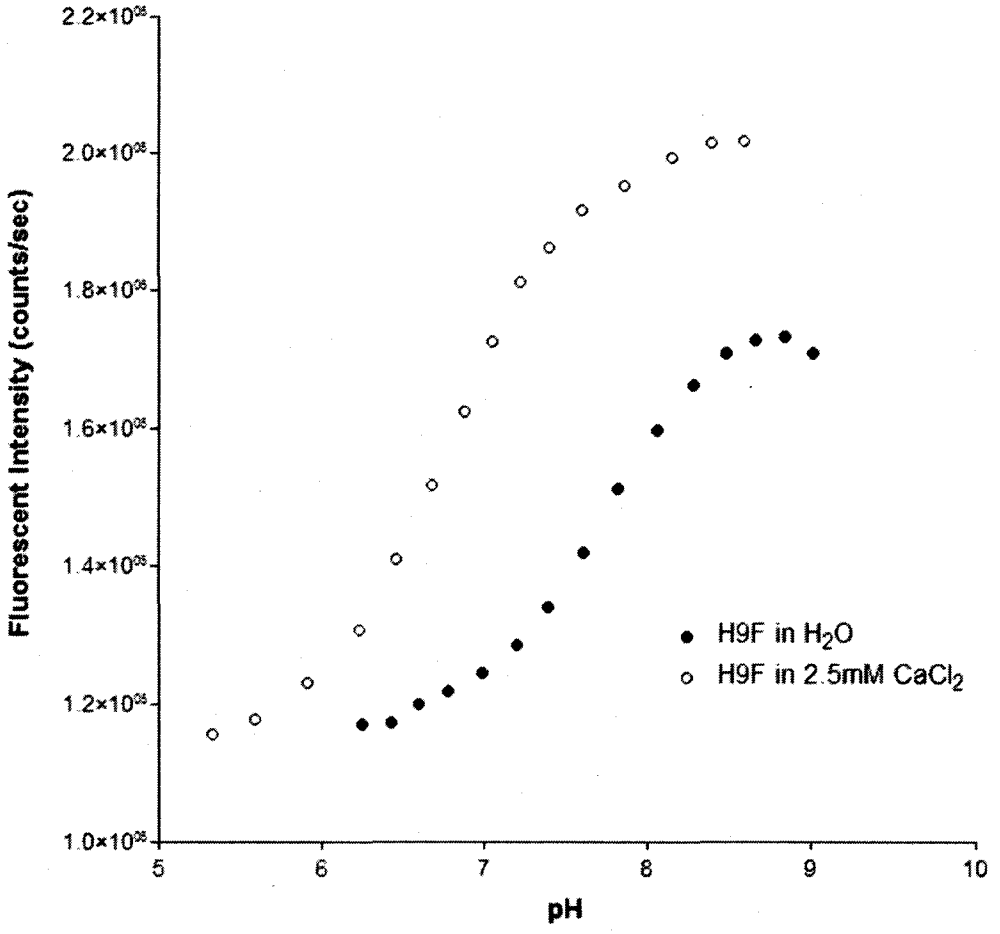

Figure 26. Effect of pH on the fluorescence of warfarin (0.5 μM) bound to H9F (10 μM) in the absence and presence of 2.5 mM $CaCl_2$. The pH was adjusted with addition of aliquots of 0.1 N NaOH and if necessary, the pH was brought down to 5-6 with 0.1 N HCl at the start of titration. The fluorescence was measured at 380 nm with excitation at 320 nm.

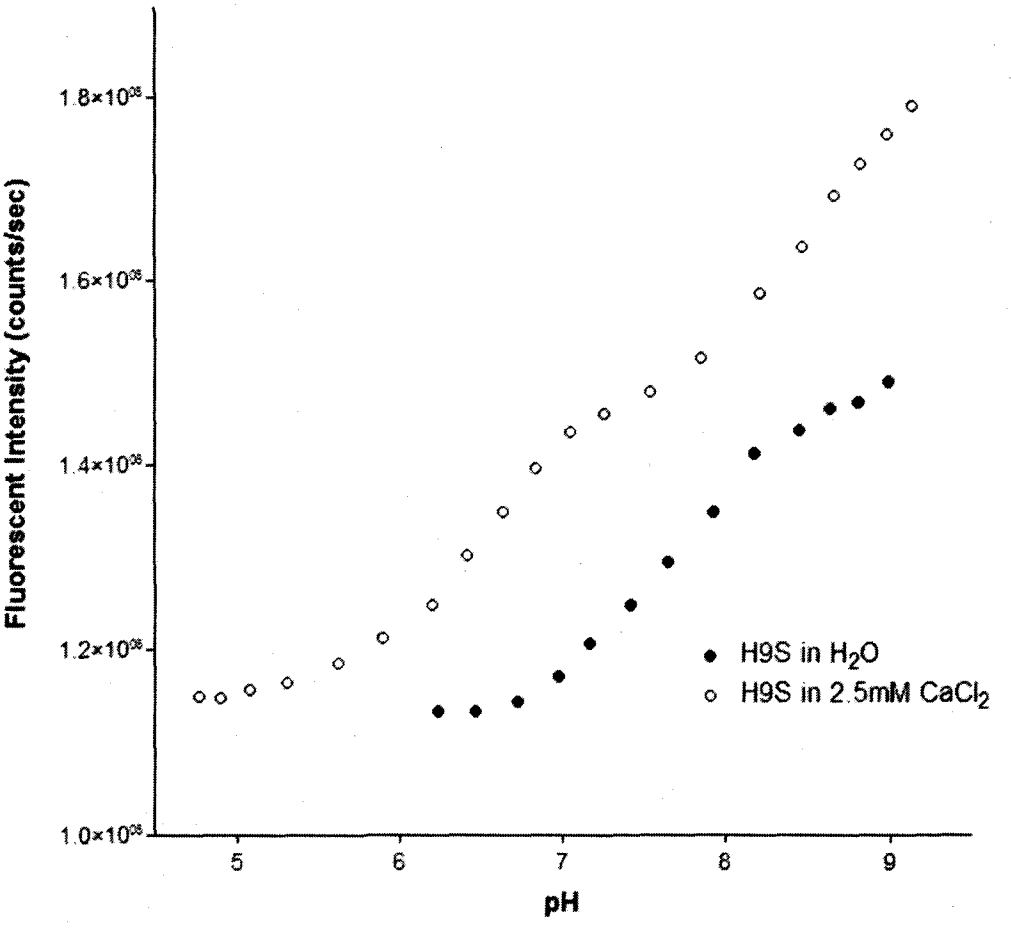

Figure 27. Effect of pH on the fluorescence of warfarin (0.5 μM) bound to H9S (10 μM) in the absence and presence of 2.5 mM $CaCl_2$. The pH was adjusted with addition of aliquots of 0.1 N NaOH and if necessary, the pH was brought down to 5-6 with 0.1 N HCl at the start of titration. The fluorescence was measured at 380 nm with excitation at 320 nm.

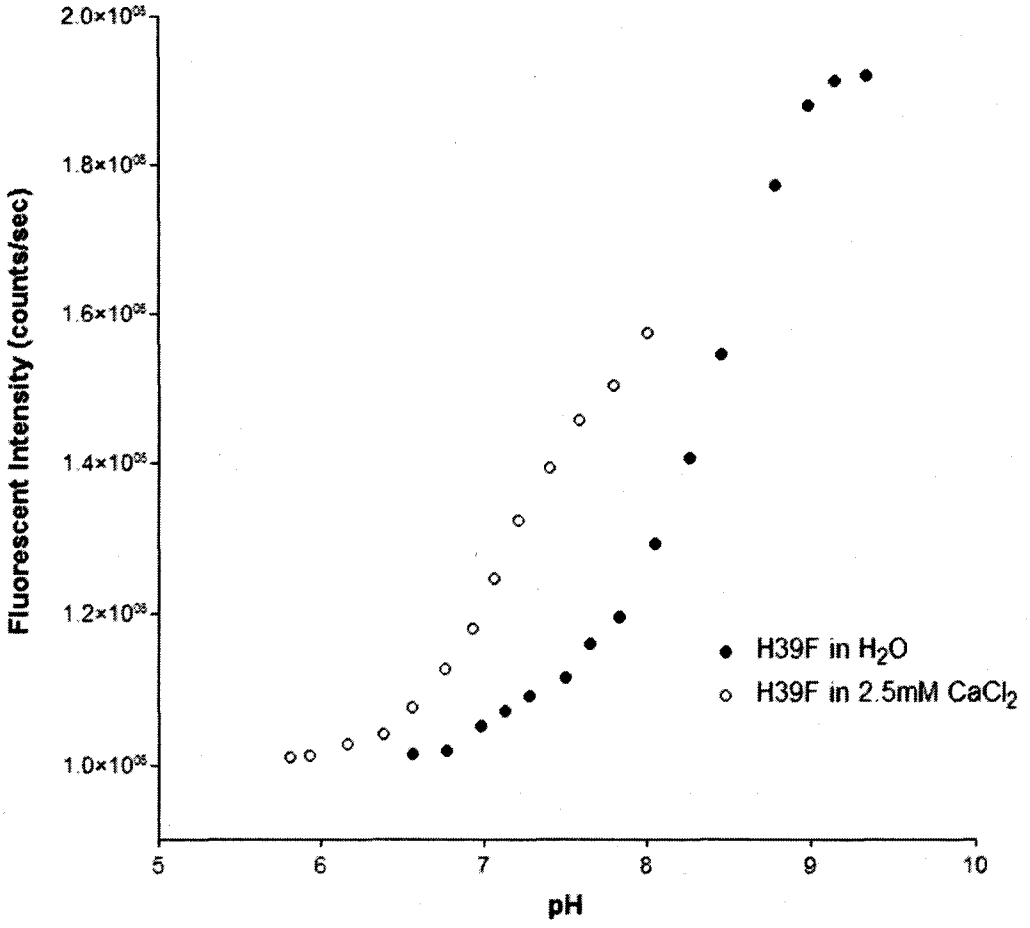

Figure 28. Effect of pH on the fluorescence of warfarin (0.5 μM) bound to H39F (10 μM) in the absence and presence of 2.5 mM $CaCl_2$. The pH was adjusted with addition of aliquots of 0.1 N NaOH and if necessary, the pH was brought down to 5-6 with 0.1 N HCl at the start of titration. The fluorescence was measured at 380 nm with excitation at 320 nm.

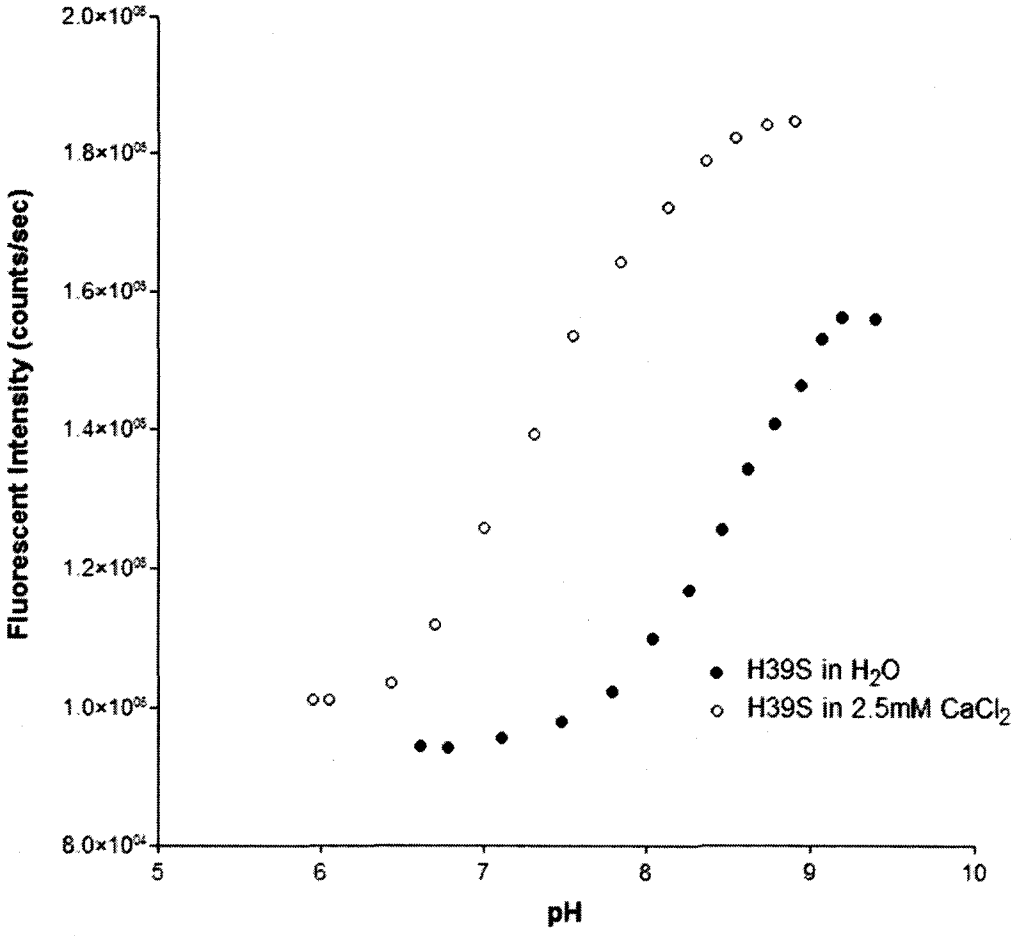

Figure 29. Effect of pH on the fluorescence of warfarin (0.5 μM) bound to H39S (10 μM) in the absence and presence of 2.5 mM $CaCl_2$. The pH was adjusted with addition of aliquots of 0.1 N NaOH and if necessary, the pH was brought down to 5-6 with 0.1 N HCl at the start of titration. The fluorescence was measured at 380 nm with excitation at 320 nm.

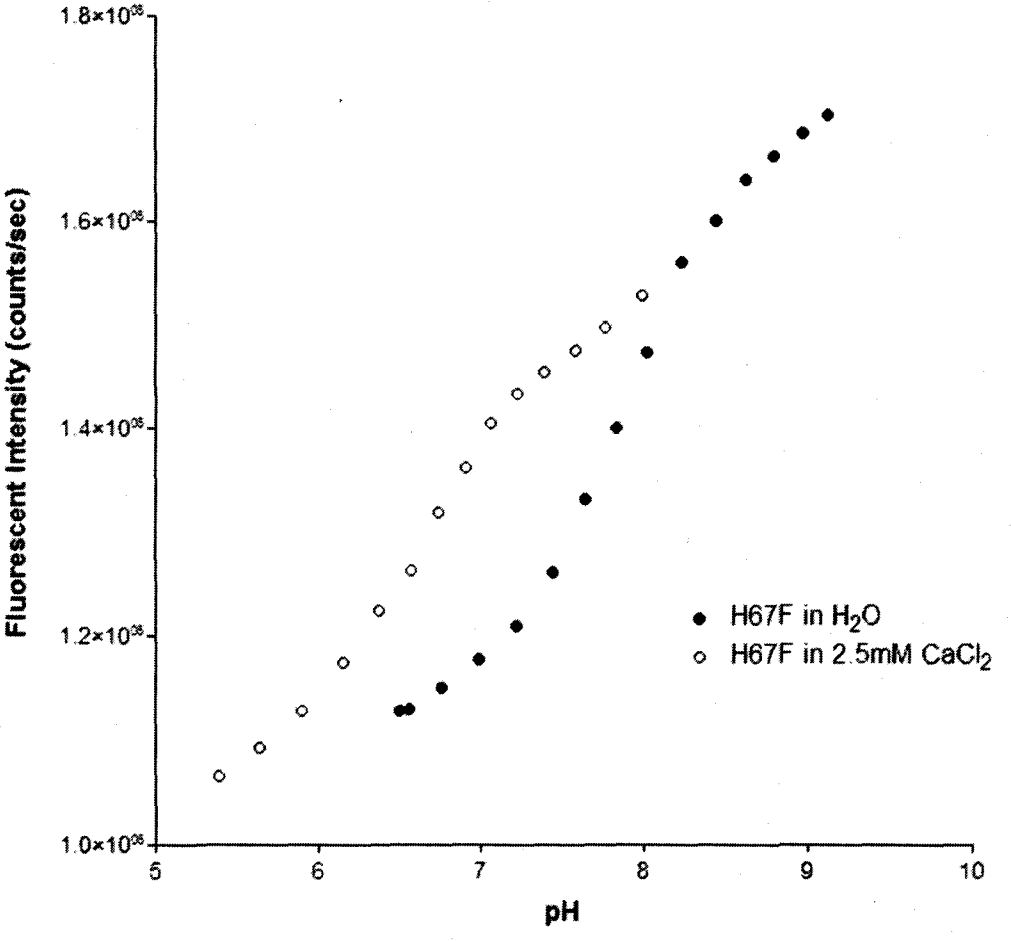

Figure 30. Effect of pH on the fluorescence of warfarin (0.5 μM) bound to H67F (10 μM) in the absence and presence of 2.5 mM $CaCl_2$. The pH was adjusted with addition of aliquots of 0.1 N NaOH and if necessary, the pH was brought down to 5-6 with 0.1 N HCl at the start of titration. The fluorescence was measured at 380 nm with excitation at 320 nm.

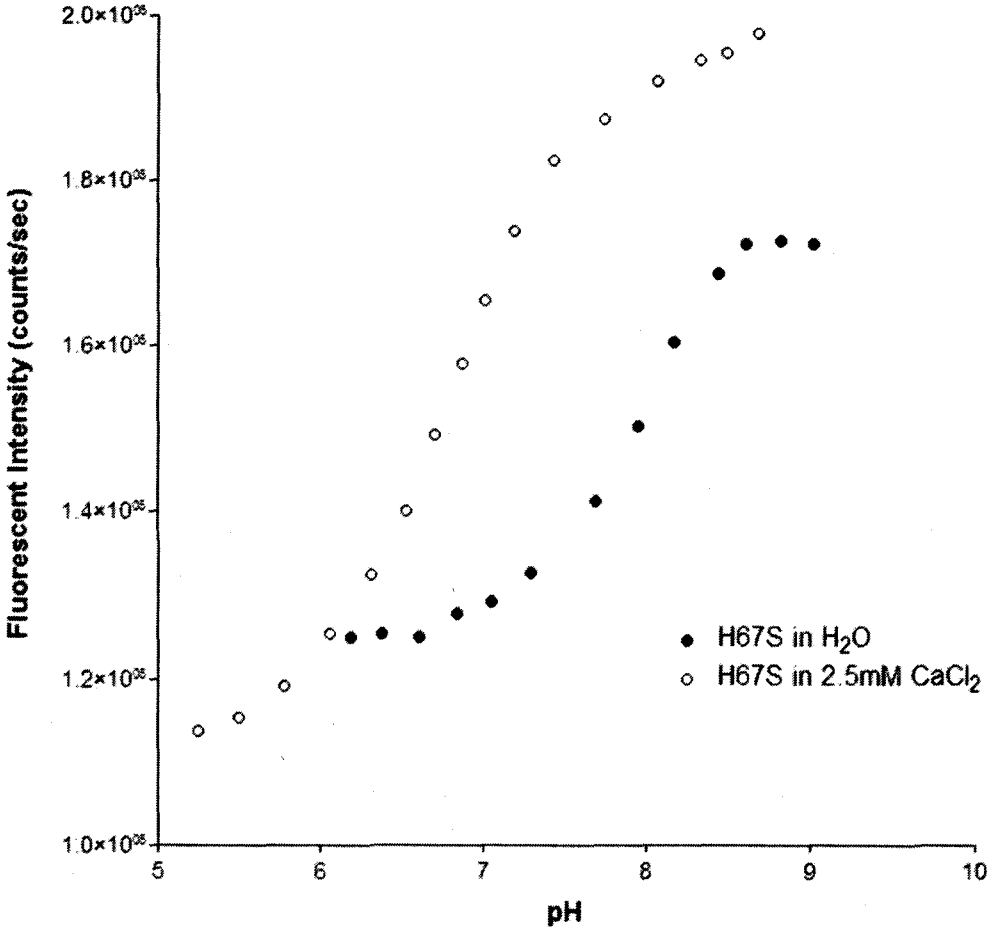

Figure 31. Effect of pH on the fluorescence of warfarin (0.5 μM) bound to H67S (10 μM) in the absence and presence of 2.5 mM $CaCl_2$. The pH was adjusted with addition of aliquots of 0.1 N NaOH and if necessary, the pH was brought down to 5-6 with 0.1 N HCl at the start of titration. The fluorescence was measured at 380 nm with excitation at 320 nm.

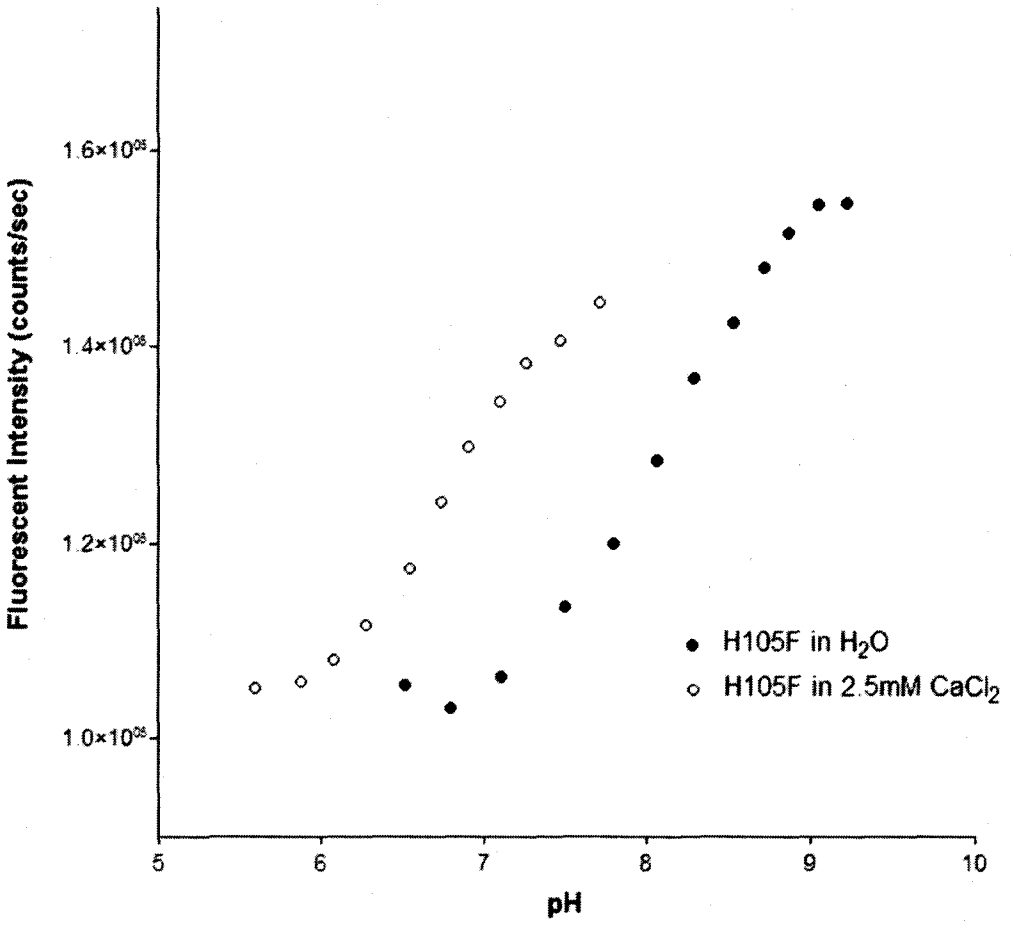

Figure 32. Effect of pH on the fluorescence of warfarin (0.5 μM) bound to H105F (10 μM) in the absence and presence of 2.5 mM $CaCl_2$. The pH was adjusted with addition of aliquots of 0.1 N NaOH and if necessary, the pH was brought down to 5-6 with 0.1 N HCl at the start of titration. The fluorescence was measured at 380 nm with excitation at 320 nm.

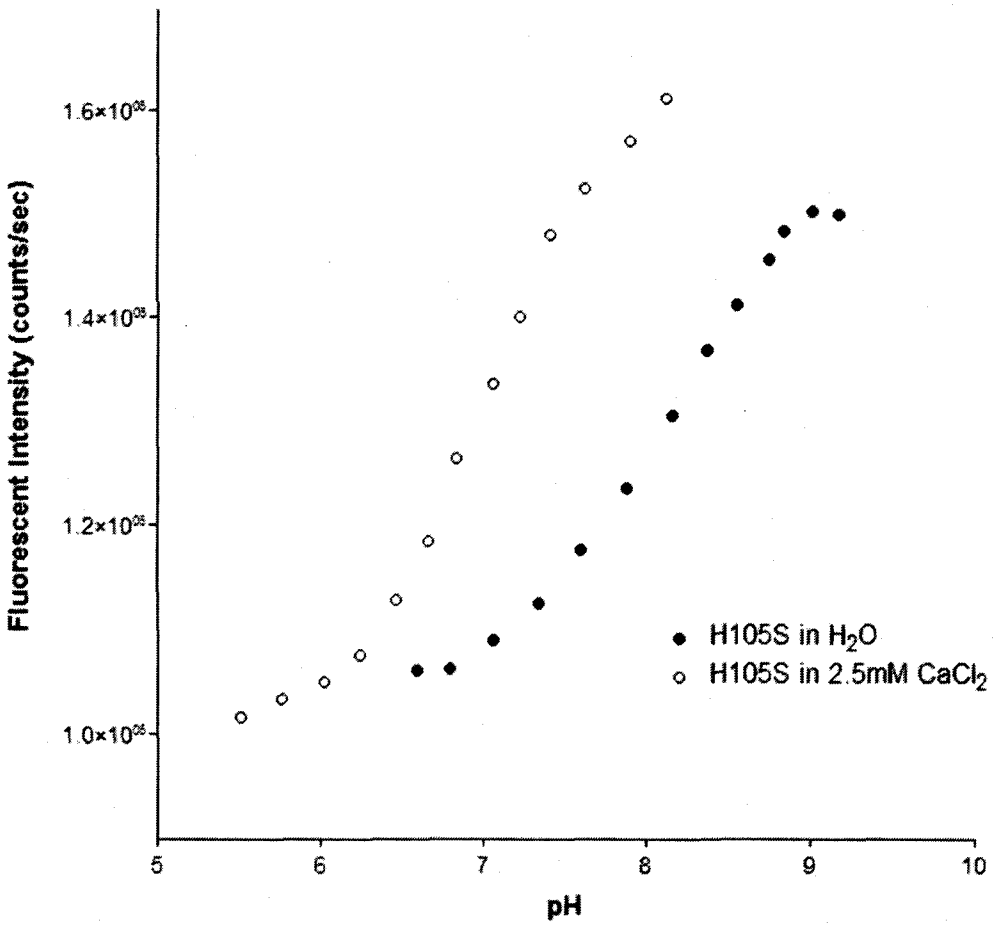

Figure 33. Effect of pH on the fluorescence of warfarin (0.5 μM) bound to H105S (10 μM) in the absence and presence of 2.5 mM $CaCl_2$. The pH was adjusted with addition of aliquots of 0.1 N NaOH and if necessary, the pH was brought down to 5-6 with 0.1 N HCl at the start of titration. The fluorescence was measured at 380 nm with excitation at 320 nm.

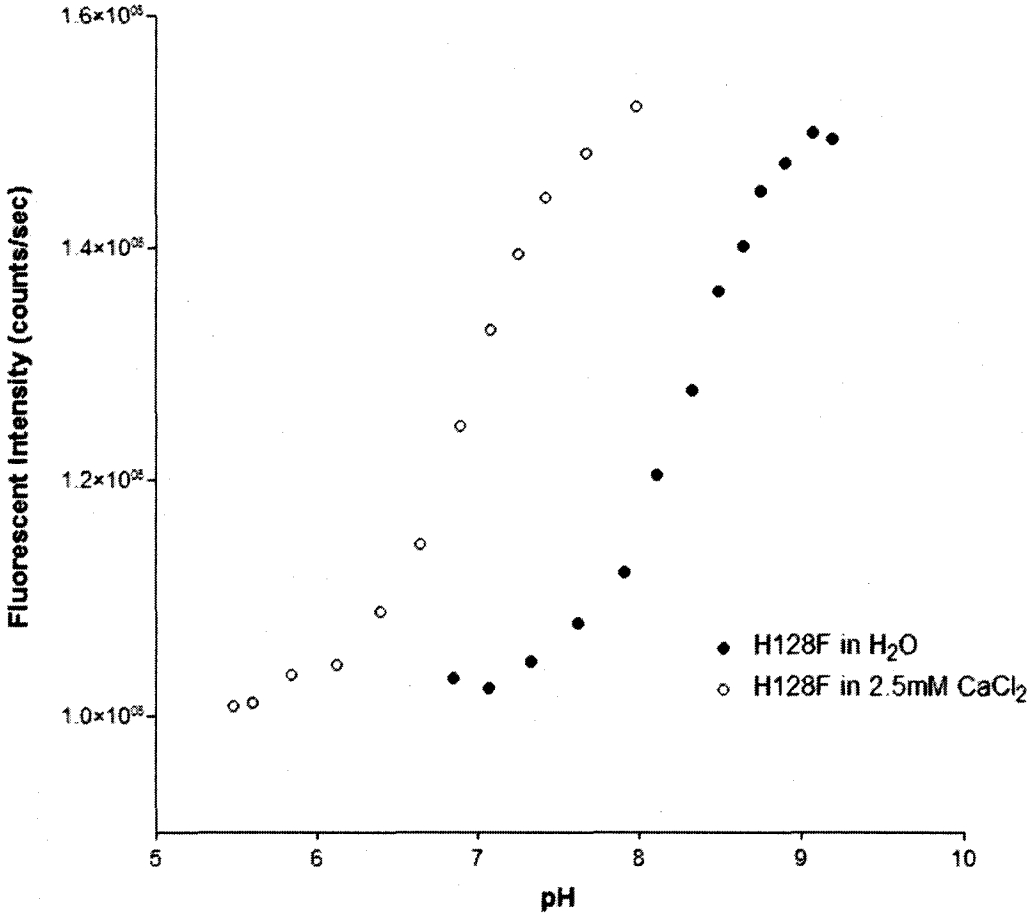

Figure 34. Effect of pH on the fluorescence of warfarin (0.5 μM) bound to H128F (10 μM) in the absence and presence of 2.5 mM $CaCl_2$. The pH was adjusted with addition of aliquots of 0.1 N NaOH and if necessary, the pH was brought down to 5-6 with 0.1 N HCl at the start of titration. The fluorescence was measured at 380 nm with excitation at 320 nm.

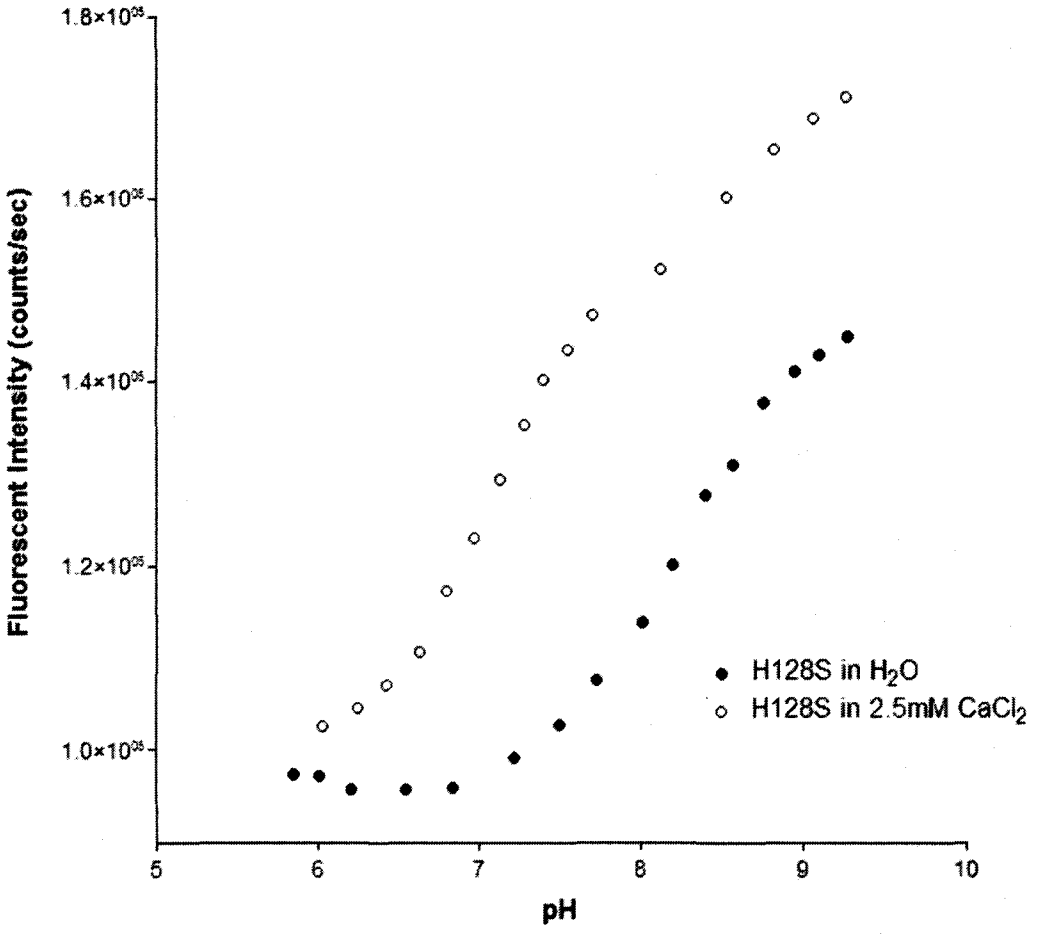

Figure 35. Effect of pH on the fluorescence of warfarin (0.5 μM) bound to H128S (10 μM) in the absence and presence of 2.5 mM $CaCl_2$. The pH was adjusted with addition of aliquots of 0.1 N NaOH and if necessary, the pH was brought down to 5-6 with 0.1 N HCl at the start of titration. The fluorescence was measured at 380 nm with excitation at 320 nm.

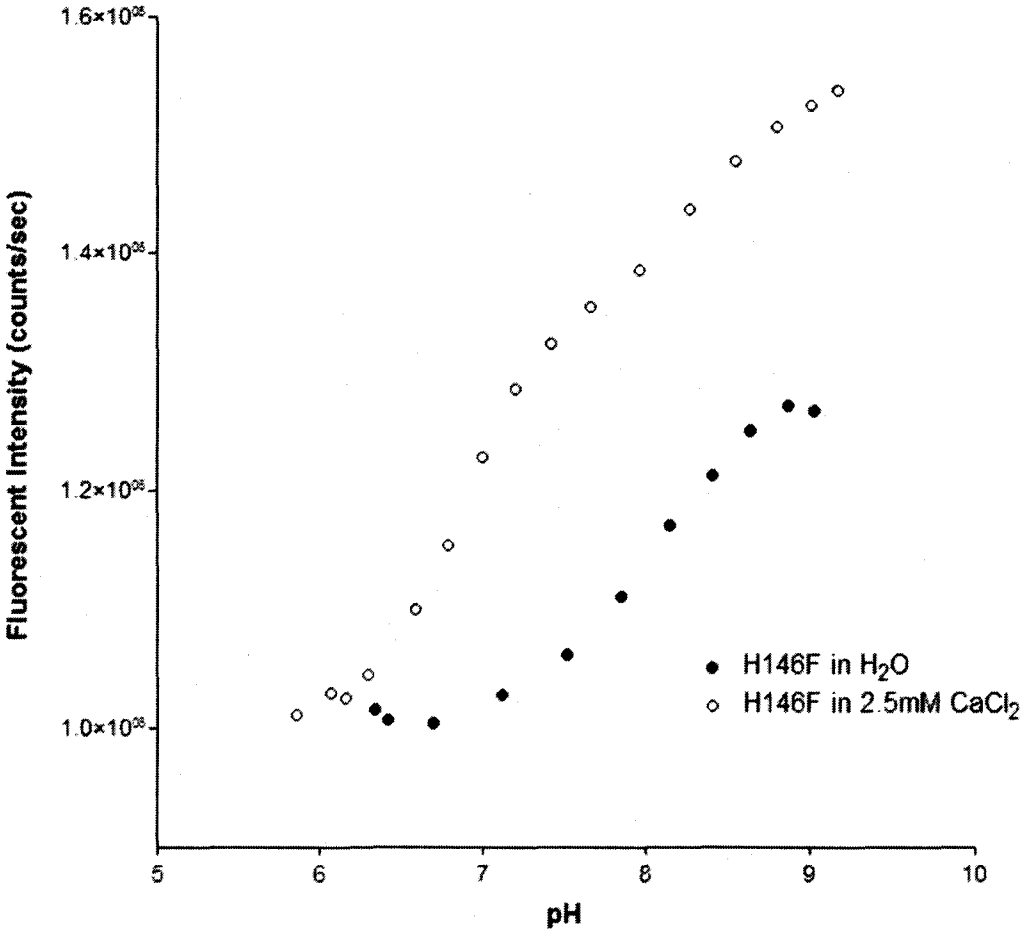

Figure 36. Effect of pH on the fluorescence of warfarin (0.5 μM) bound to H146F (10 μM) in the absence and presence of 2.5 mM $CaCl_2$. The pH was adjusted with addition of aliquots of 0.1 N NaOH and if necessary, the pH was brought down to 5-6 with 0.1 N HCl at the start of titration. The fluorescence was measured at 380 nm with excitation at 320 nm.

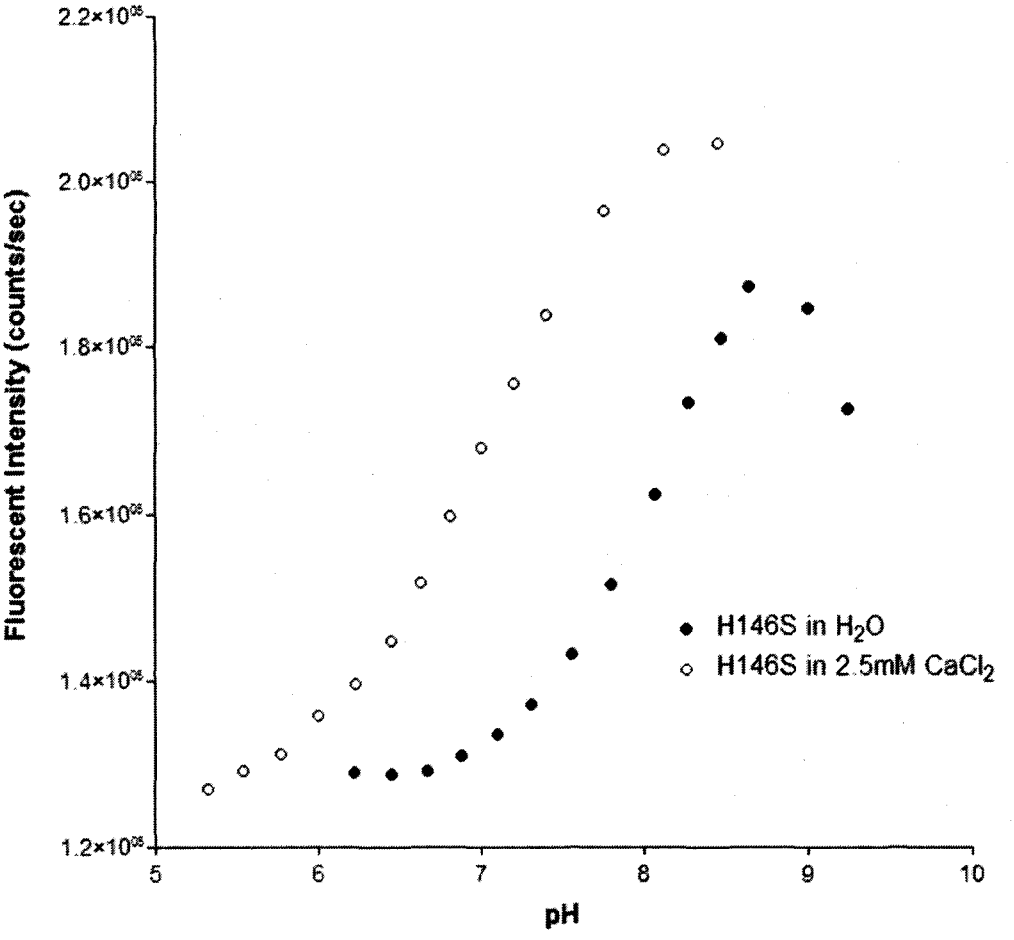

Figure 37. Effect of pH on the fluorescence of warfarin (0.5 μM) bound to H146S (10 μM) in the absence and presence of 2.5 mM $CaCl_2$. The pH was adjusted with addition of aliquots of 0.1 N NaOH and if necessary, the pH was brought down to 5-6 with 0.1 N HCl at the start of titration. The fluorescence was measured at 380 nm with excitation at 320 nm.

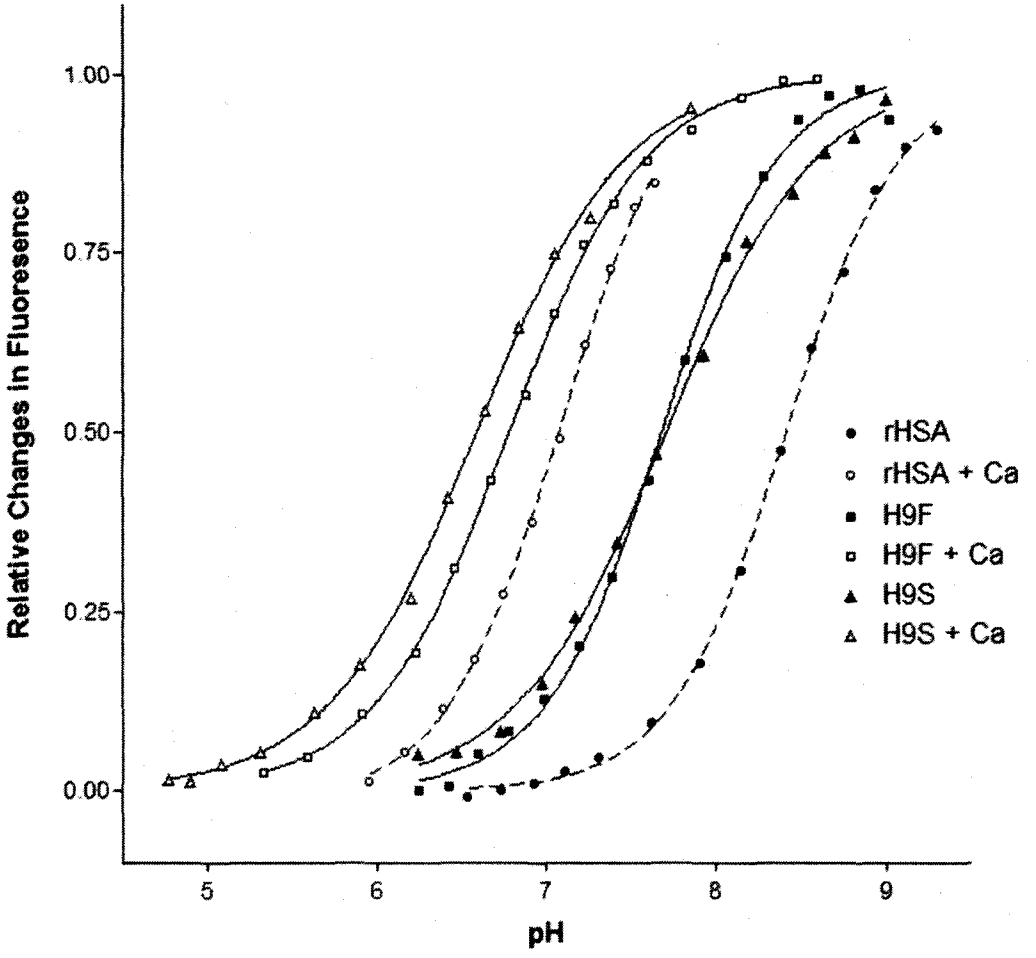

Figure 38. Fractional changes in the fluorescence of warfarin (0.5 μM) bound to H9F or H9S (10 μM) in the absence or presence of 2.5 mM $CaCl_2$ as a function of pH. The curves represent the theoretical curves fit to the data. For ease of comparison, the data for rHSA were also presented with the curves in broken lines.

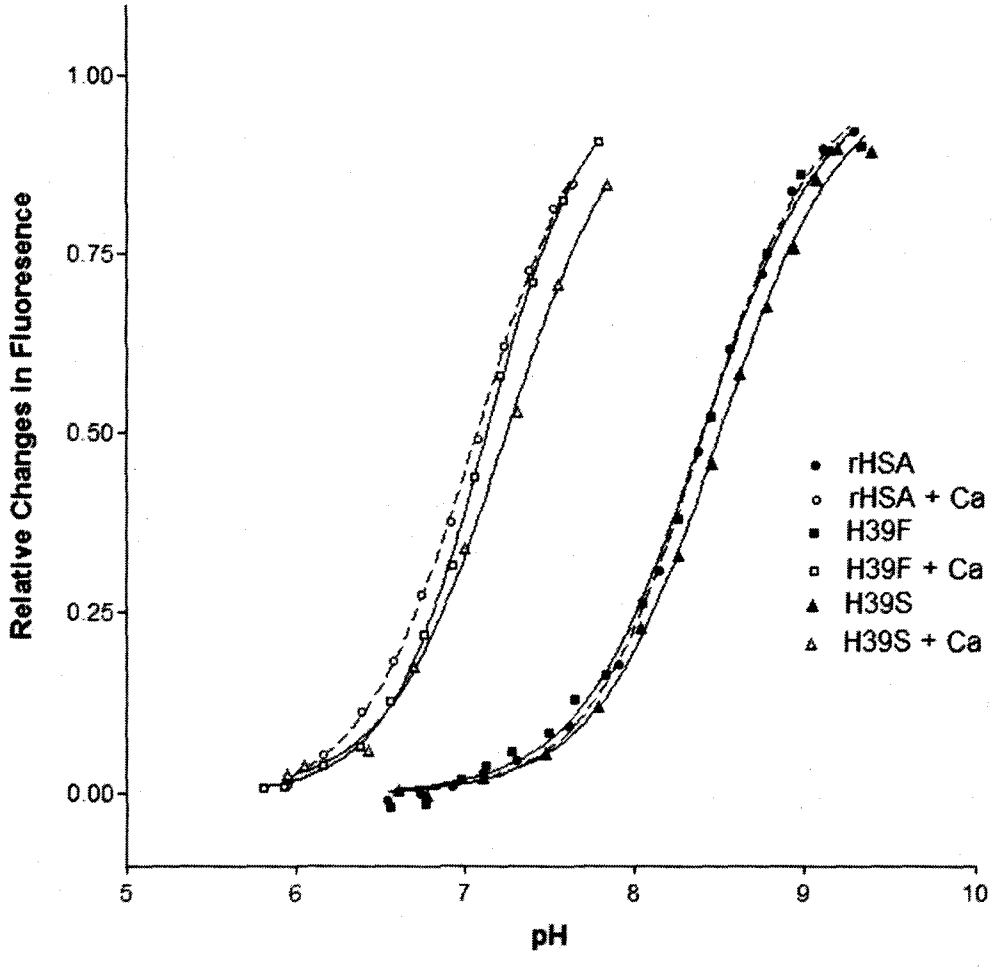

Figure 39. Fractional changes in the fluorescence of warfarin (0.5 μM) bound to H39F or H39S (10 μM) in the absence or presence of 2.5 mM $CaCl_2$ as a function of pH. The curves represent the theoretical curves fit to the data. For ease of comparison, the data for rHSA were also presented with the curves in broken lines.

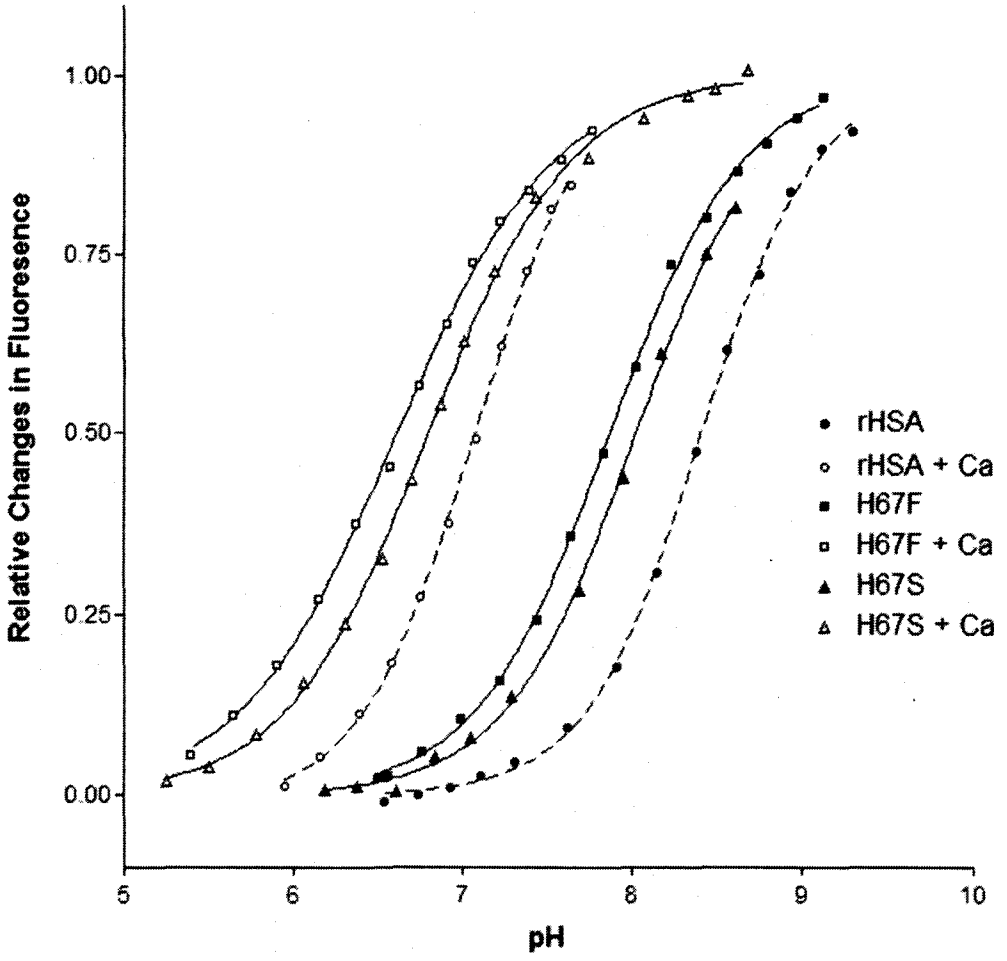

Figure 40. Fractional changes in the fluorescence of warfarin (0.5 μM) bound to H67F or H67S (10 μM) in the absence or presence of 2.5 mM $CaCl_2$ as a function of pH. The curves represent the theoretical curves fit to the data. For ease of comparison, the data for rHSA were also presented with the curves in broken lines.

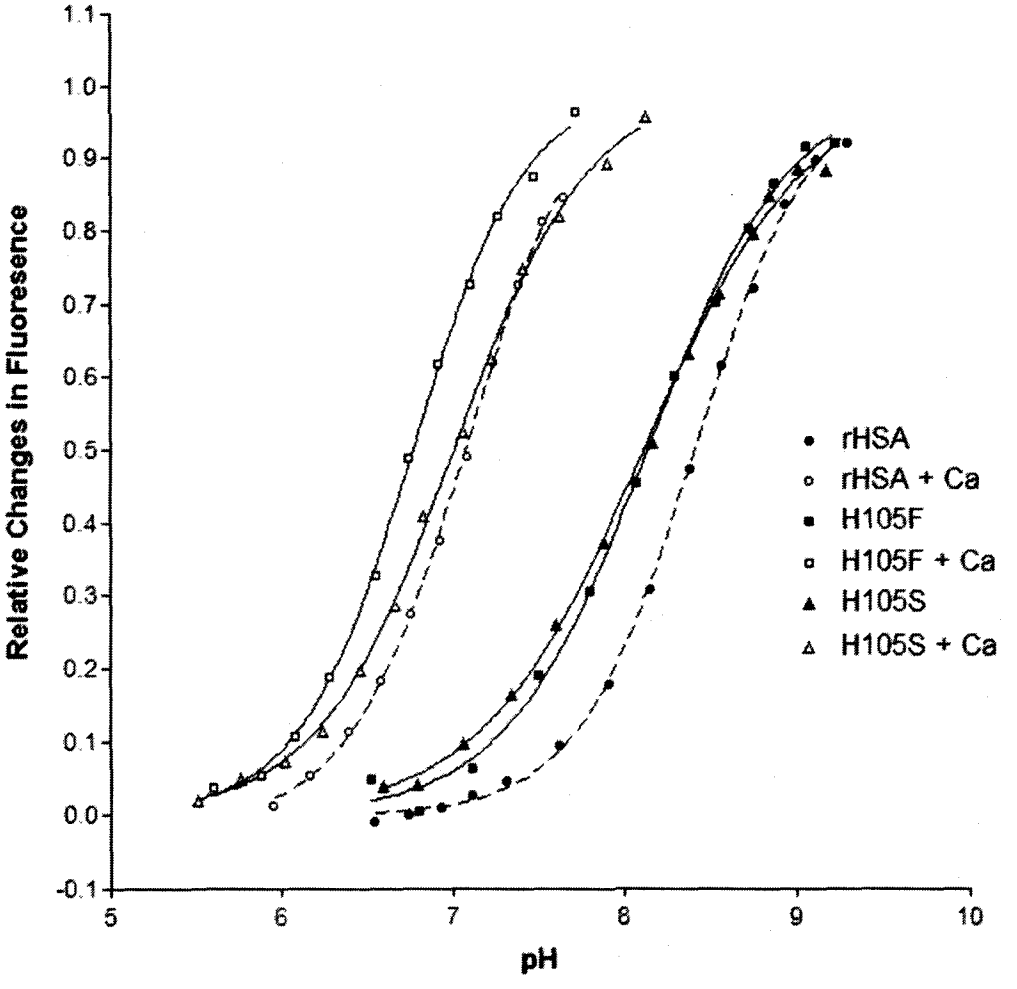

Figure 41. Fractional changes in the fluorescence of warfarin (0.5 μM) bound to H105F or H105S (10 μM) in the absence or presence of 2.5 mM $CaCl_2$ as a function of pH. The curves represent the theoretical curves fit to the data. For ease of comparison, the data for rHSA were also presented with the curves in broken lines.

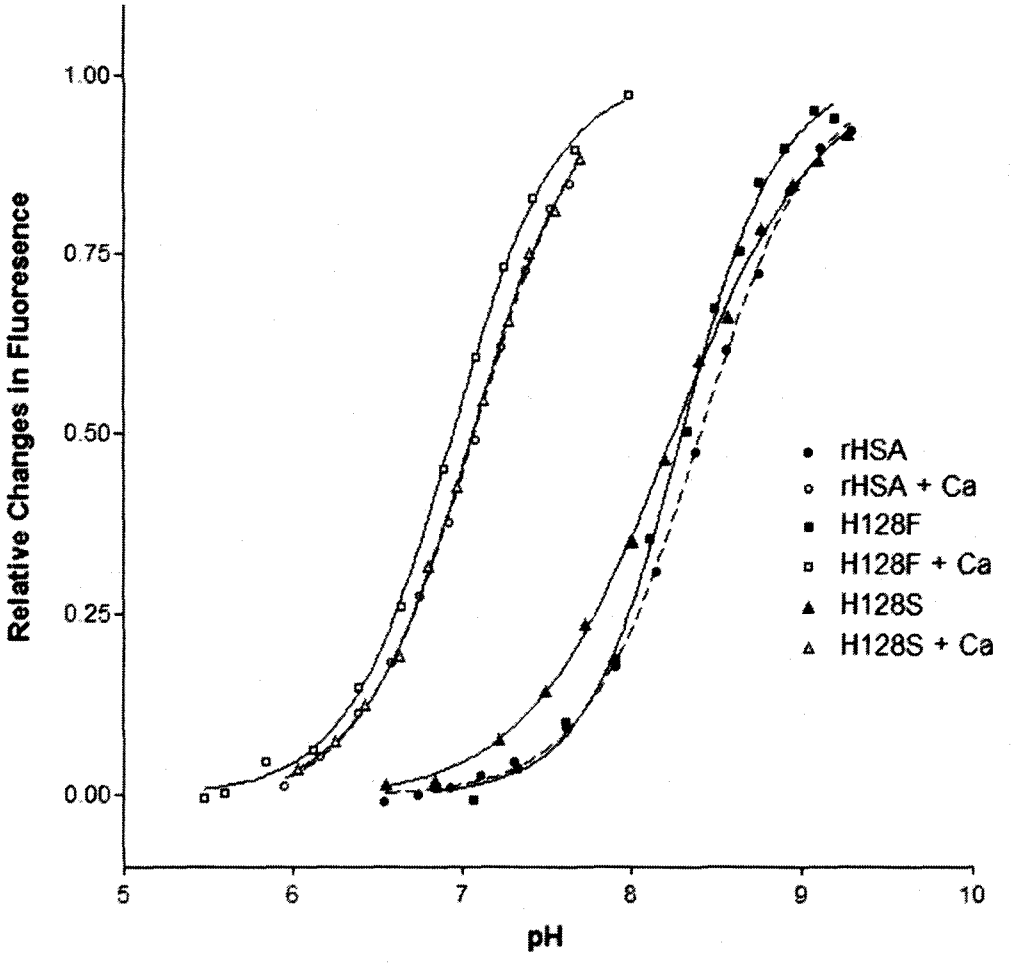

Figure 42. Fractional changes in the fluorescence of warfarin (0.5 μM) bound to H128F or H128S (10 μM) in the absence or presence of 2.5 mM $CaCl_2$ as a function of pH. The curves represent the theoretical curves fit to the data. For ease of comparison, the data for rHSA were also presented with the curves in broken lines.

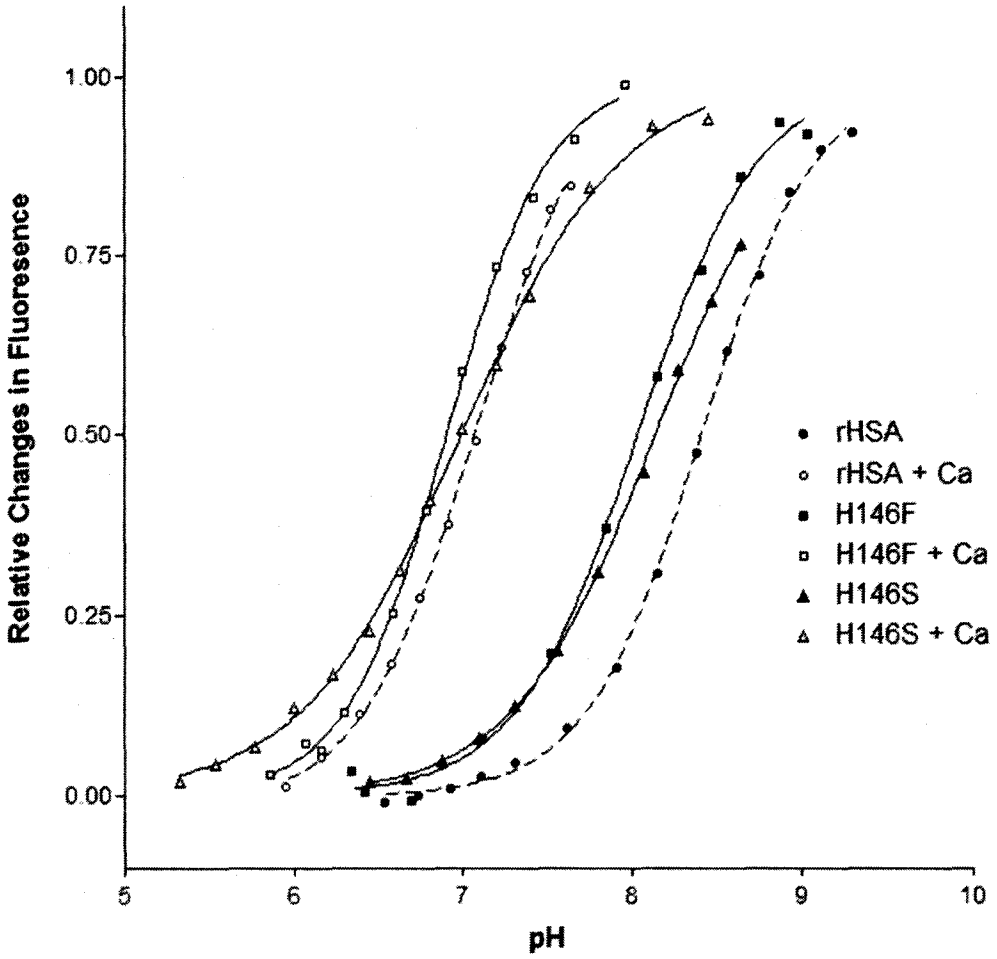

Figure 43. Fractional changes in the fluorescence of warfarin (0.5 μM) bound to H146F or H146S (10 μM) in the absence or presence of 2.5 mM $CaCl_2$ as a function of pH. The curves represent the theoretical curves fit to the data. For ease of comparison, the data for rHSA were also presented with the curves in broken lines.

Table 2. pH_{50} and Hill constant values for the HSA species in the presence and in the absence of $CaCl_2$. The protein solutions were titrated with 0.1 N NaOH in the absence and in the presence of 2.5 mM C_aCl_2 and the pH of a solution was, if needed, brought to appropriate pH with HCl before titration started.

Mutants	pH_{50} (H_2O)	Hill constant (H_2O)	pH_{50} (2.5 mM C_aCl_2)	Hill constant (2.5 mM C_aCl_2)
rHSA	8.41	1.29	7.09	1.25
H9F	7.68	1.27	6.79	1.08
H9S	7.71	0.99	6.59	0.99
H39F	8.41	1.21	7.13	1.50
H39S	8.51	1.21	7.25	1.26
H67F	7.87	1.10	6.62	0.94
H67S	8.03	1.13	6.80	1.03
H105F	8.14	1.06	6.77	1.33
H105S	8.11	0.93	7.01	1.11
H128F	8.30	1.53	6.95	1.40
H128S	8.25	1.02	7.07	1.35
H146F	8.03	1.22	6.91	1.45
H146S	8.14	1.03	7.00	0.92

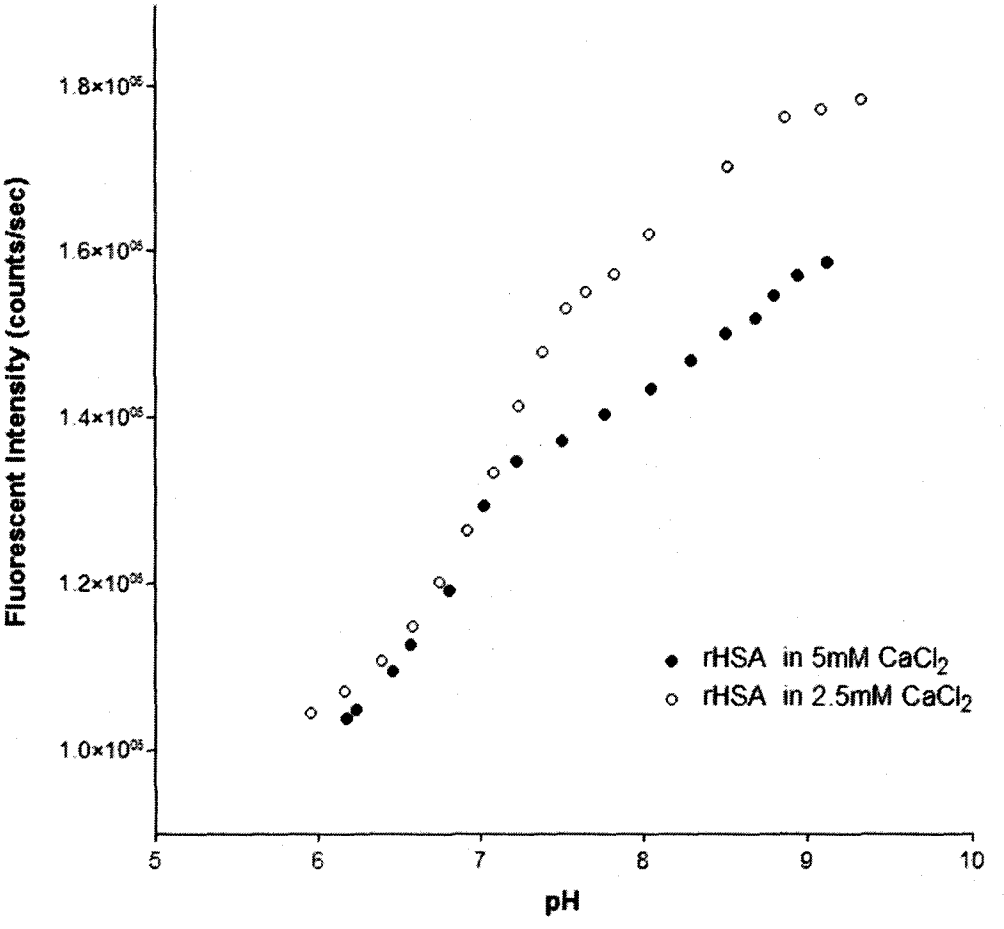

Figure 44. Effect of pH on the fluorescence of warfarin (0.5 μM) bound to rHSA (10 μM) in the presence of 2.5 mM and 5 mM $CaCl_2$. The pH was adjusted with addition of aliquots of 0.1 N NaOH and if necessary, the pH was brought down to 5-6 with 0.1 N HCl at the start of titration. The fluorescence was measured at 380 nm with excitation at 320 nm.

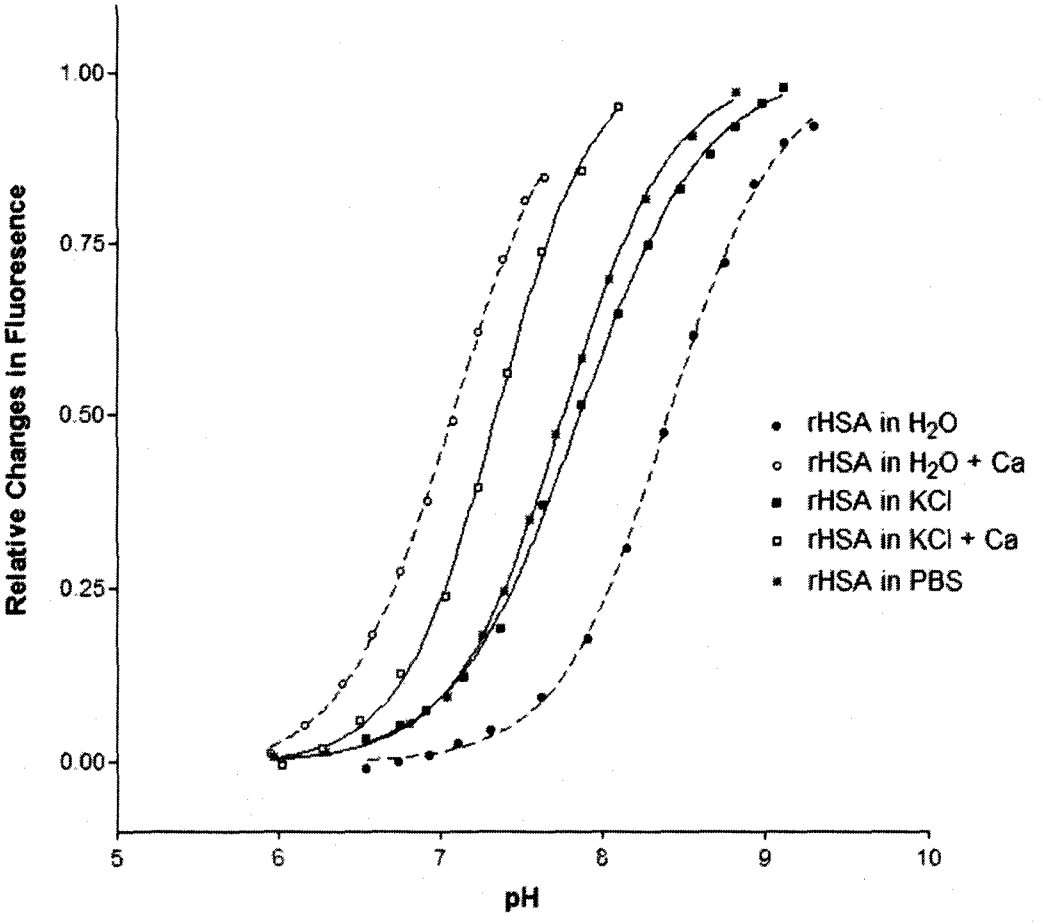

Figure 45. The effect of ionic strength on the pH titrations of warfarin-rHSA complex. The data are presented as fractional changes in fluorescence of warfarin (0.5 μM) bound to rHSA (10 μM) in the absence or presence of 2.5 mM $CaCl_2$ in different buffers as a function of pH. The concentration of KCl was 150 mM. The curves represent the theoretical curves fit to the data. The data for rHSA without buffer were presented with the curves in broken lines.

DISCUSSION

It can be reasoned that the only residues undergo dissociation/association of protons over a pH ranges of 6 to 9 are the imidazole groups of the histidine residues and the terminal amino group of HSA (Bos *et al.*, 1989b). Thus histidine residues must play a dominant role in the N-B transition. The linkage of a conformational change to a histidine residue is expected to cause a change in the pK of the histidine residue, as is well theorized by biophysical chemists. Because the N-B transition of HSA occurs at slightly elevated pH relative to the normal pK of 6.5 – 7.0 in a protein (Cantor and Schimmel, 1980a), the protonated form of the imidazole group must be stabilized by interactions, probably electrostatic in character, between the positively charged histidine residue and other residues in the neighborhood in the tertiary structure. Previous studies suggested that most probably five histidine residues are involved the N-B transition (Janssen *et al.*, 1981; Labro and Janssen, 1986; Droge *et al.*, 1983; Bos et al, 1989b). Results from ^{1}H NMR and acid/base titration experiments with two large proteolytic fragments of HSA lead Bos *et al.* (1989b) to predict that in domain I at least five histidine residues play a dominant role in the N-B transition. In the present work, this prediction has been confirmed and the assignment of the specific five residues resolved.

The N-B transition has been commonly described by the allosteric two-state model of Monod, Wyman and Changeux (1965). For example, when the proton is considered as the ligand, having the higher affinity for the N conformation, the allosteric two-state model can be used to describe the behavior of the N-B transition (Janssen *et al.*, 1981). Mathematical treatment of the two-state model can be found in a book by Cantor

and Schimmel (1980b). Briefly, in the absence of ligands, two conformations R_0 and T_0 are in equilibrium

$$R_0 \leftrightarrow T_0$$

with the allosteric constant $L = T_0 / R_0$. When the L is far greater than 1, the system will be found mainly in the T_0 conformation in the absence of ligands. The microscopic dissociation constant of a ligand for the two conformational states R_0 and T_0 is defined as K_R and K_T respectively. K_R/K_T is defined as c. A key assumption for the model is the conservation of symmetry of the properties of the protomers involved. A protomer is defined as a structural unit that bears one site for each of the various ligands. When L >>1, c < 1 (i.e., R is the high affinity state, which is the N form in the case of the N-B transition) and the number of protomers > 1, cooperativity in ligand binding will occur. However, the Hill constant for this cooperativity has often been confused with the observed Hill constant for the fraction of B (or 1 - N) versus pH when the two-state model is applied to the N-B transition. The former is the "saturation function" while the latter is the "function of state" (as defined in the original paper), which is the observed function in most of the studies reported of the N-B transition.

It is reasonable to assume that the substitution of noncharged residue for a histidine residue involved in the N-B transition by mutagenesis will favor the B conformation since the original histidine residue is expected to take part in the formation of salt bridges that stabilize the N conformation. In terms of the two-state model, such a mutant will have an increased L. By computer simulation, the following observation was made: an increase in L would shift the midpoint pH of the transition, i.e., the state function, to a lower pH value; the larger the pK of the original histidine residue, the

greater the shift of the midpoint (or pH_{50}) to a lower pH value; the Hill constant would stay almost constant (data not shown).

The results of the present work were in good agreement with the simulation. For example, five out of the six histidine residue examined showed pH_{50} shift toward low pH while the Hill constant showed no dramatic changes. In a previous study (Bos *et al.*, 1989b), the pKs of the five histidine residues corresponding to the five resonances (1 to 5 in the original paper) assigned to domain I were estimated to be 7.39, 7.49, 7.37, 7.76 and 7.28, respectively, which correlate impressively well with the changes in pH_{50} for the mutants. It is tempting to map the His9 to 7.76, H46 to 7.49, H105/H146 to 7.39/7.37, and H128 to 7.28.

The two-state model requires that the protomers are in equivalent positions and the conformational changes are symmetric, i.e., the protomers change state in a concerted manner. The requirement can only be approximately met in the case of HSA since it is a single-chain protein and no true equivalence/symmetry can be found. This departure from true symmetry might be augmented in the presence of calcium ions, which could be the origin of the complex titration curve observed for HSA species in the work presented here. The differences in the titration behavior may reflect differences in the calcium binding details. It is of interest to note that in a previous work (Lambert *et al.*, 1981), the titration behavior of HSA observed by CD experiments displayed a similar pattern (i.e., the inflection of the titration curve at about pH 7.5 in the presence of calcium ions) to what was observed by fluorescence techniques in the current work, thought no attention was paid to the phenomenon in that paper.

The effects of ionic strength on the midpoint of the N-B transition strongly suggest that electrostatic interactions play a principal role in the transition, which is consistent with many previous investigations (e.g., Leonard *et al.*, 1963; Bos *et al.*, 1988)) except with the one reported by Wilting *et al.* (1979).

The discovery made in the present study agrees favorably with what the published X-ray crystallographic structure of HSA suggests with respect to pK shifts of the histidine residues in domain II of HSA. The individual contact surface and neighbor residues of the six histidine residues in domain I that may be involved in the N-B transition are shown in Figures 46 to 51, respectively. The nitrogen atoms are in blue and oxygen atom in red. All the atoms shown in a figure are less than 7Å away from the contact surface. The figures were produced using the program Protein Explorer (Martz, 2002). A histidine residue that contributes to the transition is expected to both possess a usually high pK for the imidazole moiety and take part in stabilizing the N conformation of HSA, which would shift the pH_{50} to a higher value. Consistent with the large contribution of H9 to the N-B transition, i.e., raising the pH_{50} of the transition to within the physiological pH (under conditions of physiological concentration of calcium ions and physiological ionic strength), The imidazole group of His9 is in close contact with Asp13 and the carboxyl groups of Asp 255 and Glu6 are less than 7Å away from His9. The combined negative electric field is expected to increase the pK of His9. The local structure around Asp 255 may contribute to the interface between domain II and domain I. Similar electro-static interactions can be found around His67: Asp 249 is in close contact with His67; Glu95 and Glu252 are within 7Å distance of His67, again suggesting that negatively-charged residues from domain II, i.e., Asp255 and Glu252 are also

involved in the stabilization of the N conformation of HSA, which in turn lends evidence to the important role of His67 as well as that of H9 in the transition. In the case of His105, Asp107 and Glu86 are within the 7Å range. Since there is no direct interaction between His105 and any charged residue of domain II, His105 may contribute to the stabilization of the N-conformation by stabilizing a favorable local conformation of domain I that may be less tightly coupled to the more global N conformation, which may account for the reduced effect of His105 in the N-B transition compared to His9 or H67. For H146, Asp108, a distant neighbor in primary structure, is within the 7Å range. In the case of H128, only neighbors close in primary structure, Asp129 and Glu131 are close by, which suggests smaller contribution to the N-B transition. In excellent agreement with the results in the present work, there is no negatively-charged residue in the spatial neighbor of H39 strongly dismissing its involvement in the N-B transition.

The results also suggest that the substitution of serine or phenylalanine for histidine residue does not cause dramatic perturbation in the local or global structure of HSA, which is in agreement with the theory proposed by Bordo and Argos (1991). Based on the available 3-D structures of globin proteins, Bordo and Argos defined the structural equivalence of residues and suggested exchange matrices that serve as guidelines for 'safe' amino acid substitutions with a minimal structural impact. Based on the exchange matrices and published mutagenesis experiments (e.g., Markiewicz *et al.*, 1994), serine and phenylalanine were chosen as the safe residues in order to minimize changes in characteristics of the introduced residues other than the charge.

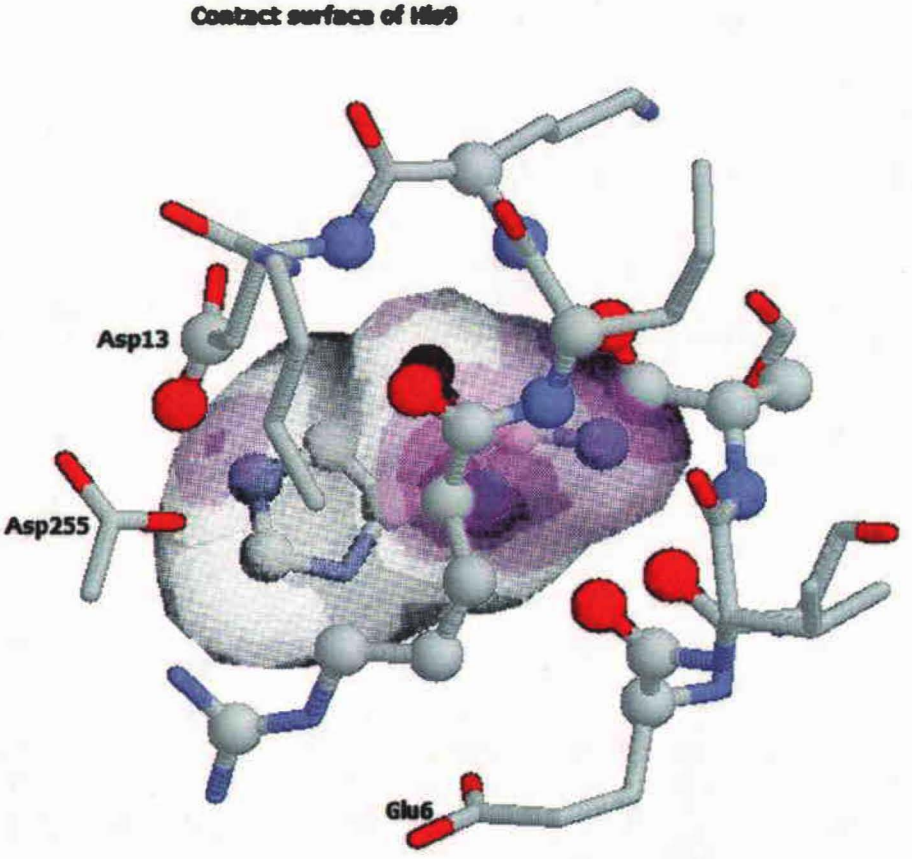

Figure 46. Contact surface and neighbor residues of His9. Nitrogen atoms are in blue and oxygen atom in red. The figure was produced using the program Protein Explorer (Martz, 2002).

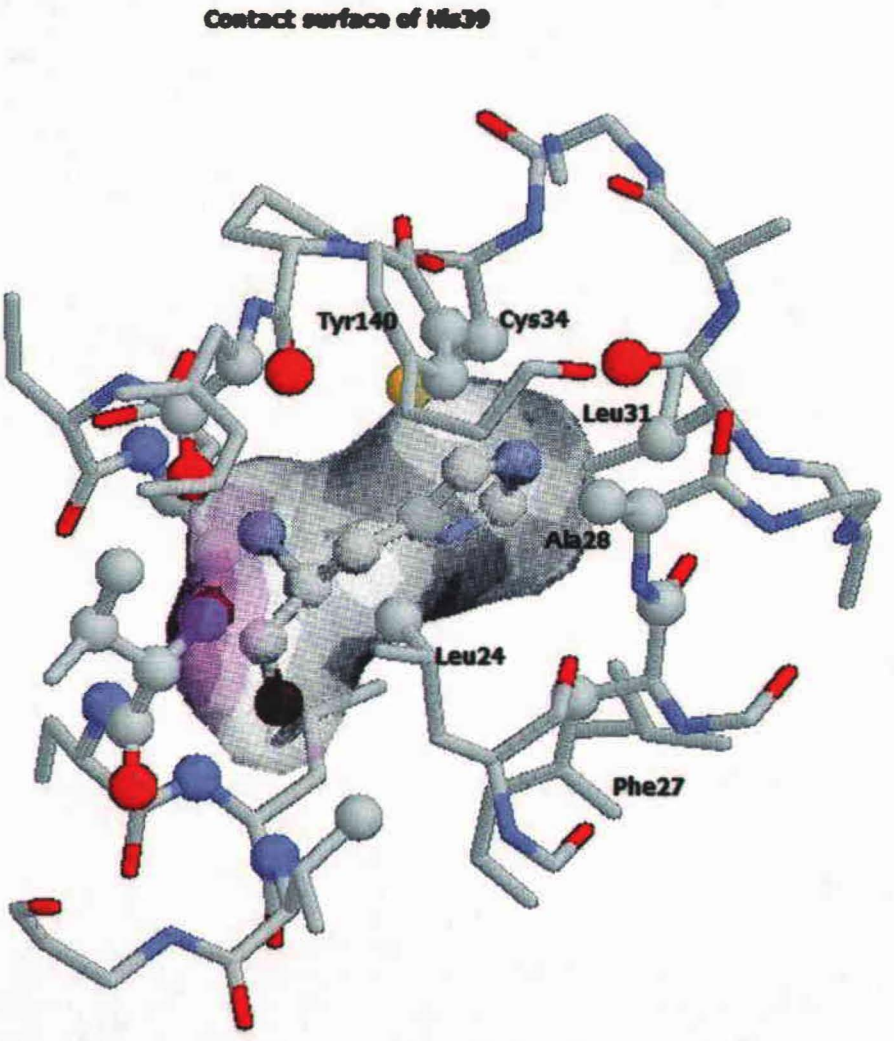

Figure 47. Contact surface and neighbor residues of His39. Nitrogen atoms are in blue and oxygen atom in red. The figure was produced using the program Protein Explorer (Martz, 2002).

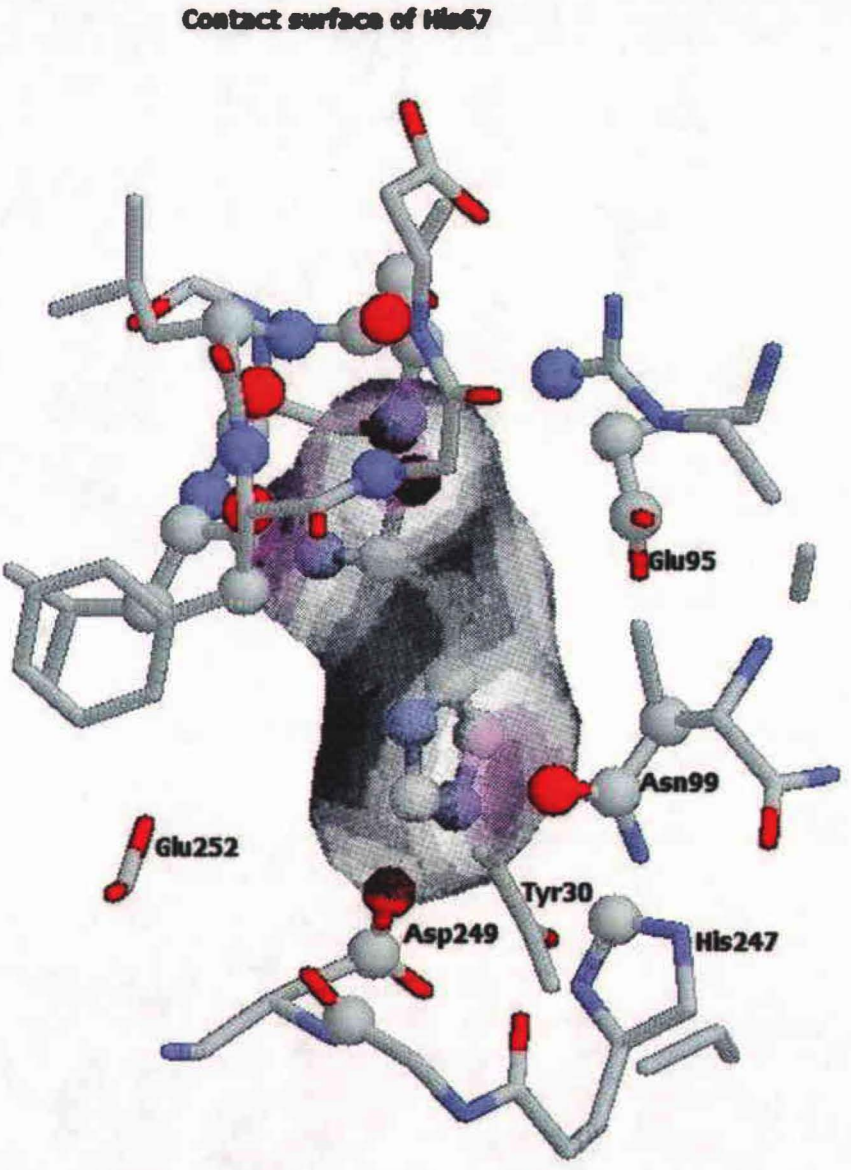

Figure 48. Contact surface and neighbor residues of His67. Nitrogen atoms are in blue and oxygen atom in red. The figure was produced using the program Protein Explorer (Martz, 2002).

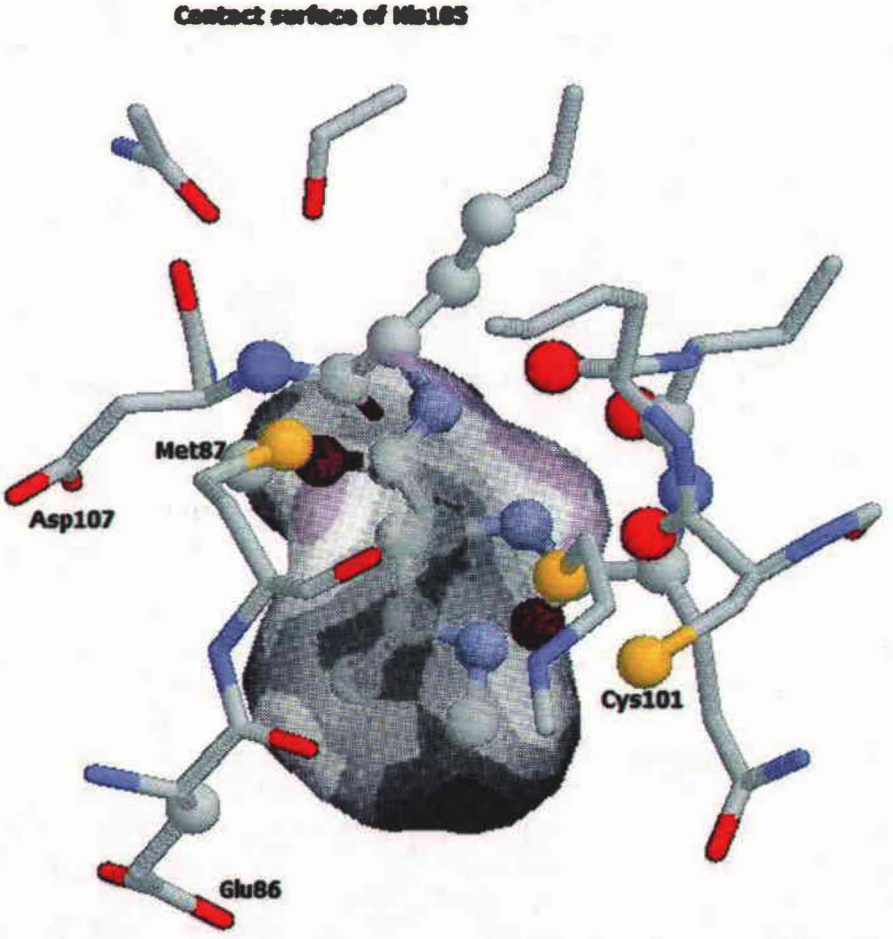

Figure 49. Contact surface and neighbor residues of His105. Nitrogen atoms are in blue and oxygen atom in red. The figure was produced using the program Protein Explorer (Martz, 2002).

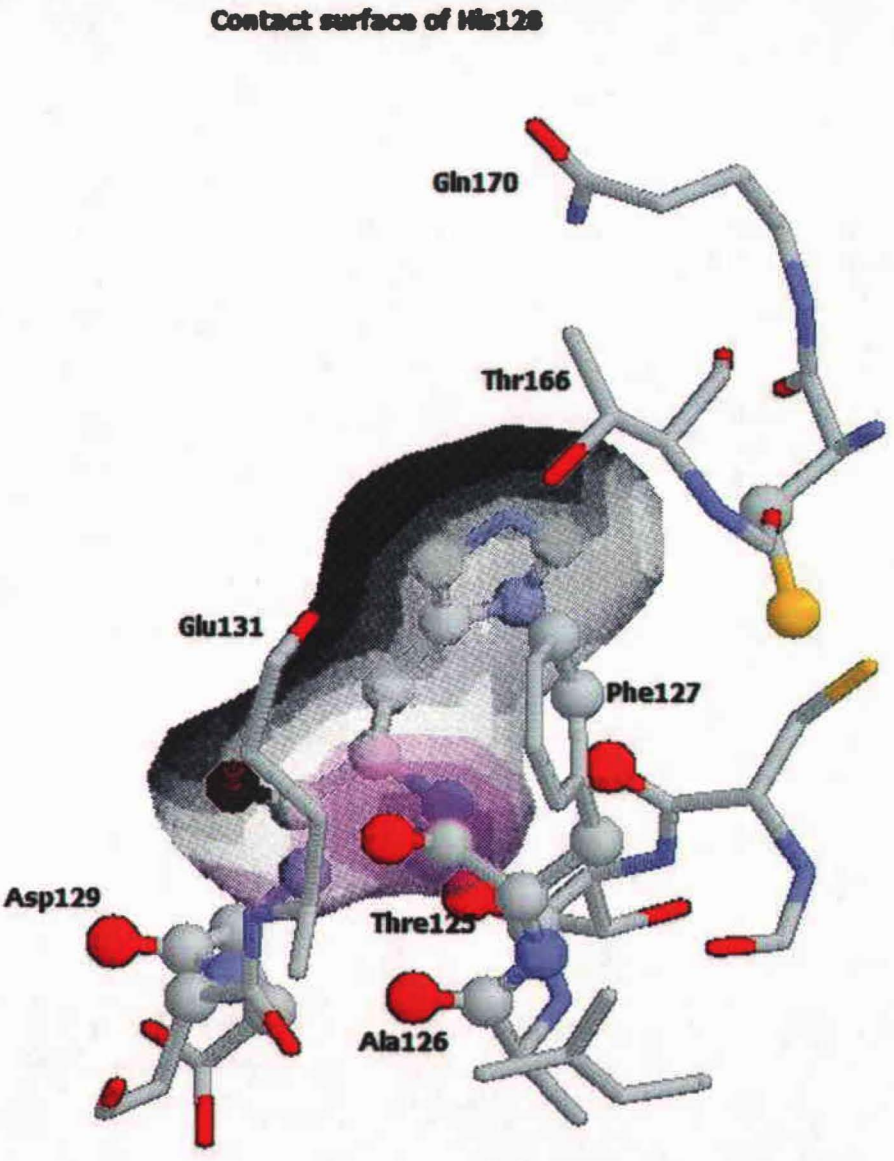

Figure 50. Contact surface and neighbor residues of His128. Nitrogen atoms are in blue and oxygen atom in red. The figure was produced using the program Protein Explorer (Martz, 2002).

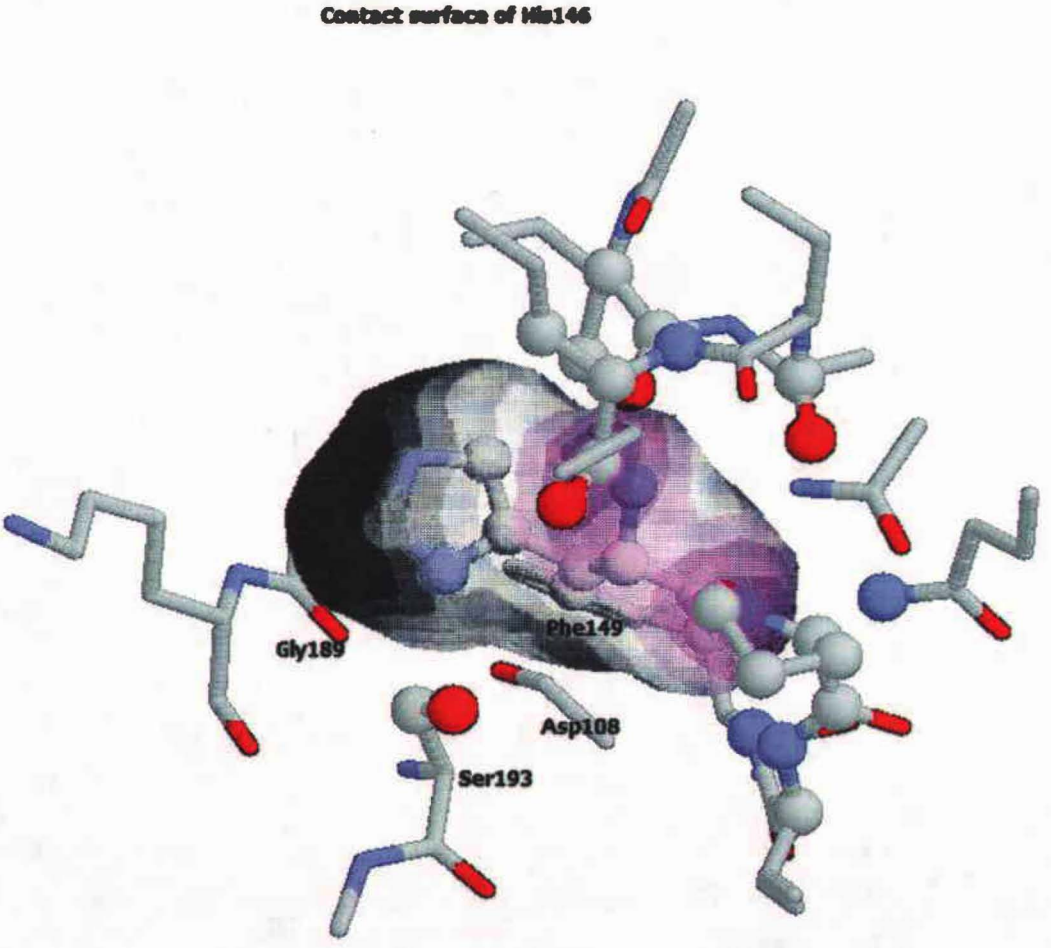

Figure 51. Contact surface and neighbor residues of His146. Nitrogen atoms are in blue and oxygen atom in red. The figure was produced using the program Protein Explorer (Martz, 2002).

CHAPTER 4
STUDY OF THE STRUCTURAL BASIS FOR HSA-MEDIATED CATALYSIS OF PROSTAGLANDIN METABOLISM

Our present study was undertaken to obtain insights into the HSA/prostaglandin interaction by comparing the rate at which specific site-directed mutants of HSA with substitutions in subdomain IIA catalyze the breakdown of 15-keto-PGE_2 to the keto-enol tautomer intermediate and to the final reaction product PGB_2. Since the spectroscopic assay technique which monitors absorbance at 505 nm has been well-validated in a previous study (Fitzpatrick *et al.* 1984) and is inexpensive and technically easy to carry-out, we chose it to assay various subdomain IIA mutants for their ability to convert 15-keto-PGE_2 to the keto-enol tautomers. The following recombinant HSA species were studied: wild type recombinant (wtrHSA), K195M, K199M, F211V, W214L, R218M, R218H, R218P, R222M, H242V, and R257M. Recombinantly produced fragments corresponding to domains I, II and III of HSA were also produced and assayed in a manner identical to full-length HSA. Part of this study has resulted in a publication (Yang *et al.*, 2002).

MATERIALS AND METHODS

Synthesis and purification of recombinant HSA

Introduction of mutations into the HSA coding region

Specific mutations were introduced into the HSA coding region in a plasmid vector containing the entire HSA coding region (pHiL-D2 HSA) using standard techniques as previously described (Petersen *et al.* 1996, 1997, 2000).

Expression of recombinant HSA

Each pHiL-D2 HSA expression cassette coding for a particular HSA mutant was introduced into the yeast species *Pichia Pastoris* by electroporation. A yeast clone which contained the expression cassette stably integrated into the chromosomal DNA was isolated in each case.

Verification of the DNA sequence of HSA clones

The total genomic DNA from each *Pichia Pastoris* clone used to produce a particular HSA species was isolated using standard techniques. The genomic DNA isolated from each clone was used as template to amplify the entire HSA coding region by PCR. For each clone, the entire HSA coding region was sequenced using the dideoxy nucleic acid chain termination technique, and the translation product corresponding to this sequence was found to match a previously published HSA sequence at all amino acid positions except for the mutation introduced into a particular HSA mutant.

Purification of recombinant HSA

The secreted HSA was isolated from growth media as follows. The medium was brought to 50% saturation with ammonium sulfate at room temperature. The temperature was then lowered to 4°C, and the pH was lowered to 4.4, the isoelectric point of HSA. The precipitated protein was collected by centrifugation and resuspended in distilled water. Dialysis was carried-out for 72 hours against 100 volumes of phosphate buffered saline (PBS) (137 mM NaCl, 2.7 mM KCl, 4.3 mM Na_2HPO_4, 1.4 mM KH_2PO_4, pH 7.4) with one change of buffer. The solution was loaded onto a column of Cibacron Blue immobilized on Sepharose 6B (Sigma, St. Louis, MO). After the column was washed with 10 bed volumes of PBS, HSA was eluted with 3 M NaCl. The eluent was dialyzed against PBS and passed over a column of Lipidex-1000 (Packard Instruments) to remove hydrophobic ligands possibly bound to HSA (Glatz and Veerkamp 1983). The resulting protein exhibited only one band on SDS-PAGE. Protein concentrations were determined by the BCA method, a modification of the Lowry procedure in which bicinchoninic acid is substituted for tartrate.

Synthesis and purification of recombinant HSA fragments

We used a protocol that was a modification of a previously published technique to express and purify domains I, II, and III of HSA (Dockal *et al.* 1999). The specifics of our methodology follow.

Cloning of coding regions for domains I, II and III

Using pHilD-2 HSA as template the following three sets of DNA oligonucleotides were used to amplify each HSA domain by PCR.

Domain I (amino acid positions 1-197)

5' DNA primer: 5' GTATCTCTCGAGAAAAGAGAGGCTGAAGCTGATGCACACAAGAGTGAGG 3'

3' DNA primer: 5' GCGGTGAGCGAATTCTTATCTCTGTTTGGCAGACGAAG 3'

Domain II (amino acid positions 189-385)

5'DNA primer: 5' GTATCTCTCGAGAAAAGAGAGGCTGAAGCTGGGAAGGCTTCGTCTGCCAAACAG 3'

3' DNA primer: 5' GCGGTGAGCGAATTCTTACTGAGGCTCTTCCACAAGAGG 3'

Domain III (amino acid positions 381-585)

5' DNA primer: 5' GTATCTCTCGAGAAAAGAGAGGCTGAAGCTGTGGAAGAGCCTCAGAATTTAATC 3'

3' DNA primer: 5' GCGGTGAGCGAATTCTTATAAGCCTAAGGCAGCTTGAC 3'

All amplified fragments were digested with the DNA restriction enzymes *Xho*I and *EcoR*I. It should be noted that the DNA fragment corresponding to domain III was only partially digested with *Xho*I since it contained an internal *Xho*I site. A DNA fragment containing full length domain III was isolated from the partial digest with *Xho*I and used for *EcoR*I digestion and cloning. The yeast expression vector pPIC9, which contains the alpha mating factor secretion signal sequence, was also digested with *Xho*I and *EcoR*I. All fragments were ligated into pPIC9 in frame with the alpha mating factor secretion signal sequence, which was shown to be cleaved at the expected position liberating the translation product of the cloned cDNA fragment for each of the domains.

Verification of DNA sequence of clones and protein expression and purification

The methods used to verify the DNA sequence of each yeast clone expressing a particular domain was identical to that used to analyze clones expressing full length HSA.

Since all three HSA domains bound to Cibacron Blue Sepharose, the HSA domains were expressed and purified using methods identical to those used to purify full-length HSA.

Spectroscopic assay of 15-keto-prostaglandin E_2 (15 keto-PGE_2) breakdown

Background

As shown in Figure 52, 15-keto PGE_2 is converted to 15-keto PGB_2 through a keto-enol tautomer intermediate which has a peak absorbance at 505 nM (Fitzpatrick *et al.* 1984). That study verified that the breakdown of 15-keto PGE_2 to the keto-enol tautomers, could be accurately monitored by measuring the absorbance at 505 nm of a solution containing 15-keto-PGE_2 as a function of time (Fitzpatrick *et al.* 1984). By monitoring absorbance at 505 nm it was also shown in the above study that albumin from different species catalyzed the breakdown of 15-Keto-PGE_2 to the keto-enol tautomer intermediate at different rates, presumably as a result of differences in the binding site structure. This previously validated assay system was used with minor modifications. The previously determined extinction coefficient of 35,000 at 505 nm (Fitzpatrick *et al.* 1984) for the keto-enol tautomers can be used in the following measurements to convert measured A_{505nm} values to keto-enol tautomer concentrations.

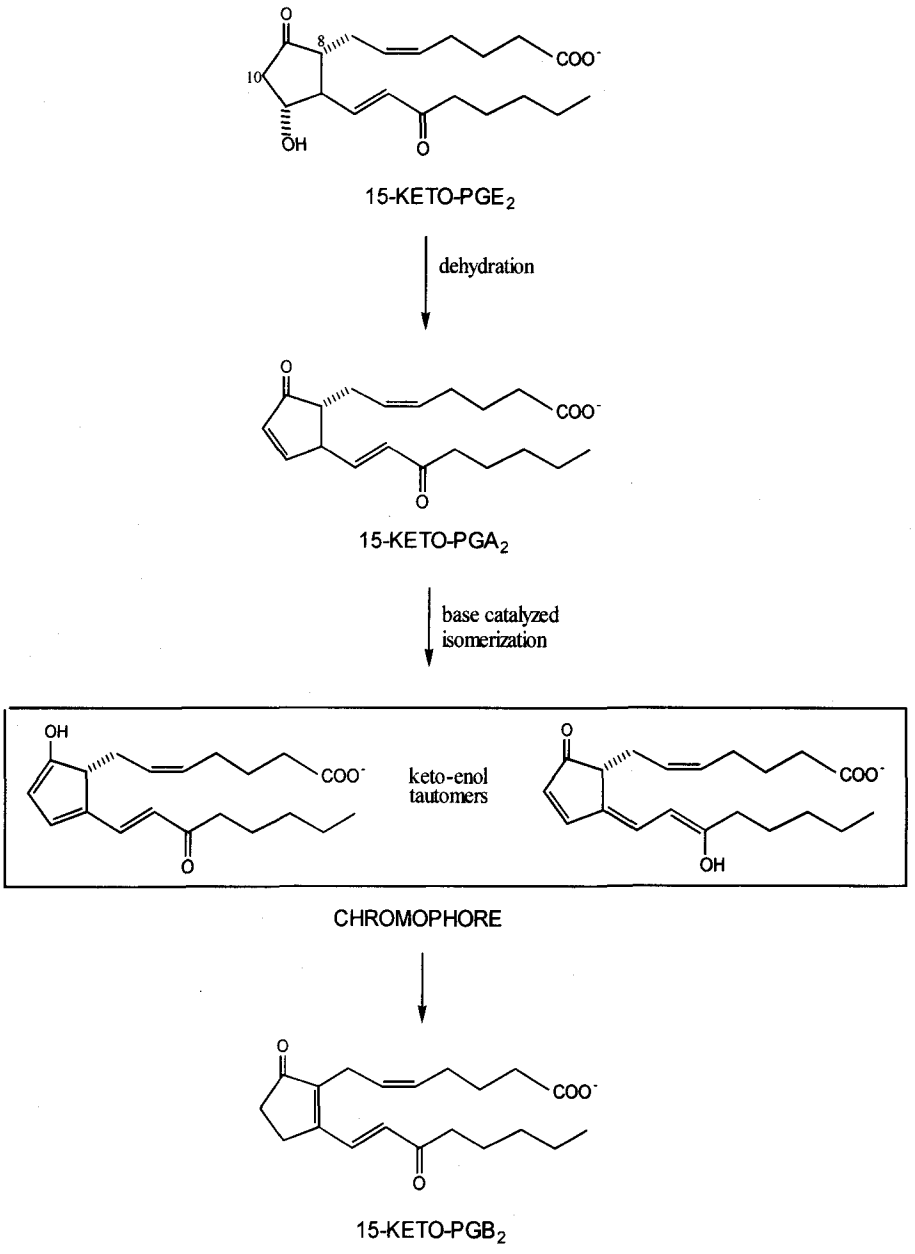

Figure 52. Proposed mechanism by which 15-Keto-PGE_2 is converted to 15-keto-PGB_2 (Fitzpatrick, Liggett and Wynalda, 1984). The spectroscopic assay employed in the present study monitors the formation of the keto-enol tautomeric hybrid of 15-keto-PGA_2, which absorbs light at 505 nm.

General experimental parameters

One mg of 15-keto-PGE_2 was dissolved in 200 µl of ethanol and 10 µl containing 50 µg was aliquoted into 20 1.5 ml-Eppendorf tubes. The ethanol was removed from each tube by vacuum drying. For each experiment, the 50 µg of dried prostaglandin in one tube was dissolved in 20 µl of PBS. Each assay contained 2 µl of dissolved prostaglandin (5 µg) and 98 µl of a particular HSA sample at a concentration of 5 mg/ml in PBS. The initial mole ratio of 15-keto-PGE_2/HSA was 2:1 (140 µM 15-keto-PGE_2/70 µM HSA). As a control for prostaglandin breakdown in the absence of HSA, assays were run containing 2 µl of dissolved prostaglandin (5 µg) and 98 µl of PBS (5 mg/ml). Additionally, a control was run using 5 mg/ml commercial bovine serum albumin (BSA) since a previous study had shown that BSA has a catalytic rate for the above process much lower than HSA. For each assay the 100 µl solution was transferred to an ultra-micro quartz spectrophotometer cuvette designed for measuring absorbance using sample volumes of 50 µl or greater (Sigma). The path length of the cuvette was 1 cm. For each albumin species the blank consisted of a sample containing the same albumin species but lacking 15-keto-PGE_2. For the control assay in which the breakdown of 15-keto-PGE_2 was monitored in PBS in the absence of albumin a solution of PBS lacking albumin and 15-keto-PGE_2 was used as a blank. For all samples assayed absorbance at 505 nm was determined at 1 h, 2 h, 4 h, 6 h, 8 h, 16 h, and 26 h after mixing together the assay components. Reactions were carried-out at 25 °C in a constant temperature incubator. Samples were only exposed to light when withdrawn from the incubator for absorbance measurements.

Analysis of data

The calculation of an approximate relative rate constant for the formation of the keto-enol tautomers for each species from the absorbance at 505 nm after 1 h was as follows. The absorbance at 505 nm after 1 h determined for wild type HSA was set equal to 1. The normalized rate constants for all other HSA species are equal to (A505nm at 1 h) / (A505nm at 1 h of wild type HSA). All experiments were done three times and the relative rate constants shown are the average of three determinations. To estimate the relative rate constant for the conversion of keto-enol tautomers to the final product, that is, 15-keto-PGB_2, nonlinear regression was applied to the 26-h data using the computer program GraphPad Prism (GraphPad, SanDiego, CA).

Assuming a two-step consecutive reaction model:

$$A \xrightarrow{k_1} B \xrightarrow{k_2} C$$

where A corresponds to 15-keto-PGE_2, B corresponds to 15-keto-PGA_2, which is monitored by observing the chromophore (enol tautomeric hybrid) formation, and C corresponds to 15-keto-PGB_2, the final product, the following equation was used.

$$[B] = [A]_0 \frac{k_1}{k_2 - k_1}\left(e^{-k_1 t} - e^{-k_2 t}\right)$$

As an illustration, the time course of A, B and C, based on the color formation in the presence of wild type recombinant HSA, was simulated using the above-mentioned model and is shown in Figure 53.

RESULTS

A 26-h time course showing absorbance at 505 nm, which corresponds to the amount of keto-enol tautomer as a function of time is shown as Figures 54, 55 and 56. As expected, the rate at which 15-keto-PGE_2 is converted to the keto-enol tautomers is insignificant in the absence of albumin. Our control with BSA found that wild type BSA was much less efficient than wild type HSA in catalyzing keto-enol tautomer formation, a result expected from a previous study. Most mutations in subdomain IIA had a significant effect on the kinetics of keto-enol tautomer formation (Figures 54, 55 and 56). The analysis of the time course for keto-enol tautomer formation is complicated by the fact that the keto-enol tautomeric hybrid decays to 15-keto PGB_2 (a species which does not absorb light) at a significant rate as the concentration of the keto-enol tautomers builds up (Figure 52). Based on the observation that the rate of increase in absorbance at 505 nm is linear until 2 h after the start of the reaction for all HSA species, the following approximation was made. We assumed that within 1 h after the start of the reaction, the rate of formation of 15-keto PGB_2 was insignificant because only a very small amount of its precursor, the keto-enol tautomers, had been formed. We also assumed that the concentration of the HSA substrate 15-keto-PGE_2 did not change significantly during this time period. It should be noted that the formation of 15-keto-PGA_2 and its keto-enol tautomers occur simultaneously when 15-keto-PGE_2 decomposes in the presence of HSA. The above assumptions allowed us to calculate an approximate relative rate constant for the formation of the keto-enol tautomers for each

species from the absorbance at 505 nm after 1 h as follows. The absorbance at 505 nm after 1 h determined for wild type HSA was set equal to 1. The normalized rate constants for all other HSA species are equal to (A_{505nm} at 1 h) / (A_{505nm} at 1 h of wild type HSA). All experiments were done three times and the relative rate constants shown are the average of three determinations. The approximate relative rate constants calculated for keto-enol tautomer formation for K195M, K199M, F211V, W214L, R218M, R218P, R218H, R222M, H242V, and R257M were 1.07, 0.51, 0.46, 1.77, 0.40, 0.52, 0.36, 1.59, 1.17, and 0.15, respectively (Table 3). By visual inspection of Figures 54, 55 and 56, it is clear that specific mutations affect the rate at which the keto-enol tautomer is converted to 15-keto-PGB_2. For example, for some HSA species, the A_{505nm} reaches a peak and then only decreases slightly, while for other species the A_{505nm} reaches a peak and then drops rapidly, indicating that after a certain time period the rate of 15-keto-PGB_2 formation significantly exceeds the rate of keto-enol tautomer formation for some HSA mutants. We estimated the values for step 2 (Table 3) using nonlinear regression assuming a two-step model:

15-keto-PGE_2 $\rightarrow$ chromophore (enol tautomeric hybrid) $\rightarrow$ 15-keto-PGB_2

Based on the 95% confident intervals, the computed values for step 2 are comparable to those for step 1 with regard to reliability. The values for step 1 obtained by regression (data not shown) agree well with those obtained by the simple calculation based on the data for the first h of reaction.

Domain II caused significant formation of the keto-enol tautomers, while domains I and III showed virtually no color formation (Figure 56). BSA showed an

initial rate about one third that of Domain II. The normalized rate constant observed for domain II relative to a wild type HSA was about 0.1. The above result is important in two ways. Firstly, It suggests that prostaglandins and related arachidonic acid metabolites bind to the ligand-binding site located in subdomain IIA of HSA, a result indicated by a large amount of previous circumstantial evidence, that is, competitive binding studies, X-ray crystallography. Secondly, the above result shows that some of the subdomain IIA binding site structure is maintained in a domain II fragment, independently of domains I and III. However, the reduced catalytic rate observed for domain II suggests that domains I and III play some role in stabilizing the native structure of the subdomain IIA prostaglandin-binding site.

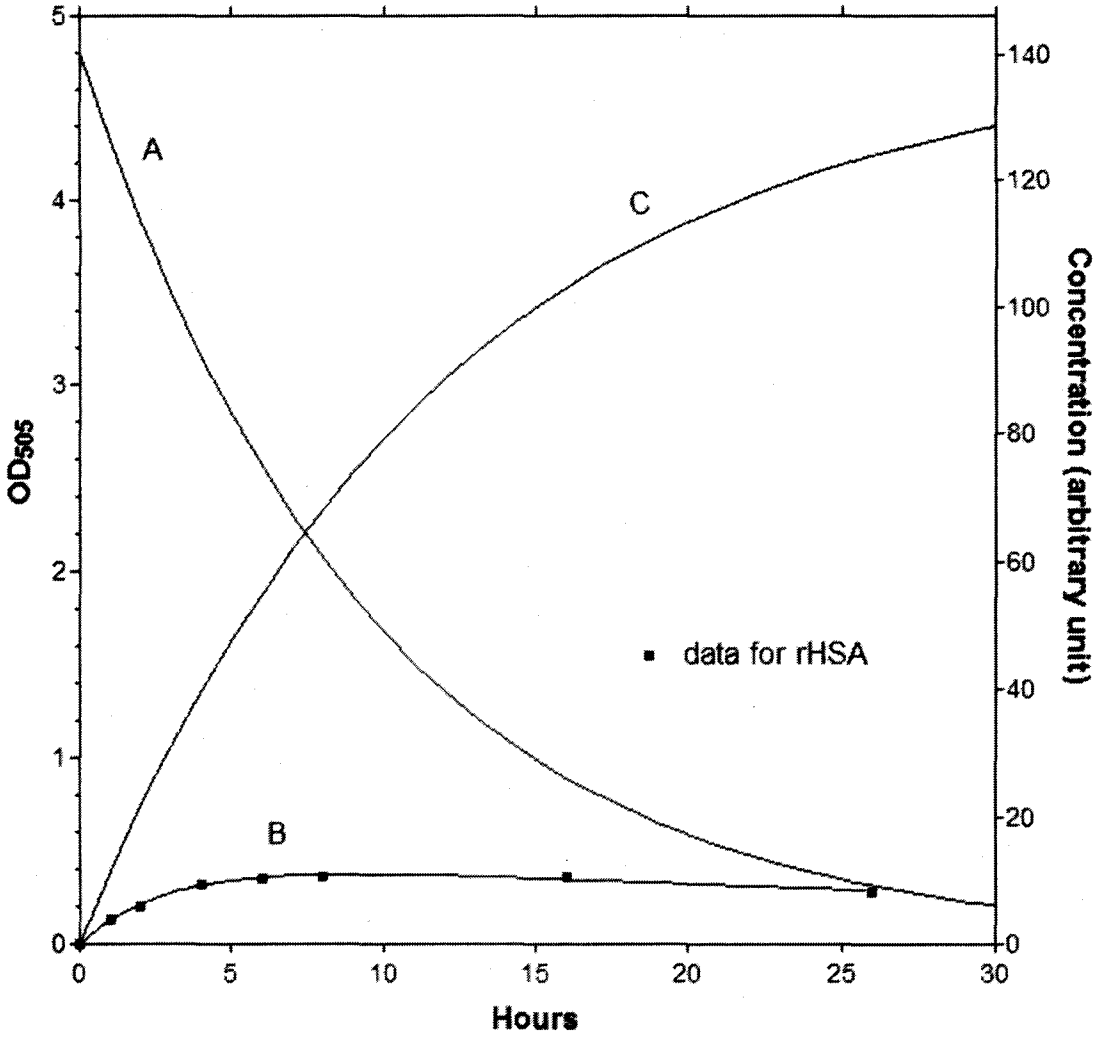

Figure 53. Time course for a two-step consecutive reaction. This simulation is based on the data for wild type recombinant HSA (points fitted by curve B) by assuming a two-step consecutive reaction model:

$$A \xrightarrow{k_1} B \xrightarrow{k_2} C$$

where A corresponds to 15-keto-PGE_2, B corresponds to 15-keto-PGA_2, which is monitored by observing the chromophore (enol tautomeric hybrid) formation, and C corresponds to 15-keto-PGB_2, the final product.

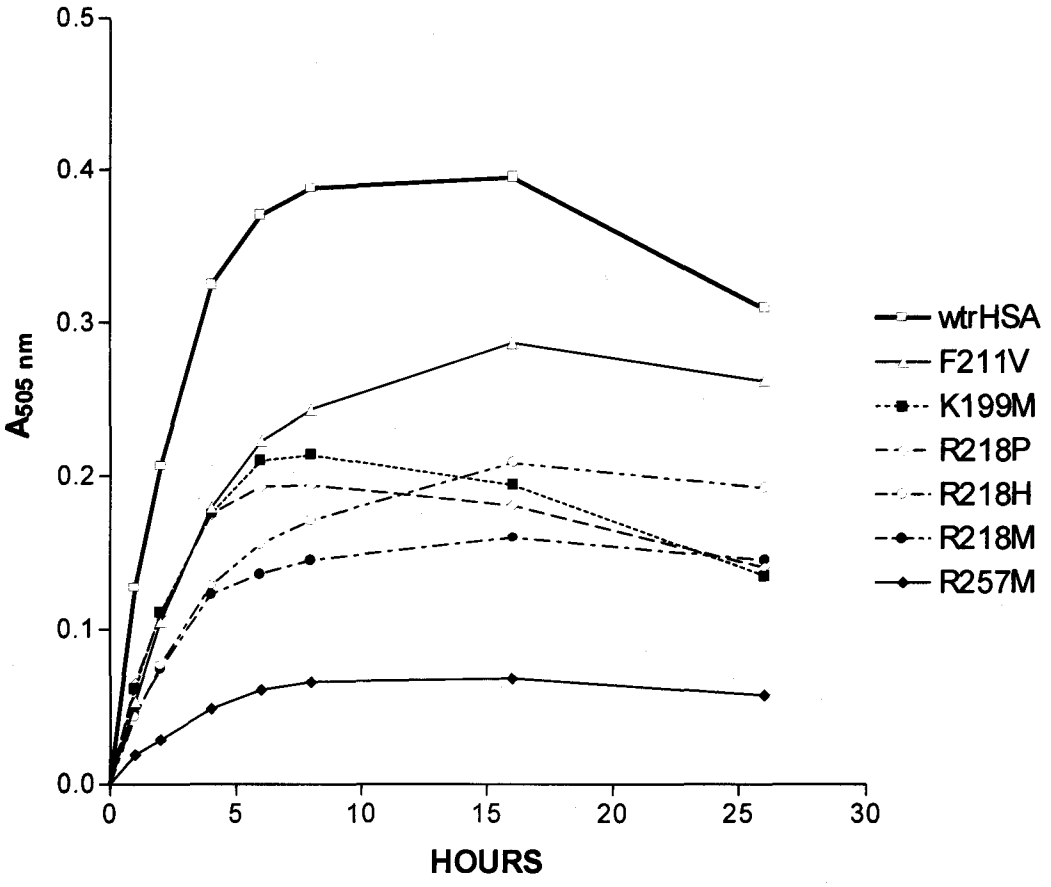

Figure 54. Effects of albumin species (group A) on 15-keto-PGE_2 catalysis. The figure shows the absorbance at 505 nm of a cuvette containing a particular albumin species or wild type HSA fragment and the same initial amount of 15-keto-PGE_2 on the ordinate. Incubation time of 15-keto-PGE_2 with a particular albumin species is shown on the abscissa in hours. The data are for wild type recombinant HSA (wtrHSA), F211V, K199M, R218P, R218H, R218M and R257M.

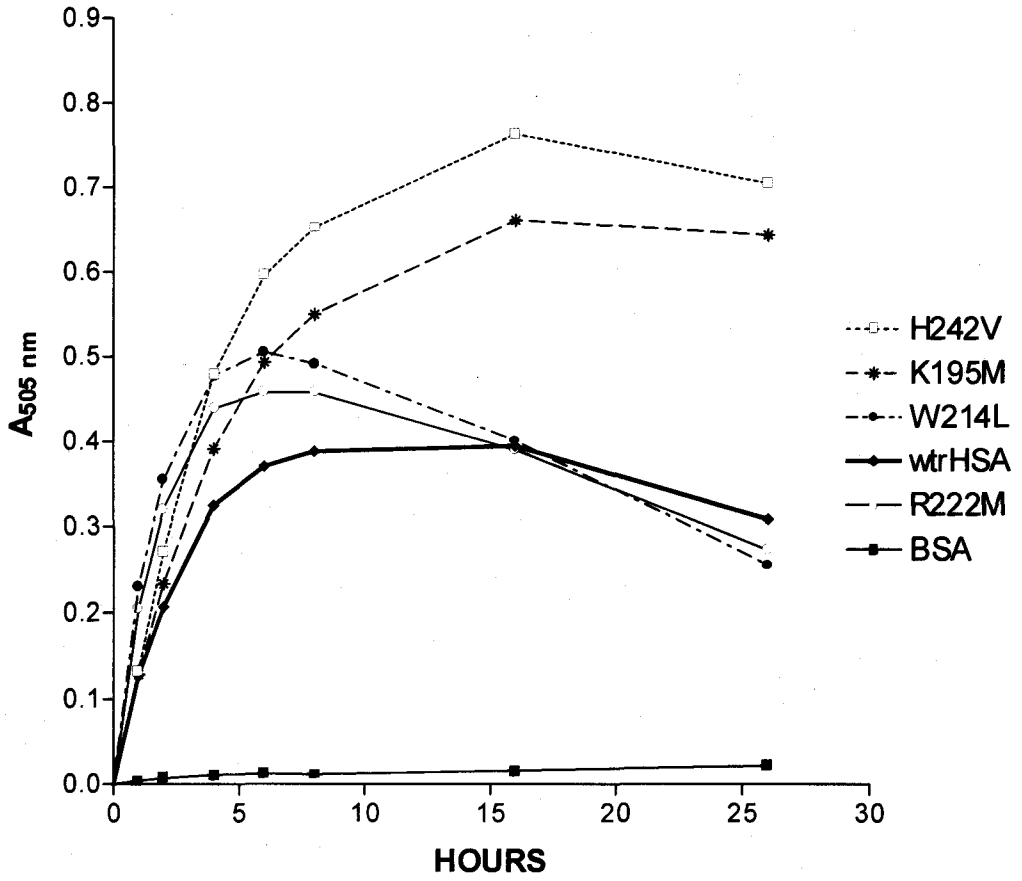

Figure 55. Effects of albumin species (group B) on 15-keto-PGE_2 catalysis. The figure shows the absorbance at 505 nm of a cuvette containing a particular albumin species or wild type HSA fragment and the same initial amount of 15-keto-PGE_2 on the ordinate. Incubation time of 15-keto-PGE_2 with a particular albumin species is shown on the abscissa in hours. The data are for wtrHSA, K195M, W214L, R222M, H242V and BSA.

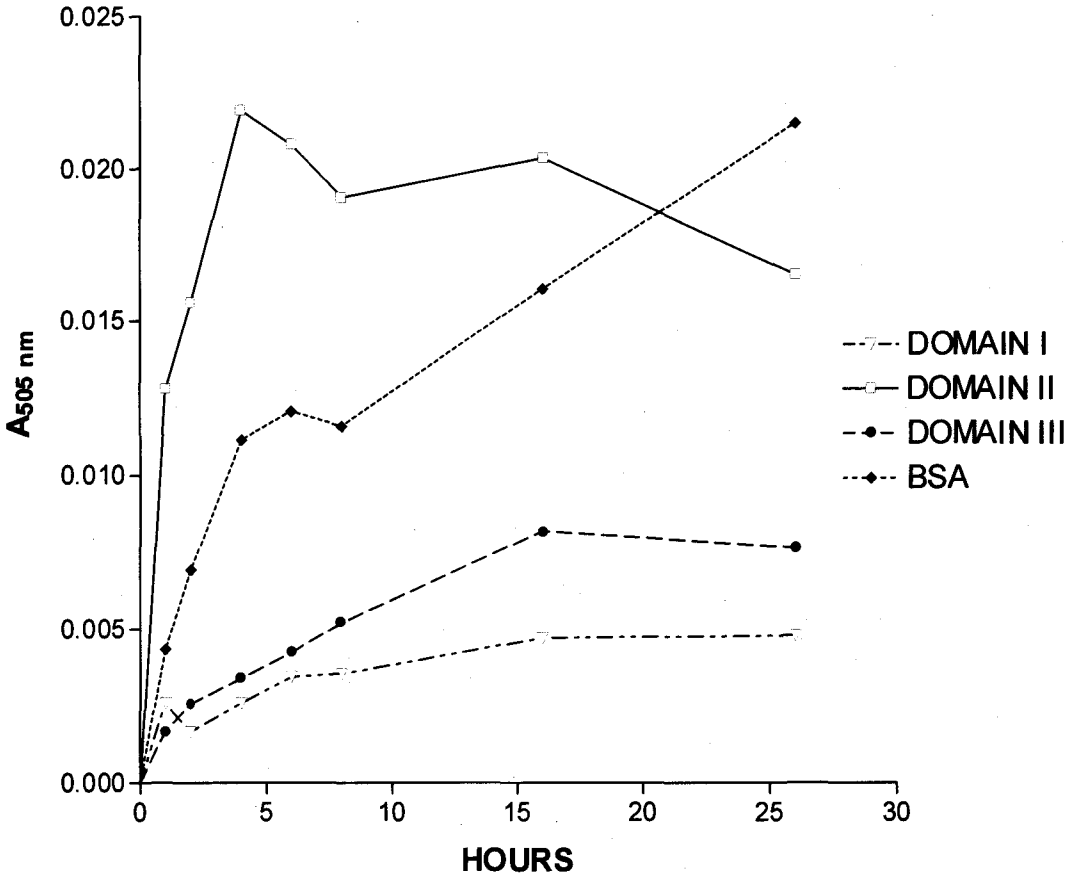

Figure 56. Effects of albumin species (group C) on 15-keto-PGE_2 catalysis. The figure shows the absorbance at 505 nm of a cuvette containing a particular albumin species or wild type HSA fragment and the same initial amount of 15-keto-PGE_2 on the ordinate. Incubation time of 15-keto-PGE_2 with a particular albumin species is shown on the abscissa in hours. The data are for recombinant fragments corresponding to Domains I, II, and III of HSA, and BSA.

Table 3. Relative rate constants for step 1 and for step 2. The values for wild type recombinant (wtrHSA) are taken as unity. The values for step 1 are calculated based on initial rate while the values for step 2 are derived by nonlinear regression assuming a two-step model:

15-keto-PGE_2 → chromophore (enol tautomeric hybrid) → 15-keto-PGB_2

Albumin species	step 1	step 2
wtrHSA	1.0	1.0
F211V	0.46	1.1
K199M	0.51	2.1
R218P	0.52	2.2
R218H	0.36	1.4
R218M	0.40	1.9
R257M	0.15	3.1
H242V	1.17	0.24
K195M	1.07	0.32
W214L	1.77	1.1
R222M	1.59	1.1

DISCUSSION

Interestingly, R218M, R218H and R218P all gave reduced catalytic rates (Figure 54) for formation of the keto-enol tautomer relative to wild type HSA. For all three of the above HSA species, the peak A_{505nm} value and initial rate of keto-enol tautomer formation were about 50% of that observed for wild type HSA. Peak A_{505nm} values were reached by about 10 h and were relatively constant until the end of the 26-h incubation, indicating an approximate steady state after 10 h, when the rates of 15-keto-PGB_2 formation and keto-enol tautomer formation are approximately equal. The peak A_{505nm} values for all three species were about half of the peak A_{505nm} for wild type HSA. Since R218P and R218H are fairly common naturally occurring HSA species, these results could be physiologically important; that is, prostaglandin metabolism could be significantly altered in patients with these genotypes. One study estimated a prevalence of 0.17 % in the general population for familial dysalbuminemic hyperthyroxinemia (Arevalo 1991), the clinical condition resulting from plasma albumin with the R218H or R218P genotype. R257M and K199M displayed normalized rate constants of 0.15 and 0.51, respectively for keto-enol tautomer formation. It should be noted that all of the substitutions described above result in the loss of a specific basic residue in subdomain IIA, either arginine or lysine, and all substitutions significantly reduced the rate of keto-enol tautomer formation.

K195M and H242V showed only slightly increased rates over wild type HSA for keto-enol tautomer formation, 1.07 and 1.17, respectively (Figure 55). However,

both species have peak A_{505nm} values almost twice that of wild-type HSA. For wild-type HSA, the A_{505nm} reaches a peak at about 8 h. After 16 h, the A_{505nm} for wild-type HSA steadily decreases, indicating that the rate of 15-keto-PGB_2 formation exceeds the rate of keto-enol tautomer formation after 16 h. For K195M and H242V, the A_{505nm} increases until 16 h and decreases only slightly after 16 h. Such a result would be consistent with the following explanation. Although the initial rates of keto-enol tautomer formation for K195M and H242V are only slightly elevated over those of wild type HSA, a decrease in the rate of 15-keto-PGB_2 formation for K195M and H242V relative to the rate of 15-keto-PGB_2 formation for wild type HSA results in a much higher peak A_{505nm} value for these two species.

F211V shows a decreased rate for keto-enol tautomer formation with a normalized rate of 0.46. The origin of this effect is unclear, but could be related to specific binding interactions between F211 and 15-keto-PGE_2. R222M and W214L exhibit initial rates for keto-enol tautomer formation of 1.59 and 1.77, respectively. Both species reach peak A_{505nm} values about 30 % greater than the peak A_{505nm} value for wild-type HSA. However, the A_{505nm} values for R222M and W214L at 26 h are actually lower than those observed for wild type HSA at 26 h, due to a more rapid drop in A_{505nm} for R222M and W214L compared to wild-type HSA from 6 to 26 h. The above result can be explained as follows. Although the initial rate of keto-enol tautomer formation is greater for R222M and W214L than for wild-type HSA, the rate of formation of 15-keto-PGB_2 for R222M and W214L is also greater than for wild-type HSA. Thus, as the concentration of the keto-enol tautomeric hybrid rises, increased 15-keto-PGB_2

formation lowers the keto-enol tautomer concentration more rapidly for R222M and W214L than for wild-type HSA.

In order to reconcile our results with previous studies, which attempt to explain the effect of HSA on prostaglandin metabolism, it is necessary to examine these previous studies in some detail. The majority of previous work supports the idea that prostaglandins bound to HSA are exposed to an alkaline microenvironment with a pH greater than or equal to 10.0. In most previous work, reaction products obtained by incubating various prostaglandins at various pH values were compared to those obtained by incubating prostaglandins with wild-type HSA. Evidence from some of the most convincing studies follows. 13,14-dihydro-15-keto-PGE_2 degrades in the presence of HSA to a unique bicyclo rearrangement product that can only be formed in buffers with a pH of approximately 10.0 or greater (Fitzpatrick *et al.* 1980; Granstrom *et al.* 1980). Another study found that albumin stabilizes PGI_2, which rapidly decomposes in aqueous buffer at neutral pH (Cho and Allen, 1978). PGI_2 is stabilized in buffers with a pH of approximately 10.0 or greater, because alkaline conditions stabilize a labile vinyl ether group that is part of PGI_2. For aqueous buffers the pH-dependent decomposition of PGE_1 and PGE_2 have been well studied (Monkhouse *et al.* 1973; Thompson *et al.* 1973; Stehle and Oesterling 1977). The main products of decomposition result from dehydration and are A- or B-type prostaglandin. The rate of decomposition increases at pH values below 2.0 and above 7.4. Between pH 2.0 and 7.4, the rate of decomposition of PGE_1 and PGE_2 is slower than at pH 7.4. Below pH 2.0, conversion of PGA_1 into PGB_1 does not occur in aqueous buffer. However, in alkaline buffers, PGA_1 and PGB_1

are both formed from PGE_1. Based on the rate at which PGA_1 and PGB_1 are formed from PGE_1 in the presence of HSA in an aqueous buffer at pH 7.4, previous authors concluded that PGE_1 and related prostaglandins bind to a site on HSA which has a local microenvironment with a pH of 10.0 or greater than 10 (Monkhouse *et al.* 1973; Thompson *et al.* 1973; Stehle and Oesterling 1977). In total, previous studies attribute the effects of subdomain IIA on prostaglandin metabolism to a general property of the binding site, alkalinity, ignoring the complexity of the binding site and suggesting that the effect of HSA binding on prostaglandin metabolism is to some extent non-specific. The large number of structurally dissimilar ligands which bind to subdomain IIA of HSA has contributed to the idea that HSA/ligand interactions are not due to detailed binding site structure and has lead to many theories of ligand binding to HSA such as that described above which lack mechanistic specificity. Our results do not conflict with the above studies in that they suggest a base-catalyzed process for the conversion of 15-keto-PGE_2 to 15-keto-PGB_2. However, our data suggest that the process is more complex and specific than previously thought.

First, the catalytic conversion of HSA bound 15-keto-PGE_2 to 15-Keto-PGB_2 is a process involving two specific steps, the first step being the formation of 15-keto-PGA_2, which is converted rapidly to its keto-enol tautomers, and the second step being the conversion of the keto-enol tautomers to 15-keto-PGB_2. These processes shall hereafter be referred to as step 1 and step 2, respectively. The rate of each step appears to be altered independently by specific amino acid substitutions. For example, the mutants K195M and H242V display slight increases in the rate of step 1, but decreases

in the rate of step 2. R222M and W214L display an increase in the rate of both step 1 and step 2.

Decreases in the rate of keto-enol tautomer formation observed for R218M, R218P, R218H, K199M, and R257M would be consistent with previous theories which hold that an alkaline microenvironment in subdomain IIA is responsible for the breakdown of 15-keto-PGE_2 and related prostaglandins. However, such a theory is contradicted by other information. For example, the mutant F211V displays a decreased rate for step 1, but the alkalinity of subdomain IIA would not be altered by such a substitution. Likewise, R222M shows increased rates for steps 1 and 2, but such a substitution would be expected to increase the alkalinity of subdomain IIA. In addition, W214L shows increased rates for steps 1 and 2, but such a substitution would not be expected to change the alkalinity of subdomain IIA.

Our results suggest that R218, R257, and K199 could play an important role in catalyzing the conversion of 15-keto-PGE_2 to 15-keto-PGA_2 and its keto-enol tautomers. In our model, any of the above residues could be located in close proximity to carbon 10 on 15-keto-PGE_2. Since the guanidino and amino groups on arginine and lysine, respectively, are strong bases, they could abstract a proton from carbon 10. Loss of the OH^- group on the adjacent carbon atom (carbon 11) would result in a base-catalyzed dehydration reaction similar to that which occurs at high OH^- concentrations. Thus, under alkaline conditions (pH 10) the reaction would be catalyzed by abstraction of a proton from carbon 10 by OH^-, whereas for HSA-bound 15-keto-PGE_2, the reaction would be catalyzed by basic amino acid residues located near carbon 10. The reduction

in the rate of step 2, the conversion of the keto-enol tautomers to 15-keto-PGB_2 observed for H242V and K195M, could be explained by the following mechanisms. K195 and/or H242 could abstract a proton from carbon 8. Alternatively, H242 could exert its effect on the rate of step 2 by modulating the pKa of K199. A previous study suggested that the pKa of K199 is decreased to 7.9 in the presence of H242, which acts as proton acceptor (Gerig and Reinheimer 1975; Carter and Ho 1994). The increased rates for steps 1 and 2 observed for R222M and W214L are more difficult to explain, but are likely to result from a tighter binding of 15-keto-PGE_2 to the subdomain IIA binding site and/or conformational changes which result in a better fit between enzyme and substrates for optimal catalysis. Clearly, R222 is not likely to be a proton acceptor in the catalytic mechanisms described above. In the X-ray structure of unliganded HSA, R222 protrudes into the center of subdomain IIA and could potentially block the binding of 15-keto-PGE_2 by steric hindrance. The reduction in the rate of catalysis observed for F211V could result from reduced binding and/or a fit between substrate and catalyst less optimal than that of wild-type HSA. In total, the breakdown of HSA-bound 15-keto-PGE_2 appears quite sensitive to subdomain IIA mutations. The present study gives two examples of naturally occurring substitutions which could affect prostaglandin metabolism. Based on our findings, it appears possible that other as yet undiscovered naturally occurring subdomain IIA substitutions could alter HSA-mediated prostaglandin metabolism, potentially impacting cardiovascular mortality.

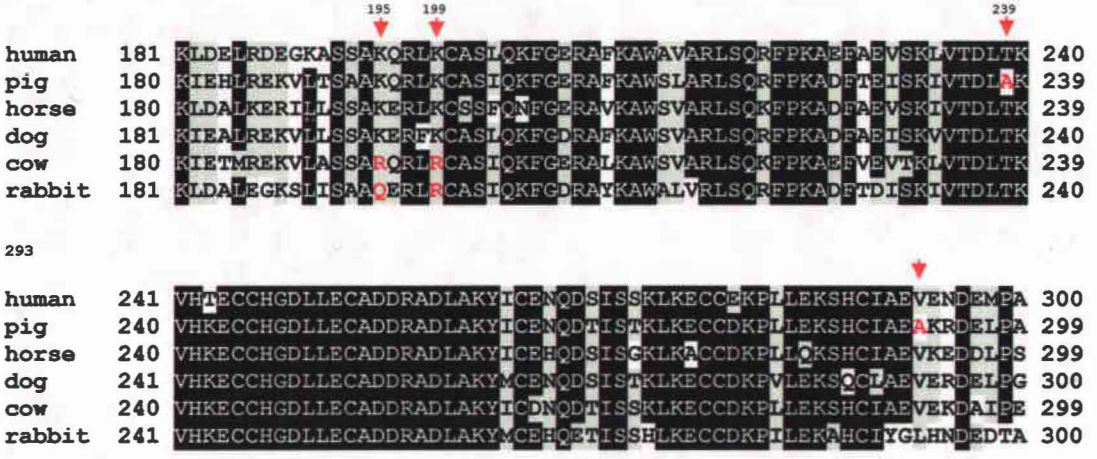

Figure 57. Sequence alignment of serum albumins from human, pig, horse, dog, cow and rabbit, focusing on domain IIA.

It is known that the side group of lysine residue has a pKa of about 10 while that of arginine residue has a pKa of equal to or greater than12 in a protein (Cantor and Schimmel, 1980a). Thus at a pH between 10 and 12, lysine residue is mainly in the deprotonated form while arginine is in the protonated form. At this pH range, lysine residue functions far better in general base catalysis than arginine residue does. Previous study has demonstrated the influence of species on albumin-15-keto-PGE2 interactions (Fitzpatrik *et al.*, 1984). Among the examined serum albumins from human, pig, horse, dog, cow and rabbit, albumin from pig exhibited the highest activity, albumins from rabbit and cow displayed virtually no activity, and albumins from human, dog and horse showed a moderate activity. Sequence alignment of domain IIA of serum albumins from human, pig, horse, dog, cow and rabbit suggests that the presence of arginine or glutamine in stead of lysine at position 195, and the presence of arginine in stead of lysine at position 199 in cow or rabbit albumin reduce the effect of the albumin-mediated catalysis (Figure 57). In addition, the change of threonine and valine to alanine at position 239 and 293 respectively may contribute to the enhanced effect of albumin from pig by reducing steric hindrance thus allowing a better fit between the binding pocket and prostaglandin molecule.

Recent work is demonstrating the importance of specific amino acid residues for certain HSA/ligand interactions. The present study continues that trend by demonstrating the specificity and complexity of the interaction between HSA and the model prostaglandin 15-keto-PGE_2. X-ray crystallographic studies which examine interactions between subdomain IIA mutants of HSA and model analogs of arachidonic

acid metabolites will be needed to unravel the many complexities of the interactions between HSA and prostaglandins. We hope that our present findings provide motivation for this future work.

CHAPTER 5
CONCLUSIONS

Human serum albumin is the most abundant protein in the blood circulation. Binding reversibly many endogenous and exogenous compounds with moderate to high affinity, HSA principally functions as a transport and depot protein. Ligand-HSA interactions affect pharmacokinetics of drugs. Due to its high concentration, HSA can assume additional functions. Structurally, it is a single chain protein with three homologous domains, each domain having distinct features. The two well-known ligand-binding sites, i.e., site I and site II, are located in Domains II and III, respectively.

Fragments have been of important use in dissecting the array of ligand binding site on HSA. In this work, domain fragments with well-defined boundaries were expressed in *Pichia pastoris* expression system and characterized. They retained many of the structural characteristics found in the domains inside the context of the whole HSA molecule. In domain II, is located the single tryptophan residue of HSA, which can be used as a sensitive probe for binding studies. Domain III-Y411W, with tyrosine at position 411 replaced by a tryptophan residue, exhibited fluorescence quenching when a quenching ligand was bound to it, which may facilitate the use of this fragment as a surrogate protein in many studies. In general, the displacement of fluorescent markers bound to a specific site on the fragments by drugs showed similar behavior as expected for the corresponding domain in the intact HSA. For example, site I specific ligands such as bilirubin, iophenoxate, phenylbutazone and warfarin, bind to domain II fragment with affinity comparable with that for intact HSA. Domain III and Domain III-Y411W

fragments bind site II specific ligands, such as ibuprofen and dansylsarcosine, as expected. Due to the lack of inter-domain interactions, small to moderate structural changes were observed in some cases when monitored by a certain method. By means of acrylamide quenching, it was found that the tryptophan residue is most accessible to solute quenching in rHSA, less accessible in domain II and least accessible in domain III-Y411W. The difference in the tryptophanyl accessibility may also reflect the inherent difference in the environments around W214 of rHSA and W411 of domain III-Y411W. In essence, the results from the fragment experiments were consistent with the current consensus on the properties of site I and site II of HSA favoring the use of fragments in future studies. A domain II construct with desirable cleavage at the secretion signal sequence was obtained and a preliminary rule for designing an efficient cleavage site has been proposed, which will make it easier to prepare new fragments.

HSA undergoes structural changes around neutral pH, known as the N-B transition, which was suggested to have physiological significance. Previous work has suggested a dominant role of five histidine residues at positions 9, 39, 67, 105, 128 or 146 of domain I in this transition. In the present work, all six residues were changed to serine and phenylalanine by using site-directed mutagenesis. And the five positions have been resolved to be 9, 67, 105, 128 and 146 and the role of the histidine residues has been confirmed. Combined with crystal structural information, the results promise to offer more insights into the molecular mechanism of this transition, which will prove valuable for a better understanding of albumin and allosteric proteins as well. The work also demonstrated the advantages of using well-designed mutants in solving complex problems in a systematic way.

The third part of the work presented attempted to provide insights into the mechanisms by which prostaglandins bound to subdomain IIA of HSA are metabolized by catalytic processes. Many arachidonic acid metabolites bind to HSA and the metabolism of these molecules is altered as a result of binding. The breakdown of the prostaglandin 15-keto-PGE_2 to 15-keto-PGA_2 and 15-keto-PGB_2 in the presence of wild type HSA and a number of subdomain IIA mutants was examined using a previously validated spectroscopic method, which monitors absorbance at 505 nm. The species examined using the above method were wild type HSA, K195M, K199M, F211V, W214L, R218M, R218P, R218H, R222M, H242V, R257M and bovine serum albumin. Previous studies on HSA mediated catalysis indicated that the breakdown of HSA bound prostaglandins results from an alkaline microenvironment in the binding site. Our results showed that the catalytic breakdown of HSA-bound 15-keto-PGE_2 to 15-keto-PGB_2 results from two specific processes, which are modulated by specific amino acid residues. Specifically, some amino acid residues modulate the rate of step one, the conversion of 15-keto-PGE_2 to 15-keto-PGA_2, while other residues modulate the rate of step 2, the conversion of 15-keto-PGA_2 to 15-keto-PGB_2. Some residues modulate the rate of step 1 and 2. In total, while our results support the involvement of certain basic amino residues in the catabolism of HSA-bound 15-keto-PGE_2 our data suggest that metabolism of HSA-bound prostaglandins may be a more complex and specific process than previously thought.

REFERENCES

Ancell, H. 1839. Course of lectures on the physiology and pathology of the blood and the other animal fluids. Lancet 1: 222.

Arevalo, G. 1991. Prevalence of familial dysalbuminemic hyperthyroxinemia in serum samples received for thyroid testing. Clin. Chem. 37: 1430-1431.

Behrens, P.Q., Spiekerman, A.M., and Brown, J.R. 1975. Structure of human serum albumin. Fed. Proc. Fed. Am. Soc. Exp. Biol. 34: 591.

Bhagavan, N.V., Lai, E.M., Rios, P.A., Yang, J., Ortega-Lopez, A.M., Shinoda, H., Honda, S.A., Rios, C.N., Sugiyama, C.E., Ha, C.E. 2003. Evaluation of human serum albumin cobalt binding assay for the assessment of myocardial ischemia and myocardial infarction. Clin Chem. 49(4):581-5.

Bordo, D., Argos, P. 1991. Suggestions for "safe" residue substitutions in site-directed mutagenesis. J. Mol. Biol. 217(4):721-9.

Bos, O.J., Fischer, M.J., Wilting, J., and Janssen, L.H. 1988a. Drug-binding and other physicochemical properties of a large tryptic and a large peptic fragment of human serum albumin. Biochim. Biophys. Acta. 953(1):37-47.

Bos, O.J., Fisher, M. J., Witling, J., Janssen, L.H. 1989a. Mechanism by which warfarin binds to human serum albumin. Stopped-flow kinetic experiments with two large fragments of albumin. Biochem. Pharmacol. 38:1979-1984.

Bos, O.J., Labro, J.F., Fisher, M.J., Witling, J., Janssen, L.H. 1989b. The molecular mechanism of the neutral-to-base transition of human serum albumin. Acid/base titration and proton nuclear magnetic resonance studies on a large peptic and a large tryptic fragment of albumin. J. Biol. Chem.264:953-959.

Bos, O.J., Remijn, J.P., Fischer, M.J., Witling, J., Janssen, L.H. 1988b. Location and characterization of the warfarin binding site of human serum albumin. A comparative study of two large fragments. Biochem. Pharmacol. 37:3905-3909.

Brown. J. R. and shokley, P, 1982. Serum albumin: Structure and characterization of its ligand binding sites. (1982) In: Lipid-protein interactions (Jost, P.C. and Griffith, O.H. eds.). vol. 1.pp. 25-68. John Wiley, New York.

Campbell, W.B., and Halushka, P.V. 1996. Lipid-derived autoacids: ecosanoids and platelet-activating factor. In Goodman and Gilman's the pharmacological basis of

therapeutics, 9th Ed. (eds. Hardman, J.G., Limbard, L.E., Molinoff, P.B., Ruddon, R.W. and Gilman, A.G.), pp. 601-616, McGraw-Hill, New York, NY.

Cantor C.R., and Schimmel, P.R. 1980a. Biophysical Chemistry: The Conformation of Biological Macromolecules, W. H. Freeman Company, New York.

Cantor C.R., and Schimmel, P.R. 1980b Biophysical Chemistry: The Behavior of Biological Macromolecules, W. H. Freeman Company, New York.

Carter, D.C., and Ho, J.X. 1994. Structure of serum albumin. Adv. Prot. Chem. 45: 153-201.

Cho, M., and Allen, M. 1978. Chemical stability of prostacyclin (PGI_2) in aqueous solutions. Prostaglandins 15: 943-954.

Curry, S., Brick, P., and Franks, N.P. 1999. Fatty acid binding to human serum albumin: new insights from crystallographic studies. Biochim Biophys Acta. 1441(2-3):131-40.

Curry, S., Mandelkow, H., Brick, P., and Franks, N.P. 1998. Crystal structure of human serum albumin complexed with fatty acid reveals an asymmetric distribution of binding sites. Nature Struct. Biol. 5: 827-835.

Dockal, M, Carter D.C, Ruker, F. 2000. Conformational transitions of the three recombinant domains of human serum albumin depending on pH. J. Biol. Chem. 275:3042-3050.

Dockal, M., Carter D.C., Ruker, F. 1999. The three recombinant domains of human serum albumin. Structural characterization and ligand binding properties. J. Biol. Chem. 274: 29303-29310.

Dockal, M., Chang, M., Carter, D.C., Ruker, F. 2000. Five recombinant fragments of human serum albumin-tools for the characterization of the warfarin binding site. Protein Sci. 9: 1455-1465.

Droge, J.H., Janssen, L.H., and Wilting, J. 1983. Allosteric properties of the oxyphenbutazone--human serum albumin complex. Pharm Weekbl Sci. 5(5):228-33.

Eftink, M.R., Ghiron, C.A..Biochemistry. 1976. Exposure of tryptophanyl residues in proteins. Quantitative determination by fluorescence quenching studies. 15(3):672-80.

Fehske, K.J., Muller, W.E. 1978. The interaction of iopanoic and iophenoxic acids with human serum albumin. Res Commun Chem Pathol Pharmacol. 19(1):119-27.

Figge, J., Rossing, T.H., and Fencle, V. 1991. The role of serum proteins in acid-base equilibria. J. Lab. Clin. Med. 120: 713-719.

Fischer, M.J., Bos, O.J., van der Linden, R.F., Wilting, J., and Janssen, L.H. 1993. Steroid binding to human serum albumin and fragments thereof. Role of protein conformation and fatty acid content. Biochem Pharmacol. 45(12):2411-6.

Fitzpatrick, F.A., Aguirre, F., Pike, J.E., and Lincoln, F.H. 1980. The stability of 13,14-dihydro-15-keto-PGE2. Prostaglandins 19: 917-931.

Fitzpatrick, F.A., and Wynalda, M.A. 1981. Albumin-lipid interactions: Prostaglandin stability as a probe for characterizing binding sites on vertebrate albumins. Biochem. 20: 6129-6134.

Fitzpatrick, F.A., Liggett, W.F., and Wynalda, M.A. 1984. Albumin-eicosanoid interactions: A model system to determine their attributes and inhibition. J. Biol. Chem. 259: 2722-2727.

Fitzpatrick, F.A., Morton, D.R., and Wynalda, M.A. 1981. Albumin stabilizes leukotriene A4. J. Biol. Chem. 257: 4680-4683.

Folco, G., Granstrom, E. and Kindahl, H. 1977. Albumin stabilizes thromboxane A2. FEBS Lett. 82: 321-324.

Foster, J.F. 1977. Some aspects of the structure and conformational properties of serum albumin. In "Albumin, Structure, Function, and Uses" (Rosenoer, V. M. and Rothschild, M..A.. eds.), pp.53-84. Pergaamon, New York.

Geisow, M.J., and Beaven, G.H. 1977. Physical and binding properties of large fragments of human serum albumin. Biochem J. 163(3):477-84.

Gerig, J.T., and Reinheimer, J.D. 1975. Modification of human serum albumin with trifluoromethyl-substituted aryl halides and sulfonates. *J Am Chem Soc.***97**: 168-73.

Gillum, R.F. 2000. Assessment of serum albumin concentration as a risk factor for stroke and coronary disease in African Americans and whites. J. Natl. Med. Assoc. 92: 3-9.

Gillum, R.F., Makuc, D.M. 1992. Serum albumin, coronary heart disease, and death Am. Heart J. 123: 507-513.

Glatz, J.F.C., and Veerkamp, J.H. 1983. Removal of fatty acids from serum albumin by Lipidex 1000 chromatography. J. Biochem. Biophys. Methods 8: 57-61.

Goldwasser, P., Feledman, J. 1997. Association of serum albumin and mortality risk. J Clin. Epidemiol. 50: 693-703.

Granstrom, E., Hamberg, M., Hansson, G., and Kindahl, H. 1980. Chemical instability of 15-keto-13,14-dihydro- PGE2: the reason for low assay reliability. Prostaglandins 20: 933-957.

Gueriguian, J.L. 1976. Prostaglandin-macromolecule interactions. I. Noncavalent binding of prostaglandins A1, E1, F2, and E2 by human and bovine serum albumins. J. Pharm. Exp. Therap. 197: 391-401.

Ha, C.E., Petersen C.E., Park D.S., Bhagavan N.V. 2000. Investigations of the effects of ethanol on warfarin binding to human serum albumin. J. Biomed. Sci. 7:114-121.

Ha, C.E., Petersen, C.E., Park, D., Harohalli, K., and Bhagavan, N.V. 1999. Identification of key amino acid residues involved in specific interactions between digoxin and human serum albumin. J. Biochem. Mol. Biol. & Biophys..2:201-207.

Hagag, N., Birnbaum, E.R., and Darnall, D.W. 1983. Resonance energy transfer between cysteine-34, tryptophan-214, and tyrosine-411 of human serum albumin. Biochemistry. 22(10):2420-7.

Harmsen, B.J., De Bruin, S.H., Janssen, L.H., Rodrigues, de Miranda, J.F., and Van Os, G.A. 1971. pK change of imidazole groups in bovine serum albumin due to the conformational change at neutral pH. Biochemistry. 10(17):3217-21.

He, X.M., and Carter, D.C. 1992. Atomic structure and chemistry of human serum albumin. Nature 358: 208-215.

Janssen, L.H., Van Wilgenburg, M.T., and Wilting, J. 1981. Human serum albumin as an allosteric two-state protein. Evidence from effects of calcium and warfarin on proton binding behaviour. Biochim. Biophys. Acta. 669(2):244-50.

Kasai-Morita, S., Horie, T., and Awazu, S. 1987. Influence of the N-B transition of human serum albumin on the structure of the warfarin-binding site. Biochim. Biophys. Acta 915:277-283.

Keaney, J.F. Jr., Simon, D.I., Stamler, J.S., Jaraki, O., Scharfstein, J., Vita, J.A., and Loscalzo, J. 1993. NO forms an adduct with serum albumin that has endothelium-derived relaxing factor-like properties. J. Clin. Invest. 91(4):1582-9.

Kjeldsen, T., Pettersson, A.F., Drube, L., Kurtzhals, P., Jonassen, I., Havelund, S., Hansen, P.H., and Markussen, J. 1998. Secretory expression of human albumin domains in Saccharomyces cerevisiae and their binding of myristic acid and an acylated insulin analogue. Protein Expr Purif. 13(2):163-9.

Kosa, T., Maruyama, T., Sakai, N., Yonemura, N., Yahara, S., and Otagiri, M. 1998. Species differences of serum albumins: III. Analysis of structural characteristics and ligand binding properties during N-B transitions. Pharm. Res. 15:592-598.

Kragh-Hansen, U., and Vorulm, H. 1993. Quantitative analyses of the interaction between calcium ions and human serum albumin. Clin Chem 39:202-8.

Kragh-Hansen, U., Chuang, V.T., and Otagiri, M. 2002. Practical aspects of the ligand-binding and enzymatic properties of human serum albumin. Biol Pharm Bull. 25(6):695-704.

Labro, J.F, and Janssen, L.H. 1986. A proton nuclear magnetic resonance study of human serum albumin in the neutral pH region. Biochim. Biophys.Acta.873:267-278.

Lakowicz, J.R. 1986. Fluorescence studies of structural fluctuations in macromolecules as observed by fluorescence spectroscopy in the time, lifetime, and frequency domains. Methods Enzymol. 131:518-67.

Leonard, W.J., Jr., Vijai, K.K., and Foster, J.F. 1963. A structural transformation in bovine and human plasma albumins in alkaline solution as revealed by rotatory dispersion studies. J. Biol. Chem. 238:1984-1988.

Levine, R.L. 1977. Fluorescence-quenching studies of the binding of bilirubin to albumin. Clin Chem. 23(12):2292-301.

Liu, R., Meng, Q., Xi, J., Yang, J., Ha, C.E., Bhagavan, N.V., and Eckenhoff, R.G. 2004. Comparative binding character of two general anesthetics for sites on human serum albumin. Biochem J. Feb 3 [Epub ahead of print]

Markiewicz, P., Kleina, L.G., Cruz, C., Ehret, S., Miller, J.H. 1994. Genetic studies of the lac repressor. XIV. Analysis of 4000 altered Escherichia coli lac repressors reveals essential and non-essential residues, as well as "spacers" which do not require a specific sequence. J. Mol. Biol. 240(5):421-33.

Martz, Eric. 2000. Protein Explorer: Freeware for 3D visualization of macromolecular structure, FASEB J. 14:22.

Maruyama, T., Lin, C.C., Yamasaki, K., Miyoshi, T., Imai, T., Yamasaki, M., and Otagiri, M. 1993. Binding of suprofen to human serum albumin. Role of the suprofen carboxyl group. Biochem. Pharmacol. 45(5):1017-26.

Meloun, B., Moravek, L., and Kostka, V. 1975. Complete amino acid sequence of human serum albumin. FEBSLett. 58(1): 134-137.

Monkhouse, D., Van Campen, L. and Aguiar, A. 1973. Kinetics of dehydration and isomerization of prostaglandins E1 and E2, J. Pharm. Sci. 62: 576-580.

Monod, J., Wyman, J., and Changeux, J.P. 1965. On the nature of allosteric transitions: a plausible model. J. Mol. Biol. 12:88-118.

Narazaki, R., Maruyama, T., and Otagiri, M. 1997. Probing the cysteine 34 residue in human serum albumin using fluorescence techniques. Biochim. Biophys. Acta. 1338(2):275-81.

Park, D.S., Petersen, C.E., Ha, C., Harohalli, K., Feix, J.B., and Bhagavan, N.V. 1999. Expression of a human serum albumin fragment (consisting of subdomains IA, IB, and IIA) and a study of its properties. IUBMB Life. 48(2):169-74.

Pedersen, K.O. 1971. Binding of calcium to serum albumin. I. Stoichiometry and intrinsic associationi constant at physiological pH. Ionic strength, and temperature. Scand. J. Clin. Lab. Invest. 28:459-69.

Peters, T. Jr. 1996. All about Albumin: biochemistry, genetics, and medical applications. Academic Press, New York.

Petersen CE, Ha CE, Mandel M, Bhagavan, NV. Expression of a human serum albumin variant with high affinity for thyroxine. Biochem. Biophys. Res. Commun. 1995;214:1121-1129.

Petersen, C.E., Ha, C.E., Curry, Stephen, and Bhagavan, N.V. 2002. Probing the structure of the warfarin-binding site on human serum albumin using site-directed mutagenesis. Proteins: Structure, Function, and Genetics 47:116-125.

Petersen, C.E., Ha, C.E., Harohalli, K., Park, D., and Bhagavan, N.V. 1997. Mutagenesis studies of thyroxine binding to human serum albumin define important structural characteristics of subdomain 2A. Biochemistry 36:7012-7017.

Petersen, C.E., Ha, C.E., Harohalli, K., Park, D.S., and Bhagavan, N.V. 2000. Familial dysalbuminemic hyperthyroxinemia may result in altered warfarin pharmacokinetics. Chemico-Biol. Inter. 124:161-172.

Petersen, C.E., Ha, C.E., Jameson, D.M., and Bhagavan, N.V.1996. Mutations in a specific human serum albumin thyroxine binding site define the structural basis of familial dysalbuminemic hyperthyroxinemia. J.Biol. Chem 271:19110-19117.

Petitpas, I., Bhattacharya, A.A., Twine, S., East, M., and Curry, S. 2001. Crystal structure analysis of warfarin binding to human serum albumin: Anatomy of drug site I. J. Biol. Chem. 276, 22804-22809.

Petitpas, I., Petersen, C.E., Ha, C.E., Bhattacharya, A.A., Zunszain, P.A., Ghuman, J., Bhagavan, N.V., and Curry, S. 2003. Structural basis of albumin-thyroxine interactions and familial dysalbuminemic hyperthyroxinemia. Proc Natl Acad Sci U S A. 100(11):6440-5.

Raz, A. 1972. Interaction of prostaglandins with blood plasma proteins: Comparative binding of prostaglandins A2, F2 and E2 to human plasma proteins. Biochem. J. 130: 631-636.

Rahman, M.H., Maruyama, T., Okada, T., Yamasaki, K., and Otagiri, M. 1993. Study of interaction of carprofen and its enantiomers with human serum albumin--I. Mechanism of binding studied by dialysis and spectroscopic methods. Biochem. Pharmacol. 46(10):1721-31.

Remuzzi, G., Mecca, G., Marchesis, D., Livio, M., de Gaetano, G., Doanti, M.B., and Silver, M.J. 1979. Platelet hyperaggregability and the nephrotic syndrome. Thromb. Res. 16: 345-354.

Silver, M.J., Smith, J.B., Ingerman, C.M., and Kocsis, J.J. 1973. Arachidonic acid-induced human platelet aggregation and prostaglandin formation. Prostaglandins 4: 863-875.

Smith, P.K., Krohn, R.I., Hermanson, G.T., Mallia, A.K., Gartner, F.H., Provenzano, M.D., Fujimoto, E.K., Goeke, N.M., Olson, B.J., and Klenk, D.C. 1985 Measurement of protein using bicinchoninic acid.Anal Biochem.150(1):76-85.

Spector, A.A. 1986. In Biochemistry and Biology of Plasma Lipoproteins. Edited by Scanu A.M. and Spector A.A. published by Marcel Dekker, Inc. page 247-279.

Stamler, J.S., Jaraki, O., Osborne, J., Simon, D.I., Keaney J, Vita, J., Singel, D., Valeri, C.R., and Loscalzo, J. 1992 Nitric oxide circulates in mammalian plasma primarily as an S-nitroso adduct of serum albumin. Proc. Natl. Acad. Sci. U.S.A. 89(16):7674-7.

Stehle, R., and Oesterling, T. 1977. Stability of prostaglandin E1 and dinoprostone (prostaglandin E2) under strongly acidic and basic conditions. J Pharm. Sci. 66: 1590-1595.

Steiner, R.F., Roth, J., and Robbins, J. 1966. The binding of thyroxine by serum albumin as measured by fluorescence quenching. J. Biol. Chem. 241(3):560-7.

Subramaniam, R., Fan, X. J., Scivittaro, V., Yang, J., Ha, C. E., Petersen, C. E,, Surewicz, W. K., Bhagavan, N. V., Weiss, M. F., and Monnier, V. M. 2002. Cellular oxidant stress and advanced glycation endproducts of albumin: caveats of the dichlorofluorescein assay. Arch Biochem Biophys. 400(1):15-25.

Sudlow, G., Birkett, D.J., and Wade, D.N. 1973. Spectroscopic techniques in the study of protein binding: the use of 1-anilino-8-naphthalenesulphonate as a fluorescent probe for the study of the binding of iophenoxic and iopanoic acids to human serum albumin. Mol. Pharmacol. 9(5):649-57.

Sudlow, G., Birkett, D.J., and Wade, D.N. 1975. Spectroscopic techniques in the study of protein binding. A fluorescence technique for the evaluation of the albumin binding and displacement of warfarin and warfarin-alcohol. Clin Exp. Pharmacol. Physiol. 2:129-140.

Sudlow, G., Birkett, D.J., and Wade, D.N. 1976. Further characterization of specific drug binding sites on human serum albumin. Mol. Pharmacol.12:1052-1061.

Sugio, S., Kashima, A., Mochizuki, S., Noda, M., and Kobayashi, K. 1999. Crystal structure of human serum albumin at 2.5 A resolution. Protein Eng 12:439-46.

Takamura, N., Haruta, A., Kodama, H., Tsuruoka, M., Yamasaki, K., Suenaga, A., and Otagiri, M. 1996. Mode of interaction of loop diuretics with human serum albumin and characterization of binding site. Pharm Res. 13(7):1015-9.

Takamura, N., Rahman, M.H., Yamasaki, K., Tsuruoka, M., and Otagiri, M. 1994. Interaction of benzothiadiazides with human serum albumin studied by dialysis and spectroscopic methods. Pharm Res. 11(10):1452-7.

Thompson, G., Collins, J., and Schmalzried, L. 1973. Total rate equation for decomposition of prostaglandin E2. J Pharm. Sci. 62: 1738-1739.

Unger, W.G. 1972. Binding of prostaglandin to human serum albumin J. Pharm. Pharmac. 24: 470-477.

Wanwimolruk, S., and Birkett, D.J. 1982. The effects of th N-B transition of human serum albumin on the specific drug-binding sites. Biochim. Biophys. Acta; 709:247-255.

Watanabe, T., Narumiya, S., Shimizu, T., and Hayaishi, O. 1982. Characterization of the biosynthetic pathway of prostaglandin D2 in human platelet-rich plasma. J. Biol. Chem. 257: 14847-14853.

Williams, T.F. 1992. Serum albumin, aging and disease. J Clin Epidemiol. 45(3):205-6.

Wilting, J., van der Giesen, W.F., Janssen, L.H., Weideman, M.M., Otagiri, M., and Perrin, J.H. 1980. The effect of albumin conformation on the binding of warfarin to human serum albumin. The dependence of the binding of warfarin to human serum albumin on the hydrogen, calcium, and chloride ion concentrations as studied by circular dichroism, fluorescence, and equilibrium dialysis. J. Biol. Chem. 255(7):3032-7.

Wynalda, N.A., and Fitzpatrick, F.A. 1980. Albumins stabilize prostaglandin I2. Prostaglandins 20: 853-861.

Yang, J., Petersen, C.E., Ha, C., and Bhagavan NV. 2002. Structural insights into human serum albumin-mediated prostaglandin catalysis. Protein Sci. 11:538-545.

Zurawski, V.R., Jr, Foster, and J.F. 1974. The neutral transition and the environment of the sulfhydryl side chain of bovine plasma albumin. Biochemistry. 13(17):3465-71.